New Mexico GEOLOGY

Spring 2019
Volume 41, Number 1

New Mexico Bureau of Geology and Mineral Resources / A Research Division of New Mexico Tech

New Mexico GEOLOGY

Spring 2019
Volume 41, Number 1

Cover

The Loma de las Cañas northeast of Socorro is a northeast-southwest oriented ridge composed of lower Permian sedimentary rocks. These are strata of the Yeso Group overlain by the Glorieta Sandstone capped by the lower part of the San Andres Formation. In the foreground, reddish brown sandstone and siltstone of the Arroyo de Alamillo Formation of the Yeso Group crop out as low benches and in gullies. The lower slope of the Loma is strata of the Torres Member of the Los Vallos Formation that are variegated beds of salmon-colored siltstone, gray gypsum and black dolomite. The prominent red beds above them are the Joyita Member of the Los Vallos Formation, and the thick gray gypsum interval below it is the Cañas Member. Above the Joyita Member, which is the uppermost unit of the Yeso Group, tabular beds of yellow and brown sandstone are the Glorieta Sandstone, and they are capped by dark gray, bedded limestones of the lower part of the San Andres Formation. In 1904, Clarence Luther Herrick (1858–1904), one of the pioneers of New Mexico geology, published the first description of the strata of the Loma de las Cañas. Herrick thought most of these strata are of Triassic and Jurassic age, but decades of subsequent research on the regional stratigraphy and biostratigraphy has firmly established their early Permian age. *Photograph and caption by Spencer G. Lucas.*

A publication of the
New Mexico Bureau of Geology and Mineral Resources
A Research Division of the
New Mexico Institute of Mining and Technology
Science and Service
ISSN 0196-948X

New Mexico Geology is an online publication available as a free PDF download from the New Mexico Bureau of Geology and Mineral Resources website. Subscribe to receive email notices when each issue is available at geoinfo.nmt.edu/publications/subscribe.

Editorial Matter: Articles submitted for publication should follow the guidelines at geoinfo.nmt.edu/publications/periodicals/nmg/NMGguidelines.html.
Address inquiries to Bruce Allen, Geologic Editor, New Mexico Bureau of Geology and Mineral Resources 801 Leroy Place, Socorro, NM 87801. For telephone inquiries call (575) 835-5177 or send an email to NMBG-NMGeology@nmt.edu

The Cretaceous System in central Sierra County, New Mexico

Spencer G. Lucas, New Mexico Museum of Natural History, Albuquerque, NM 87104, spencer.lucas@state.nm.us
W. John Nelson, Illinois State Geological Survey, Champaign, IL 61820, jnnelson@illinois.edu
Karl Krainer, Institute of Geology, Innsbruck University, Innsbruck, A-6020 Austria, Karl.Krainer@uibk.ac.at
Scott D. Elrick, Illinois State Geological Survey, Champaign, IL 61820, elrick@illinois.edu

Abstract

Upper Cretaceous sedimentary rocks are exposed in central Sierra County, southern New Mexico, in the Fra Cristobal Mountains, Caballo Mountains and in the topographically low Cutter sag between the two ranges. The ~2.5 km thick Cretaceous section is assigned to the (ascending order) Dakota Formation (locally includes the Oak Canyon [?] and Paguate [?] members), lower interval of the Mancos Formation (Graneros, Greenhorn, and Carlile members), Tres Hermanos Formation (Atarque, Campana, and Fite Ranch members), D-Cross Member of the Mancos Formation, Gallup Formation, Flying Eagle Canyon Formation, Ash Canyon Formation, and the McRae Group, consisting of the José Creek, Hall Lake, and Double Canyon formations. The name Tokay Tongue of the Mancos Formation is abandoned as an unnecessary term that reduces lithostratigraphic precision. The new name Campana Member of the Tres Hermanos Formation is proposed to replace the preoccupied (duplicate) name, Carthage Member. The terms Mesaverde Formation (Group) and Crevasse Canyon Formation are no longer applied to part of the Cretaceous section in Sierra County. Instead, these strata are the Flying Eagle Canyon Formation (new name) and redefined Ash Canyon Formation. The very thick McRae Formation is raised in rank to the McRae Group, and its constituent members are raised to formations. The Double Canyon Formation is a new lithostratigraphic unit comprising the upper part of the McRae Group. Ammonite and inoceramid bivalve biostratigraphy indicates that the lower interval of the Mancos Formation is of middle Cenomanian-early Turonian age, the Atarque Member of the Tres Hermanos Formation is early Turonian, the D-Cross Member of the Mancos Formation is middle Turonian, and the Gallup Formation is late Turonian. Vertebrate biostratigraphy indicates that the lower part of the Hall Lake Formation is Lancian (late Maastrichtian) in age. Depositional environments of the Cretaceous strata in Sierra County are both marine and nonmarine. They range from offshore marine (lower interval and D-Cross Member of the Mancos Formation), to shoreline deposition of various types (part of the Dakota Formation, the Atarque and Fite Ranch members of the Tres Hermanos Formation, and the Gallup Formation), to nonmarine fluvial channel and floodplain deposits (part of the Dakota Formation, Campana Member of the Tres Hermanos Formation, Flying Eagle Canyon Formation, Ash Canyon Formation, and the entire McRae Group). A comprehensive understanding of the Cretaceous strata in Sierra County allows a more detailed interpretation of local geologic events in the context of broad, transgressive-regressive (T-R) cycles of deposition in the Western Interior Seaway, and also in terms of Laramide orogenic history: (1) T1 transgression of the seaway during middle-late Cenomanian time resulting in deposition of the Dakota Formation, Graneros Member of the Mancos Formation and Greenhorn Member of the Mancos; (2) Turonian R1 regression with deposition of the Carlile Member of the Mancos Formation and the Atarque and Campana members of the Tres Hermanos Formation; (3) late Turonian T2 transgression marked by deposition of the Fite Ranch Member of the Tres Hermanos Formation and lower D-Cross Member of the Mancos Formation; (4) R2 regression during late Turonian-early Coniacian time, with deposition of the upper sandy part of the D-Cross Member, the Gallup Formation, and the lower part of the Flying Eagle Canyon Formation; (5) no clear record of the T3, R3 or T4 events in Sierra County, but the Flying Eagle Canyon Formation likely encompasses the time from the last phase of R2 through T4 (Coniacian–Santonian); (6) R4 regression of early Campanian age and the onset of the Laramide orogeny, when deposition of the Ash Canyon Formation took place; (7) the first significant influx of volcanic detritus at the base of the McRae Group derived from the late Campanian-early Maastrichtian (~70–75 Ma) Copper Flat igneous complex; (8) onset of Hall Lake Formation deposition during the late Maastrichtian (~66–68 Ma); (9) deposition of the bulk of the Hall Lake Formation and the Double Canyon Formation, possibly extending into the Paleocene; and (10), the Love Ranch Formation of likely Eocene age representing the final pulse of the Laramide orogeny in Sierra County.

Introduction

Cretaceous sedimentary rocks are exposed in central Sierra County, southern New Mexico, in and around parts of the Fra Cristobal and Caballo Mountains, as well as in the lowlands between the two mountain ranges, the structural Cutter sag (Fig. 1). This is the most extensive outcrop area of Cretaceous rocks in southern New Mexico, and the exposed Cretaceous section is very thick, at about 2.5 km. First recognized in 1860, these Cretaceous strata have been the subject of diverse, but generally restricted, studies for more than 150 years.

Our goal here is to present the first comprehensive study of the Cretaceous sedimentary rocks in central Sierra County—their lithostratigraphy, paleontology and age, sedimentary petrography and depositional history. Our study entails revisions to the Cretaceous lithostratigraphic nomenclature used in Sierra County and provides new precision to correlation of parts of the section. Our analysis thus allows the Cretaceous strata of Sierra County to be integrated further into a broader understanding of Cretaceous geological history in New Mexico.

Some of the data collected in this study are presented in appendices to this report, which are available as a separate, downloadable file. These data include graphic depictions of measured stratigraphic sections, representative photographs of thin sections used in petrographic analyses, photographs of selected fossils, and a geologic map that shows the distribution of one of the new stratigraphic units discussed herein. Previous studies of the Cretaceous strata in Sierra County are reviewed in the appendices, which also include a summary of subsurface data in tabulated form and a geologic cross section that incorporates those data. References in the main text to items in the appendix are preceded with the letter "A" (e.g., Table A2.1).

Study area, methods, abbreviations, and conventions

The Cretaceous strata of central Sierra County are exposed from the northern tip of the Fra Cristobal Mountains (just into Socorro County) to the northern Caballo Mountains and its eastern periphery (Fig. 1). These strata extend eastward under

the Jornada del Muerto basin and westward under the Rio Grande rift. Place names used in the text are those on the relevant United States Geological Survey topographic quadrangle maps. The horizontal datum for coordinates reported herein is NAD83 (UTM meters, zone 13).

The research reported here is based primarily on fieldwork undertaken during 2013–2017, though some paleontological data were collected as early as the 1980s. This fieldwork was largely part of an effort to map the geology of the Fra Cristobal Mountains. Understanding the Cretaceous strata exposed in the Fra Cristobals necessitated fieldwork to better understand the Cretaceous strata exposed to the south, in the Cutter sag and in the northern Caballo Mountains. Data and interpretations from oil-test boreholes—archived at the New Mexico Bureau of Geology and Mineral Resources (NMBGMR) (Socorro)—were examined in order to obtain additional estimates of thicknesses of some of the Cretaceous units in the area, and are summarized herein.

Data collection included: mapping in the Fra Cristobal Mountains and the area immediately to the south and southwest of the range; measuring numerous stratigraphic sections using a 1.5 m staff and Brunton pocket transit (Fig. 2); collecting numerous rock samples for petrographic analysis; and collecting invertebrate and vertebrate fossils, primarily for biostratigraphic analysis. All fossils collected are part of the collection of the New Mexico Museum of Natural History and Science (NMMNH) in Albuquerque and bear NMMNH locality and catalog numbers. Lithofacies codes assigned to nonmarine sediments (e.g., Gt, St, etc.) are from Miall (1996, 2010). In petrographic analysis, sandstone composition was determined microscopically by identifying the different grain types at 250 equally spaced points across each thin section analyzed (Tucker, 1988), using thin section photographs and the program JMicroVision. In the petrographic analysis, Q includes monocrystalline, polycrystalline, and microcrystalline quartz, and chert. Sandstones were classified using the scheme proposed by Pettijohn et al. (1987).

As a convention in the lithostratigraphic nomenclature used here, all units are referred to as a group, formation, or member. We do not use lithologic modifiers (e.g., sandstone, shale) or the term tongue to refer to any of the formal Cretaceous lithostratigraphic units discussed here, even though those terms have been

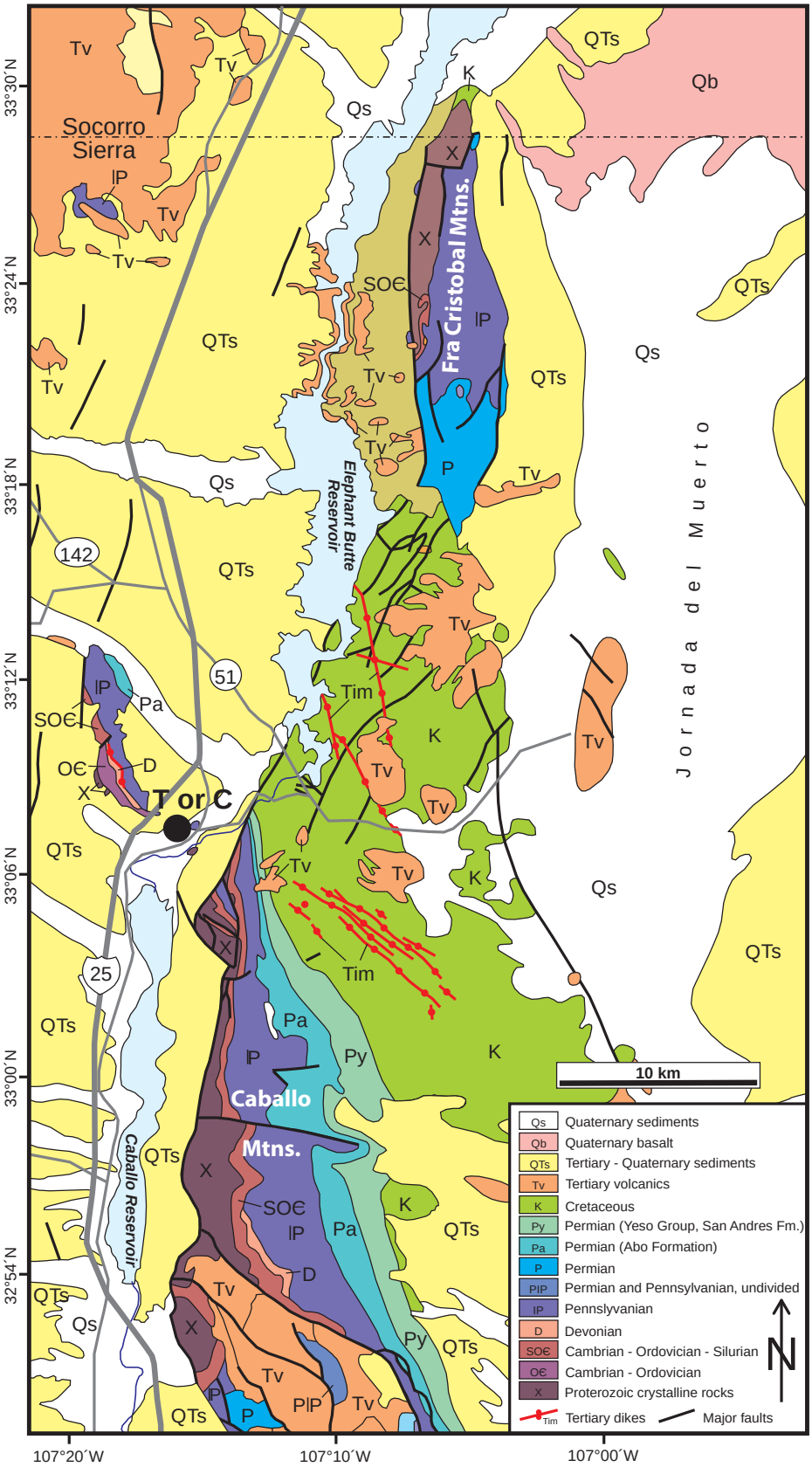

FIGURE 1. Geologic map (after NMBGMR, 2003) showing location of Cretaceous outcrops in central Sierra County, New Mexico.

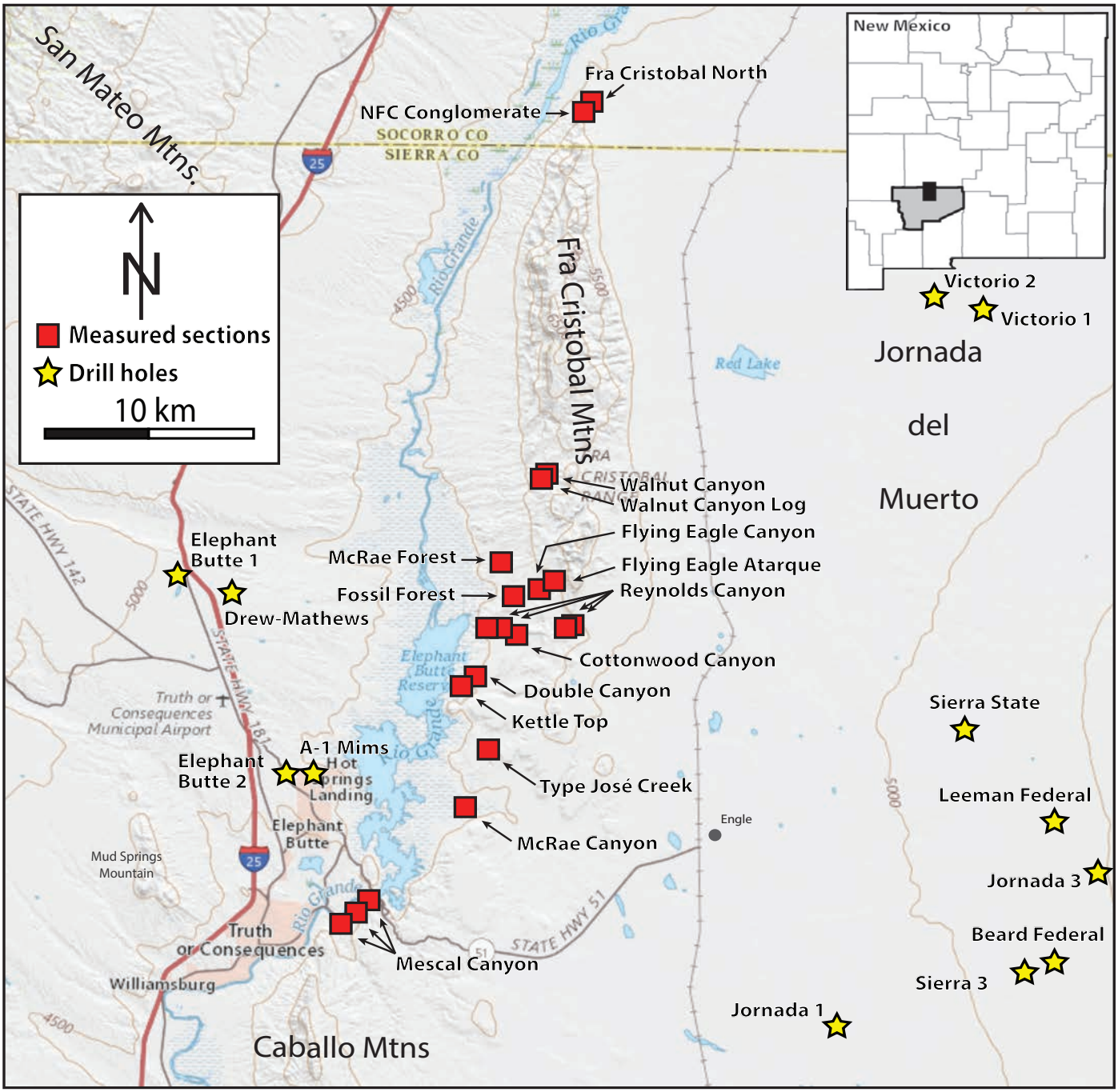

FIGURE 2. Topographic map of part of Sierra County, New Mexico, showing locations of stratigraphic sections measured for this investigation (also see Table A2.1).

used by others. The lithologic modifiers are generally inaccurate—the Mancos Shale, for example, includes lithotypes other than shale. And, the units referred to as "tongues" either do not have that geometry (e.g., the so-called tongues of the Dakota Formation) or their intertongued relationship to other units is inferential and not demonstrable in Sierra County. Therefore, we regard our convention in lithostratigraphic nomenclature as simpler and more accurate than other usages.

Previous studies

The Cretaceous strata of Sierra County have been long studied since shortly after Mexico ceded the territory that is now New Mexico to the United States in 1848. Accounts of these investigations are found in a wide array of government reports, articles in scientific journals, and unpublished theses and dissertations. From these studies, an understanding of diverse aspects of the Cretaceous section has emerged. Previous studies of Cretaceous strata in Sierra County are reviewed in Appendix 1, and the development of stratigraphic nomenclature applied to these rocks is summarized in Figure 3.

Dakota Formation

Lithostratigraphy

Introduced by Meek and Hayden (1861), Dakota is one of the most widely used

stratigraphic names in North America. Keyes (1905a) and Harley (1934) extended the term "Dakota sandstone" into Sierra County, and all subsequent authors have accepted that usage. The Dakota Formation is the stratigraphically lowest Cretaceous unit in Sierra County, cropping out in the southern Fra Cristobal Mountains, at Mescal Canyon and along the eastern front of the Caballo Mountains. At all of its outcrops, the Dakota rests disconformably on the lower Permian San Andres Formation and is overlain by the Mancos Formation. Strata beneath the Dakota along the eastern front of the Caballo Mountains were assigned to the Yeso Formation by Seager and Mack (2003), but other workers interpreted these underlying strata as San Andres Formation (Kelley and Silver, 1952; Lucas and Krainer, 2012).

We measured three stratigraphic sections of the Dakota Formation in Sierra County: (1) a complete section of the unit at Flying Eagle Canyon (Figs. 4A–C, 5A, A3.1); (2) an incomplete section at Reynolds Canyon (Fig. A3.2); and (3) a complete section in Mescal Canyon (Figs. 4D–F, 5B, A3.3). Various thicknesses of the Dakota Formation in Sierra County have been reported, including 24 and 27 m (Melvin, 1963), 49 m (Doyle, 1951), 75 m (Kelley and Silver, 1952), and 2 to 106 m (Bauer, 1989; Seager and Mack, 2003). The sections we measured document Dakota Formation thicknesses of 24 to 39 m. Data from 15 oil-test holes east and west of the Fra Cristobal Range record a thickness range of 18 to 73 m (Table A2.2).

In the southern part of the Fra Cristobal Range, the Dakota is an upward-fining succession of nearly pure quartz sandstone. Color, weathering aspect, and bedding style distinguish the Dakota from any of the Paleozoic sandstones, even in small, fault-bounded exposures. Freshly broken sandstone is nearly white, whereas weathered surfaces are stained pink, magenta, and orange. Grain size decreases from medium to coarse near the base to very fine near the top. Sand grains are rounded and well-sorted. Conglomerate at the base contains cobble-sized clasts of partially silicified, gray San Andres limestone and rounded pebbles of chert, ironstone, and jasper. Medium to thick cross-bedding in the lower part gives way to planar and wavy lamination and thin bedding in the upper part. The contact with the overlying Mancos Formation is gradational through an interval several meters thick. Good exposures of the transition zone may be viewed in the Reynolds Canyon section (Fig. A3.2) and along the southwest-trending arroyo 0.8 km northeast of Bert Cook Well in the western headwaters of Reynolds Canyon (Fig. A4.1).

At Flying Eagle Canyon, the Dakota Formation is 24 m thick and is composed almost entirely of quartzose sandstone and silica-pebble conglomerate (Figs. 4A–C, A3.1). Trough cross-bedding is the prevalent bedform, and a few beds display ripple lamination or tabular bedding. The lowest bed of the Dakota is a trough cross-bedded conglomerate containing chert and other siliceous pebbles. The conglomerate has a scoured base with local stratigraphic relief of up to

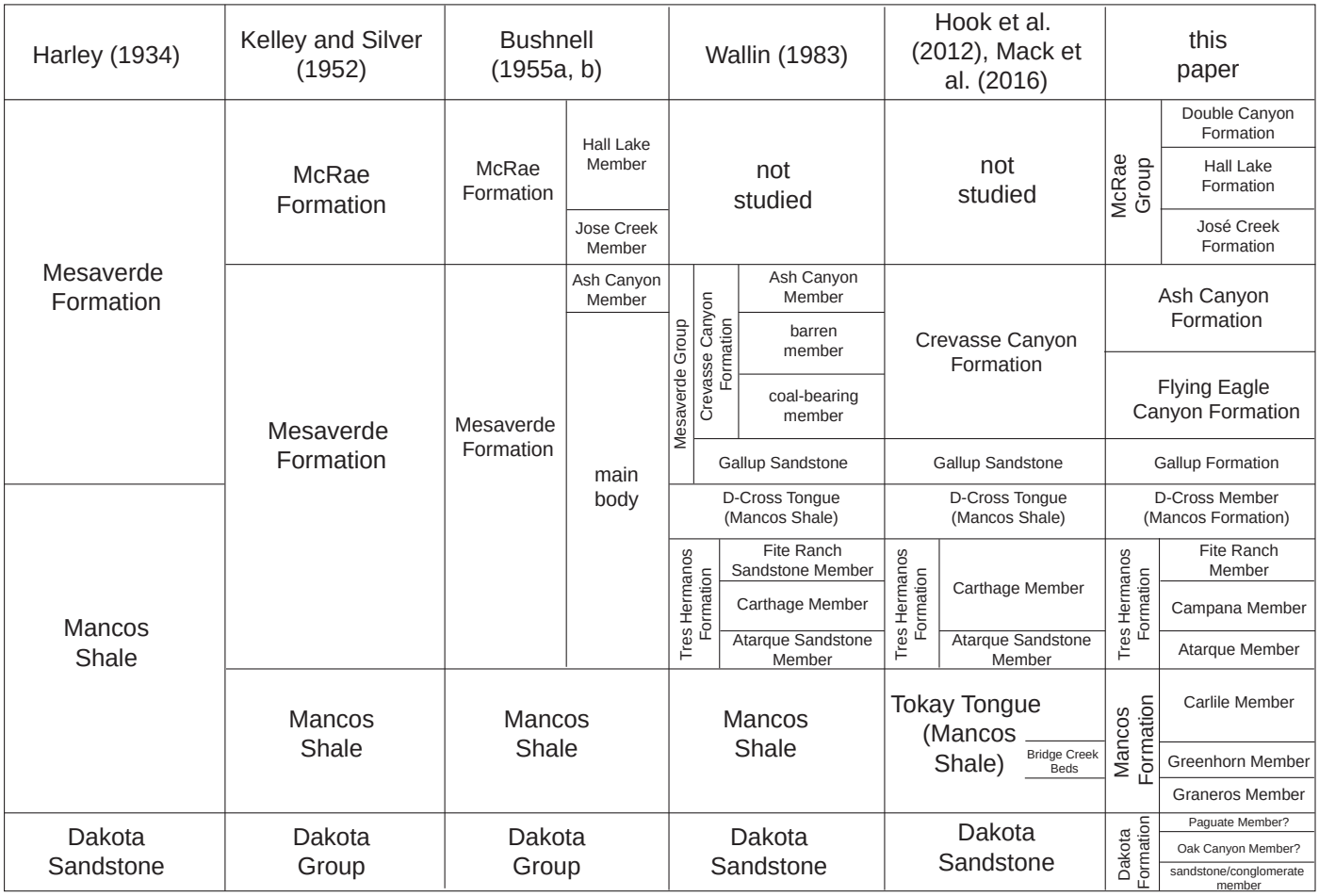

FIGURE 3. Development of Cretaceous lithostratigraphic nomenclature in Sierra County, New Mexico.

2 m on top of the San Andres Formation, and is overlain by trough cross-bedded sandstone with lenses of conglomerate containing chert pebbles. This unit is overlain by fine-grained, ripple-laminated sandstone, horizontally laminated sandstone, trough cross-bedded sandstone, and massive sandstone. The top sandstone bed of the Dakota Formation is conformably overlain by greenish-gray shale at the base of the Mancos Formation.

In Reynolds Canyon, only 7.6 m of the upper part of the Dakota Formation crops out above a fault (Fig. A3.2). These strata are very similar to the upper part of the Dakota Formation strata exposed in Flying Eagle Canyon. However, a significant difference is that the uppermost bed of the Dakota Formation is bioturbated at Reynolds Canyon, whereas it is not at Flying Eagle Canyon.

At Mescal Canyon (Figs. 4D–F, 5B, A3.3), the Dakota Formation is thicker (~39 m thick) and has a very different stratigraphic architecture than in the southern Fra Cristobal Mountains, and this stratigraphic architecture is present at all of its outcrops in the Caballo Mountains (Seager, 1995b, c; Seager and Mack, 2003). It can be divided into three intervals: basal sandstone, medial shale, and upper sandstone. The basal sandstone interval (Fig. A3.3, units 2–5) is 7.5 m thick and composed of trough cross-bedded and horizontally laminated sandstone with much oxidized fossil plant debris (Fig. 4D). The medial sandy shale interval is an ~27 m thick succession dominated by sandy shale and muddy, cross-bedded or bioturbated, thin sandstone beds and lenses (mostly <0.2 m, rarely up to about 1 m) and scattered carbonaceous debris. The uppermost sandstone interval (Fig. A3.3, units 14–16) is ~5 m thick and composed of trough cross-bedded or horizontally

FIGURE 4. Photographs of selected outcrops of the Dakota Formation in Sierra County, New Mexico. A–C, Flying Eagle Canyon section. A, Overview of upper part of Dakota Formation. B, Cross-bedded sandstone. C, Silica-pebble (e.g., quartzite, chert) conglomerate. D–F, Mescal Canyon A section. D, Cross-bedded sandstone near base. E, Overview of upper part of section showing shaley interval of Oak Canyon Member(?) overlain by sandstone beds of Paguate Member(?). F, Crustacean burrows (*Ophiomorpha*) in Paguate Member(?).

laminated sandstone with extensive bioturbation (primarily the well-known crustacean burrows *Ophiomorpha* [Fig. 4F] and *Thalassinoides*). The intensity of bioturbation mostly varies from 10 to 25% using the bioturbation index of Miller and Smail (1997), and has an ichnofabric of 2–3 (cf. Droser and Bottjer, 1986). A few beds, however, are very intensively bioturbated and have an ichnofabric of 5. The bioturbated top of this sandstone interval is very coarsely grained, locally pebbly, and is overlain by gray shale at the base of the Mancos Formation.

The Dakota Formation strata at Flying Eagle and Reynolds canyons are nonmarine sandstone and conglomerate (see below). Such strata are typically referred to as the "main body" of the Dakota Formation (e. g., Landis et al., 1973; Hook and Cobban, 2015). Owen and Owen (2005) renamed the "main body" of the Dakota Formation in northwestern New Mexico the White Rock Mesa Member. This sandstone-dominated unit has coal beds and other carbonaceous strata, unlike the Dakota "main body" in Sierra County. Therefore, we do not use the name White Rock Mesa Member for these Dakota strata in Sierra County and instead refer to them informally as the sandstone/conglomerate member of the Dakota Formation (Figs. 3, A3.3).

The Dakota Formation section at Mescal Canyon resembles part of the intertongued Dakota–Mancos succession in northern New Mexico (e.g., Landis et al., 1973; Lucas et al., 1998b; Head and Owen, 2005). Thus, most of the Dakota Formation section at Mescal Canyon (other than the upper sandstone interval) closely resembles strata of the Oak Canyon Member to the north—gray sandy shale with a few, intercalated thin sandstone beds and scattered carbonaceous debris. The cross-bedded, laminated, and extensively bioturbated sandstone interval at the top of the Dakota section in Mescal Canyon is similar to the Cubero Member, but more closely resembles the Paguate Member of the Dakota Formation to the north.

We note that at many locations in northern New Mexico, not all of the sandstone members of the Dakota Formation are present (e.g., Landis et al., 1973; Lucas et al., 1998b). This lack of continuity is not consistent with early ideas (e.g., Peterson and Kirk, 1977; Owen and Sparks, 1989) that the sandstone members of the Dakota are regressive shoreline deposits and therefore seaward tongues of a landward Dakota lithosome. Instead, the Dakota sandstone members more likely represent offshore sand bodies of discontinuous ridges, bars, and shoals that accumulated during shoreline stillstand in a generally transgressive system. During those stillstands, sand sourced from Laramidia to the west was spread across a broad and shallow shelf (Molenaar, 1983; Head and Owen, 2005). This model of

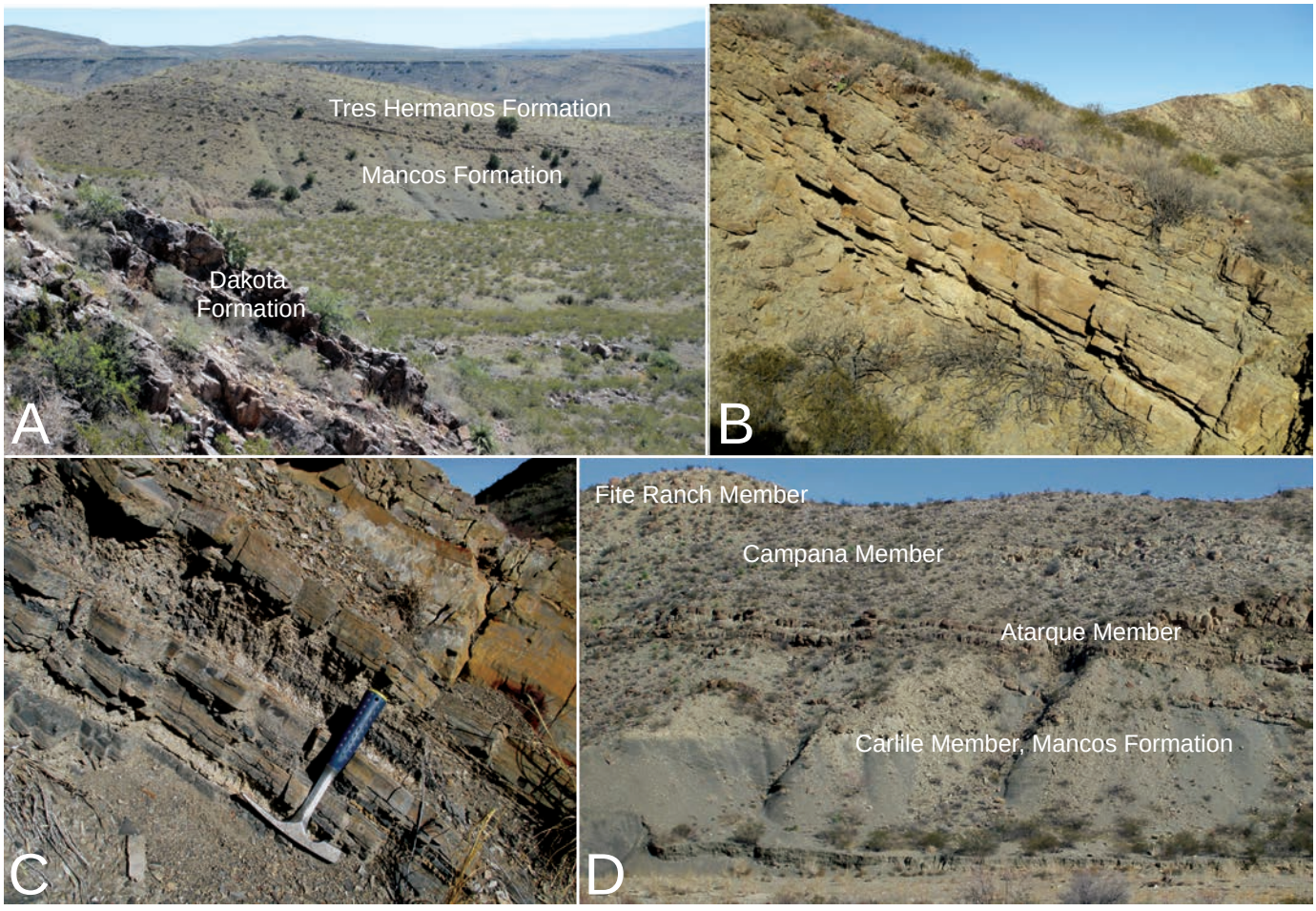

FIGURE 5. Photographs of selected outcrops of the Dakota Formation, lower interval of the Mancos Formation and Tres Hermanos Formation in Sierra County. A, Overview of lower part of Flying Eagle Canyon section looking east. Lower interval of Mancos Formation is slope-forming shale unit below Tres Hermanos Formation. B, Upper, bioturbated sandstone interval of Dakota Formation at Mescal Canyon here assigned to the Paguate Member(?). C, View of light-colored bentonite beds in Graneros Member of Mancos Formation at Mescal Canyon. D, Overview of part of Mescal Canyon A section looking approximately north, showing all three members of the Tres Hermanos Formation.

Dakota deposition needs further analysis, but it does explain why the sandstone members of the Dakota Formation are not continuous across their depositional basin.

Middle Cenomanian fossils of the *Acanthoceras amphibolum* Morrow ammonite zone are present just above the Dakota Formation at Reynolds Canyon and at Mescal Canyon (Hook et al., 2012; also see below), so correlation to the Oak Canyon, Cubero and Paguate members of the Dakota Formation is not contradicted by biostratigraphy (the Cubero and Paguate are in the zone of *A. amphibolum*). The possibility that the upper sandstone interval of the Dakota Formation at Mescal Canyon is the Cubero Member cannot be discounted, though the bedforms and intensity of bioturbation are more characteristic of the Paguate Member (cf. Lucas et al., 1998b). The possible presence of an unconformity at the base of the upper sandstone interval (Mack et al., 2016) and of the "x" bentonite just above the sandstone interval (see below) also supports a Paguate correlation.

Molenaar (1983) tentatively identified the upper sandstone interval of the Dakota Formation in Mescal Canyon as the Twowells Member, but that unit is of late Cenomanian age (ammonite zone of *Calycoceras canitaurinum* [Haas]), so it is too young to correlate to the sandstone interval at the top of the Dakota in Mescal Canyon. Tentative identification of the Oak Canyon and Paguate members of the Dakota Formation in Mescal Canyon (Fig. A3.3) thus is based primarily on stratigraphic position and lithologic resemblance, but not a correlation supported by detailed biostratigraphic data.

Paleontology and age

Other than the trace fossils *Ophiomorpha* and *Thalassinoides* (Fig. 4F), we observed no identifiable fossils in the Dakota Formation in Sierra County. Seager and Mack (2003, fig. 38) reported that fossil oysters are present in the upper part of the medial shale unit of the Dakota Formation at Mescal Canyon.

As already noted, bivalve and ammonite fossils from the lowermost Mancos Formation at Reynolds Canyon and Mescal Canyon are of middle Cenomanian age (Hook et al., 2012), so this sets a minimum age for the Dakota Formation strata. It seems most likely that all of the Dakota Formation strata in Sierra County are of Cenomanian age. However, the lower, nonmarine strata of the Dakota section, as best seen at Flying Eagle Canyon, could be of Early Cretaceous age (cf. Seager, 1981; Lucas and Estep, 1998), though no data support such an age assignment.

Sedimentary petrography

Sandstone of the Dakota Formation in Sierra County (Fig. A5.1A–B) is mostly medium grained and well-sorted, and locally contains a few larger clasts with diameters up to 5 mm, resulting in moderate to poor sorting. Most of the detrital grains are subrounded, but some grains are rounded (Fig. A5.1A–B). Microscopic study confirms the field observation that sandstone of the Dakota is quartz arenite. Monocrystalline quartz (including a few porphyry quartz grains; porphyry quartz is volcanic quartz derived from rhyolite) is the dominant grain type. Polycrystalline quartz is present in small amounts. Chert grains are a common constituent.

The larger grains are different types of microcrystalline quartz (chert), rarely displaying spherulitic texture, which indicates that these grains are derived from acidic volcanic rocks (Fig. A5.1A–B). Rarely, patches of clay minerals are present that most likely represent altered detrital feldspar grains (Fig. A5.1B). The detrital grains are cemented by quartz that is present as well-developed authigenic overgrowths (Fig. A5.1A–B). Locally, some blocky calcite cement is present. All samples plot into the field of quartz arenite (classification schemes of McBride, 1963, and Pettijohn et al., 1987), and the average composition is $Q_{99.7}F_0L_{0.3}$ (see discussion of petrofacies below).

Depositional environments

The Dakota Formation is one of the most widespread lithologic units of the Western Interior Seaway. It records the initial transgression of the Cretaceous seaway across much of New Mexico and thus represents different types of nearshore marine sedimentation. It marks the beginning of the T1 transgression of Weimer (1960; also see Molenaar, 1983), which reflects a major tectonic reorganization of the Cretaceous marine basins of the American Southwest (e. g., Mack, 1987).

As already discussed, the Dakota Formation can be divided into three units at Mescal Canyon. We interpret the lower sandstone unit as composed of fluvial channel-fill sandstones, and the middle part as thin, cross-bedded, channel-fill sandstones and thick estuarine deposits. The upper sandstone unit with abundant burrows is definitely marine, representing nearshore (shoreface) deposits. According to Seager and Mack (2003; also see Bauer, 1989), the lower and middle parts of the Dakota Formation at Mescal Canyon are fluvial deposits divided into channel and floodplain facies with eastward and northeastward paleoflow directions. Bioturbated shale and sandstone (including characteristic marine trace fossils, such as *Ophiomorpha*) near the top of the middle part indicate a marine depositional setting, and the uppermost shale bed is interpreted as lagoonal or estuarine deposits. The overlying sandstones of the upper part of the Dakota Formation display ripple lamination and bioturbation, and have been interpreted as tidal-flat deposits (Seager and Mack 2003), but are more likely shelf sandstones representing shoals and offshore bars (see above). The uppermost very coarse to pebbly sandstone is interpreted as a lag deposit representing a ravinement surface (transgressive lag) (Seager and Mack, 2003).

At Flying Eagle Canyon and Reynolds Canyon, the Dakota Formation is thinner and coarser grained; mudstone is absent. The lower part is composed of fine-grained conglomerate and sandstone, likely representing fluvial channel fills. The middle part is composed of fine-grained sandstone displaying horizontal lamination, ripple lamination and trough cross-bedding, and the upper part is composed of trough cross-bedded sandstone, all likely representing fluvial deposits.

Lower interval of Mancos Formation–Graneros, Greenhorn, and Carlile members

Lithostratigraphy

Cross and Purington (1899) gave the name Mancos Shale to a thick succession, dominantly of shale, overlying the Dakota Formation in the Mancos Valley near the town of Mancos in southwestern Colorado. Subsequently, the name Mancos was extended through large areas of western Colorado, eastern Utah, northeastern Arizona, and New Mexico. The Mancos exhibits large-scale intertonguing relationships with sandstone units that carry a wide variety of names.

The Mancos Formation forms two intervals of the Cretaceous section in Sierra County, a lower interval between the

Dakota and Tres Hermanos formations, and an upper interval between the Tres Hermanos and Gallup formations. The upper interval has consistently been termed the D-Cross Tongue (Molenaar, 1983; Seager and Mack, 2003; Hook et al., 2012), and we refer to it as the D-Cross Member (see below), although some early workers (e.g., Lee, 1907b; Darton, 1928; Harley, 1934) did not recognize an upper interval of the Mancos in Sierra County (Fig. 3). However, more than one name has been applied to the lower interval of the Mancos Formation, including Rio Salado Tongue and Tokay Tongue. This interval includes strata equivalent to and lithologically similar to the Graneros Shale, Greenhorn Limestone, and Carlile Shale of northern New Mexico (Fig. 6), so we apply these names as members to the lower interval of the Mancos Formation in Sierra County.

Hook et al. (1983) defined the Rio Salado Tongue of the Mancos Shale in west-central New Mexico as the shale-dominated stratigraphic unit between the Twowells Tongue of the Dakota Sandstone (below) and the Tres Hermanos Formation or equivalent strata of the Juana Lopez Member of the Mancos Formation (above) (Fig. 6). Hook and Cobban (2015, p. 27) coined the name Tokay Tongue in Socorro County to refer to "that portion of the Mancos Shale between the undifferentiated or main body of the Dakota Sandstone and the Tres Hermanos Formation (or offshore equivalent)" in southern New Mexico (Fig. 6). Rio Salado is a useful term where the Twowells Member of the Dakota Sandstone is present and can be identified with certainty, though the term Graneros Shale Member of the Mancos Shale has been used in a restricted sense to refer to the same interval in the southern San Juan Basin (Head and Owen, 2005; Owen et al., 2007), a usage we do not endorse. A broader use of the term Rio Salado Tongue, to refer to the entire lower interval of the Mancos Formation in Sierra County and southward (Lucas and Estep, 1998; Lucas et al., 2000; Seager and Mack, 2003) was rejected by Hook and Cobban (2015), and we also abandon that usage.

Tokay Tongue, however, is simply a synonym of the unit that Meek and Hayden (1861) long ago named the "Fort Benton group" (more commonly called Benton Group or Benton Shale: Wilmarth, 1928; Cobban and Reeside, 1952) and that has long been abandoned in favor of a more detailed lithostratigraphic terminology. In southeastern Colorado, Gilbert (1896) divided the Benton Group into three units (ascending): Graneros Shale, Greenhorn Limestone, and Carlile Shale, and those names have long been used in northern New Mexico (e.g., Rankin, 1944; Pike, 1947; Kauffman et al., 1969; Coates and Kauffman, 1973; Lucas et al., 1987). Given that the lower interval of the Mancos Formation in Sierra County is readily divided into Graneros, Greenhorn, and Carlile lithosomes (Figs. A3.1–A3.3), those names are used here. In addition, in Socorro County, where the type section of the Tokay Tongue is located, the lower Mancos can be readily divided into Graneros, Greenhorn and Carlile intervals, as was first done by Rankin (1944, p. 21–22, fig. 6) (Fig. 6).

There is another problem with application of the term Tokay Tongue in Sierra County. As originally defined, the base of the Tokay Tongue rests on the "main body" of the Dakota Formation near Carthage in Socorro County (Hook and Cobban, 2015). The "main body" of the Dakota in this area (cf. Hook, 1983; Hook and Cobban, 2015) is very similar to what we are calling the sandstone/conglomerate member of the Dakota in Sierra County. However, in the Caballo Mountains, additional Dakota strata above this member show marine influence and are likely equivalent to part of the intertongued Dakota–Mancos succession to the north (see earlier discussion). Thus, use of the name Tokay Tongue in the Caballo Mountains redefines the base of that unit upward, so it is significantly higher than at the type locality.

Hook and Cobban (1981; also see Cobban et al., 1989) also applied the old name Colorado Formation (or Shale) of White (1878) to essentially the same stratigraphic interval as the Tokay Tongue in southwestern New Mexico, so Tokay is

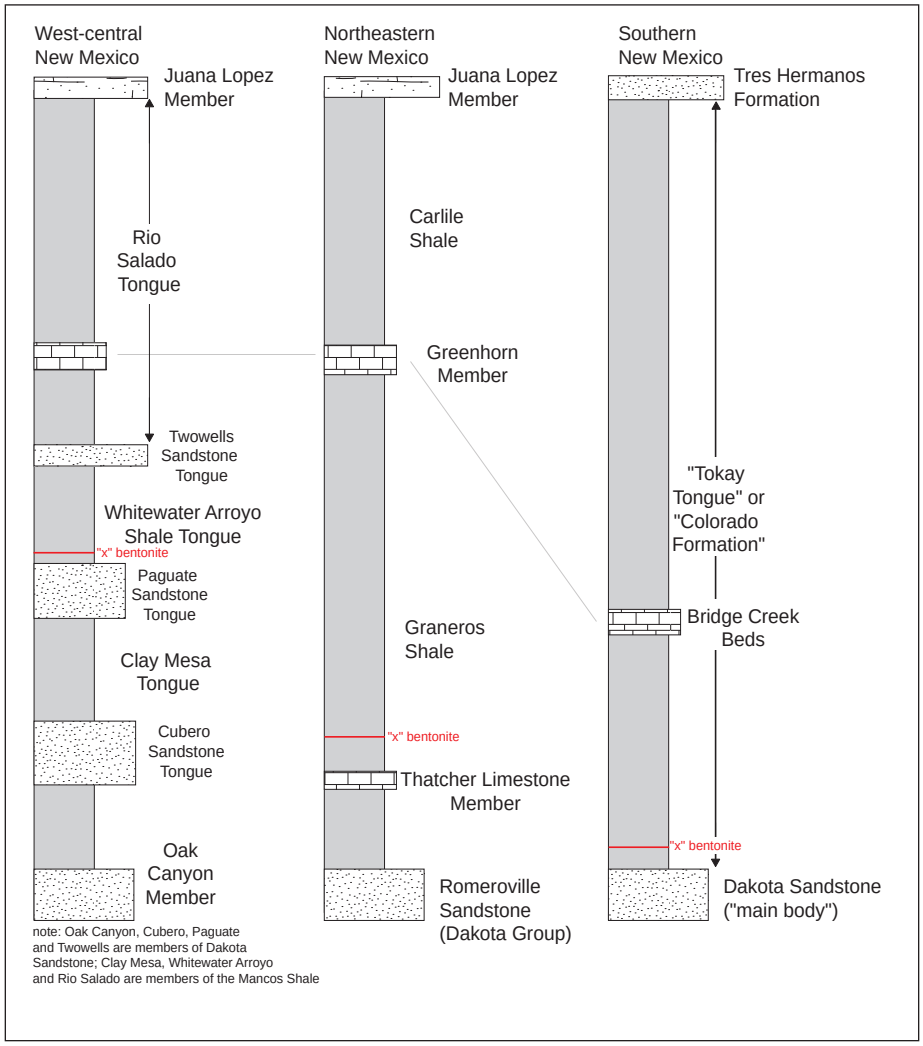

FIGURE 6. Regional stratigraphy of the Dakota–Mancos interval in New Mexico. Left column based on Owen et al. (2007); middle column based on Kauffman et al. (1969); and column on right represents Socorro County and is the nomenclature of Hook and Cobban (2015).

also a synonym of Colorado as used by Hook and Cobban, 1981 (though note that Cobban et al. [2008] did abandon the term Colorado Formation, following Molenaar [1983] and Lucas et al. [2000]). Thus, the Tokay Tongue is both a synonym of unit(s) named long ago, and its use embodies a reduction in stratigraphic precision by applying one name to a stratigraphic interval for which three names already exist and were first applied more than 70 years ago (Fig. 6). Therefore, we recommend the name Tokay Tongue be abandoned.

We also abandon the term "Bridge Creek beds" as used by Hook and Cobban (2015; also see Hook et al., 2012) to refer to the interval we term the Greenhorn Member of the Mancos Formation. This stratigraphic interval correlates to part of the Bridge Creek Member of the Greenhorn Formation on the High Plains, but is not the same unit lithologically or in terms of its lithostratigraphic extent (cf. Hattin, 1975, 1987).

The outcrop distribution of the lower interval of the Mancos Formation in Sierra

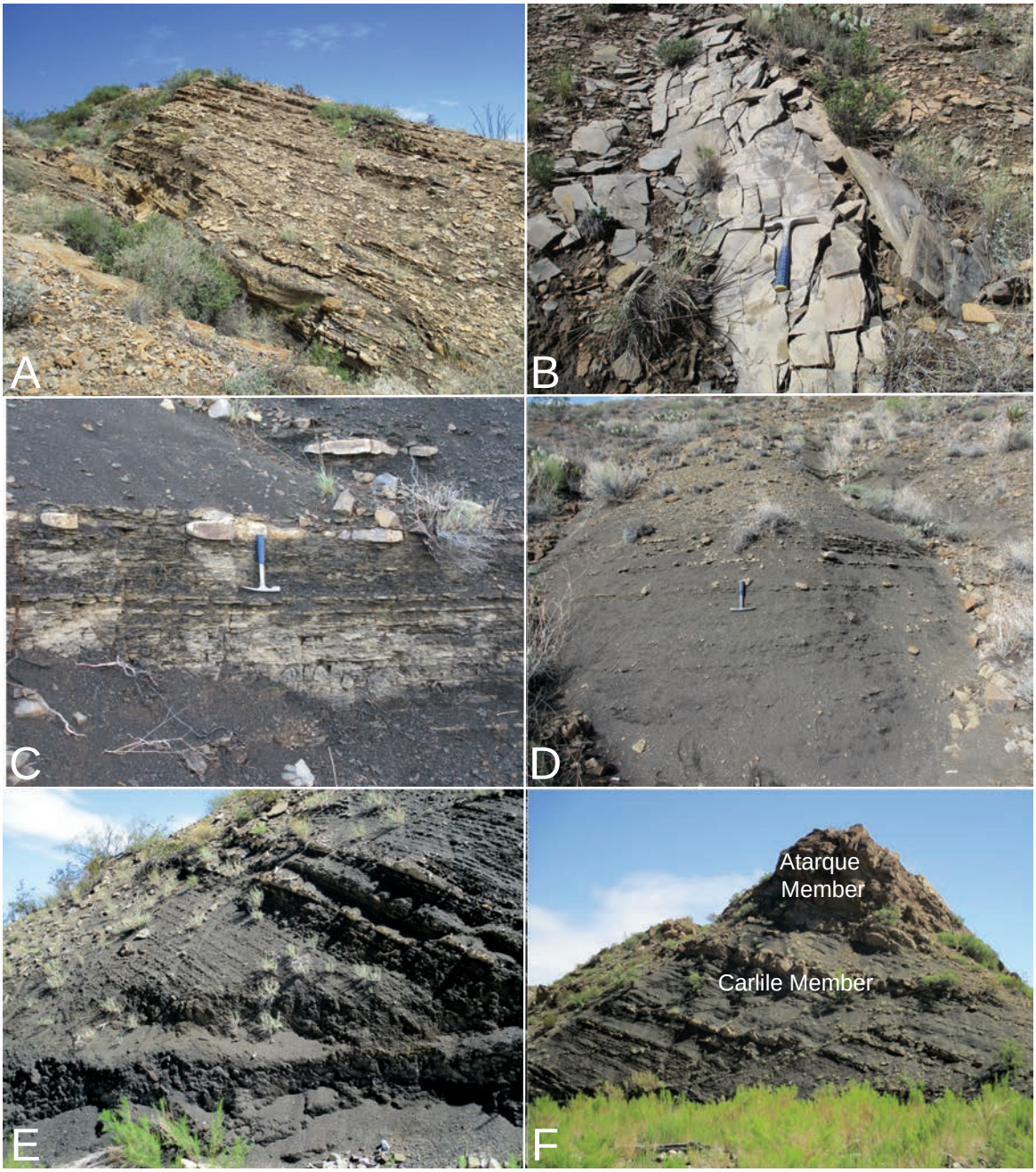

FIGURE 7. Photographs of selected outcrops of the lower interval of the Mancos Formation. A, Mescal Canyon A section, thinly interbedded sandstone and shale/siltstone of the Graneros Member of the Mancos Formation. B, Limestone bed of Greenhorn Member of Mancos Formation in Mescal Canyon A section. C, Limestone of the Greenhorn Member of the Mancos Formation in Flying Eagle Canyon section. D, Shale slope of Carlile Member of Mancos Formation in Flying Eagle Canyon section. E, Cyclically bedded shale of Carlile Member in Mescal Canyon A section. F, Upper part of Carlile Member just below cuesta formed by Atarque Member of Tres Hermanos Formation in Mescal Canyon A section.

County corresponds to that of the underlying Dakota Formation. Naturally, the Mancos is less resistant to erosion than the sandstone-dominated Dakota (below) and Tres Hermanos (above), but many excellent exposures can be found along ravines and canyons flowing to the Rio Grande (e.g., Figs. 5A, D, 7). The lower interval of the Mancos Formation crops out in the southern Fra Cristobal Mountains, at Mescal Canyon in the northern Caballo Mountains, and along the eastern base of the Caballo Mountains. Although relief is lower along the eastern flank of the Caballo Mountains, the Mancos is exposed well enough to be readily mappable on the ground and from aerial images. The lower interval of the Mancos Formation is a shale-dominated unit with a relatively thin, limestone and shale interval in its lower part, the Greenhorn Member. We measured three sections of the lower interval of the Mancos: complete sections at Flying Eagle Canyon (Figs. 5A, A3.1) and Mescal Canyon (Figs. 5C–D, 7, A3.3), and an incomplete section at Reynolds Canyon (Fig. A3.2).

Melvin (1963) reported a lower Mancos Formation thickness of 90 m but estimated it to be as much as 137 m thick southwest of Durham Ranch in the northern Caballo Mountains. Our measured stratigraphic sections indicate that the lower interval of the Mancos Formation is 113–156 m thick in Sierra County, but geometric considerations suggest thickness could be as great as 210 m in the southern Fra Cristobals. Oil-test drilling records suggest a thickness range from 85 to 132 m in central Sierra County (Table A2.2). In our measured stratigraphic sections, the lower Mancos Formation is divisible into a lower, Graneros Member (12–18 m thick), a medial, Greenhorn Member (5–13 m thick) and an upper, Carlile Member (90–136 m thick) (Figs. A3.1–A3.3). The lower, Graneros Member is characterized by gray, sandy and silty shale and interbedded sandstone (Fig. 7A), the Greenhorn by thin limestone beds intercalated with shale (Fig. 7B–C), and the Carlile by black shale with some thin, intercalated sandstone beds, especially in the upper part (Figs. 5D, 7D–F).

Overall, the lower Mancos is a succession of shale and siltstone with some thin, intercalated limestone beds. The basal 10 to 20 m (Graneros) are dark gray, weathering greenish-gray or olive-gray, silt-free to slightly silty, and calcareous. Several beds of orange-weathering bentonite less than 3 cm thick are present (Fig. 5C). The Greenhorn Member consists of shale like that of the Graneros Member, with interbeds and lenses of limestone ranging from a few cm to about 30 cm thick. The thickest limestone beds lie about 20 m above the Mancos base. A molluscan fauna, chiefly inoceramid bivalves, is present (Fig. A6.1D–E). Limestone beds are dark gray, weathering light gray and yellowish gray, and micritic. The thicker limestone beds tend to be concretionary. The upper part of the lower Mancos (Carlile) is silty shale with siltstone becoming increasingly prevalent upward. Siltstone laminae are medium gray, calcareous, and planar to wavy. The lower Mancos generally lacks the large septarian concretions that are conspicuous in the younger D-Cross Member of the Mancos. The contact with the overlying Tres Hermanos Formation is gradational through an interval several meters thick, in which sandstone beds alternate with laminated shale and siltstone (Fig. 7E–F).

At Flying Eagle Canyon, the lower interval of the Mancos is ~113 m thick and is mostly dark gray to black shale intercalated with thin (0.1–0.3 m thick) beds of ripple-laminated or bioturbated sandstone as well as some equally thin beds of sandy limestone and calcarenite (Figs. A3.1). Shale is black, except in the lowermost 2 m, where the color is greenish gray. The black shale contains a few limestone concretions (in units 64 and 68) and septarian concretions (units 69–73) in the upper part. About 18 m above the base is an ~5 m thick interval of limestone beds (0.1 and 0.3 m thick) containing bivalves, intercalated with shale containing thin lenses of limestone, that we identify as the Greenhorn Member. The shale interval below the Greenhorn Member is relatively poorly exposed at Flying Eagle Canyon but does not appear to differ significantly in lithology from shale above the Greenhorn Member.

At Reynolds Canyon (Fig. A3.2), only about 18 m of the lower interval of the Mancos Formation is exposed below a fault. As at Flying Eagle Canyon, limestone beds intercalated with shale about 17 m above the Mancos base are assigned to the Greenhorn Member. Mancos strata below the Greenhorn are gray shale with many thin sandstone interbeds and several thin bentonite layers.

At Mescal Canyon (Fig. A3.3), the lower interval of the Mancos Formation is ~156 m thick. The Greenhorn interval is about 12 m above the base of the lower Mancos in our stratigraphic section, though Hook et al. (2012, fig. 4) showed it as 59 m above the base. The Greenhorn Member is ~13 m thick. The Carlile Member of the Mancos Formation is dominantly black shale with thin intercalations of hummocky, cross-bedded sandstone (one bed, 0.6 m thick), horizontally laminated sandstone (two beds, up to 3 m thick) and many thin sandstone beds (<0.2 m thick, in the upper half). Black shale in the upper part (174–195 m) contains limestone nodules (concretions).

Seager and Mack (2003) drew attention to 5 bentonite beds. These beds are 2–4 cm thick and conspicuous in a 1.2 m thick interval of the Graneros Member (Fig. 5C) to the east of our measured section in Mescal Canyon (at UTM 293695E, 3668087N). Most important is possible identification of one of these bentonite beds near the base of the Graneros Member as the "x" bentonite (Hook et al., 2012). This widespread middle Cenomanian bentonite bed was originally $^{40}Ar/^{39}Ar$ dated at 94.93 ± 0.53 Ma (Obradovich, 1993). This date has been recalculated to 95.53 ± 0.09 Ma, and a $^{206}Pb/^{238}U$ date of 95.87 ± 0.1 Ma has been reported recently (Barker et al., 2011; Schmitz, 2012). In northwestern New Mexico, the "x" bentonite is just above the Paguate Member of the Dakota Formation (e. g., Owen et al., 2005) (Fig. 6). If identification of the "x" bentonite in Mescal Canyon by Hook et al. (2012) is correct, then the Graneros interval at Mescal Canyon is equivalent at least in part to the Whitewater Arroyo Member of the Mancos Formation in northern New Mexico (Fig. 6). This identification also supports correlation of the underlying sandstone interval at the top of the Dakota Formation to the Paguate rather than the Cubero Tongue. A similar bentonite in a similar stratigraphic position in our Reynolds Canyon section (Fig. A3.2) may also be the "x" bentonite, though actual dating or geochemical fingerprinting of these Sierra County bentonites is needed to confirm identification of the "x" bentonite.

Paleontology and age

Brief early mentions of fossils of "Benton age" (equivalent to Cenomanian–Turonian: Cobban and Reeside, 1952) from Sierra County noted by Darton (1928) are likely of invertebrate fossils from the lower Mancos Formation. Fossils from the lower Mancos Formation in Sierra County are primarily of marine bivalves and ammonites. Hook et al. (2012) listed numerous stratigraphic levels with index fossils of middle Cenomanian, late Cenomanian

and early Turonian age in the lower Mancos Formation at Mescal Canyon. Our collections from Flying Eagle and Reynolds canyons are less extensive but document Cenomanian ages in the Graneros and Greenhorn members of the Mancos Formation (Fig. A6.1).

According to the data of Hook et al. (2012), the Cenomanian–Turonian boundary is in the Greenhorn Member in Mescal Canyon. Their data indicate that the Cenomanian *Euomphaloceras septemseriatum* zone is directly overlain by the Turonian *Mammites nodosoides* zone, so six ammonite zones are missing, a substantial hiatus or unconformity within the Greenhorn interval (Mack et al., 2016). However, we observed no physical evidence of an unconformity at this stratigraphic level.

Sedimentary petrography

Thin sandstone beds intercalated in the lower part of the Mancos Formation are fine grained, well-sorted and composed of subangular to subrounded grains. The sandstone contains abundant monocrystalline quartz, and subordinately polycrystalline quartz, chert grains, and many detrital feldspar grains, including plagioclase and untwinned potassium feldspars (orthoclase). Most of the detrital feldspars are slightly altered; some feldspar grains are partly replaced by calcite. The sandstone contains brownish grains that represent altered detrital grains, probably intermediate to basaltic volcanic rock fragments. Rarely, volcanic rock fragments containing plagioclase laths are present, which are derived from intermediate to basaltic volcanic rocks. Other rare grain types are fine-grained metamorphic (phyllitic) rock fragments and micas (biotite and muscovite). The sandstone is cemented by coarse blocky calcite. The sandstones analyzed plot into the field of subarkose (cf. McBride, 1963; Pettijohn et al., 1987); the average composition is $Q_{70}F_{17}L_{13}$ (also see the later section on petrofacies).

Based on field inspection, most limestone in the lower Mancos is lime mudstone. However, one limestone bed of the Greenhorn Member (Fig. A3.1, unit 53) is composed of packstone to rudstone containing abundant echinoderm fragments, subordinately some bivalve shell fragments, many phosphatic fossil fragments (teeth, bones) and a few detrital quartz grains (Fig. A5.1C–D). The sediment is cemented by calcite.

Depositional environments

The lower interval of the Mancos Formation represents the upper part of the T1 transgression and the onset of the R1 regression of the Western Interior Seaway (Molenaar, 1983). The turnaround point is in the Greenhorn Member, which represents highstand of the Western Interior Seaway and possibly the highest sea level of the Cretaceous (e. g., Kauffman and Caldwell, 1993). Thus, the lower interval of the Mancos Formation represents a marine depositional system that is divided into: (1) offshore depositional settings that accumulated shale with intercalated beds of siltstone and fine-grained sandstone (storm layers); and (2) offshore deposits lacking storm layers, deposited below the storm wave base (Mack et al., 2016).

At Mescal Canyon, the gray and black, fissile, fossiliferous shales are marine deposits derived from suspended sediment in an offshore environment below normal wave base. Intercalated fine-grained sandstone beds displaying horizontal lamination, ripple lamination, and rare hummocky cross-bedding are storm layers (Seager and Mack, 2003). Thin limestone beds represent intervals of little clastic sediment input.

The facies of the lower interval of the Mancos Formation at Flying Eagle Canyon differs somewhat from that at Mescal Canyon (Figs. A3.1, A3.3). At Flying Eagle Canyon, the lower interval of the Mancos is composed of shale with abundant thin limestone beds and thin sandstone beds intercalated. Sandstone beds are partly bioturbated, commonly massive and more abundant in the upper part. The thick shale succession with many thin limestone and sandstone beds belongs to the lower offshore facies of Mack et al. (2016). Interpretation of the sandstone beds is difficult as the primary sedimentary structures in many beds were destroyed by bioturbation. The sandstone beds may represent storm layers. At Mescal Canyon, in the lower interval of the Mancos, intercalated sandstone beds, which probably represent storm layers, are more abundant, and limestone beds are rare except in the Greenhorn Member. At both Mescal Canyon and Reynolds Canyon, abundant sandstone beds are intercalated in the Graneros interval of the Mancos below the Greenhorn Member, and these are interpreted to represent storm beds.

The Greenhorn Member is composed of thin limestone beds alternating with shale. Limestone beds are dominantly lime mudstone at Mescal Canyon, indicating deposition from suspension. The thin, partly marly, limestone beds of the Greenhorn interval are autochthonous deposits formed from suspension during periods of little siliciclastic influx. At Flying Eagle Canyon some limestone beds contain abundant shell fragments and are partly echinoderm packstone to rudstone containing bivalve shells, bone fragments and teeth; we interpret these beds as storm layers. Subordinately, thin beds of lime mudstone are also present. Deposition of the Greenhorn Member occurred in an offshore environment near the storm wave base.

Tres Hermanos Formation

Lithostratigraphy

Herrick (1900) gave the name "Tres Hermanos sandstone" to massive yellow sandstone about 23 m thick and lying 45 to 75 m above the Dakota Formation in western Socorro and Valencia counties, New Mexico. He did not mention the origin of the name, but it probably refers to Tres Hermanos Peaks, in sec. 26, T3N, R7W, northwestern Socorro County (Dane et al., 1971). Various authors modified the definition of the unit; Hook et al. (1983) established current usage. Wallin (1983) was the first author to identify the Tres Hermanos in Sierra County (Fig. 3).

The Tres Hermanos Formation crops out in Sierra County at Flying Eagle Canyon (Figs. 5A, A3.4, A3.1) and at the head of Reynolds Canyon (Figs. 8A, A3.4) in the Fra Cristobal Mountains, and at Mescal Canyon in the northern Caballo Mountains (Figs. 5D, 7F, 8B–C, A3.3). In these areas, the Tres Hermanos forms a small hogback, bench, or cuesta between valleys underlain by older and younger shales. We measured the Tres Hermanos to be 42 m and 43 m thick at Flying Eagle and Reynolds canyons, which are closely adjacent, and 75 m thick at Mescal Canyon, about 18 km to the south. Logs of 15 oil-test holes near the Fra Cristobal Range show a thickness range of 60 to 90 m. Hence, the formation appears to thicken toward the southeast in Sierra County.

To the north, in Socorro County, the Tres Hermanos Formation is divided into three formal members: a basal sandstone interval, the Atarque Member, a medial coal-bearing interval, the Carthage Member, and an upper sandstone interval, the Fite Ranch Member (Hook et al., 1983). The same basic strati-

graphic architecture is evident in the Tres Hermanos Formation in Sierra County, so the member names used in Socorro County have also been applied in Sierra County, beginning with Wallin (1983) (Fig. 3). However, it is worth noting that the strata in Sierra County corresponding to the Carthage Member contain very little coal. Thus, Seager and Mack (2003, fig. 43) depicted a single coal bed in the Carthage Member at Mescal Canyon, but this bed is of very local extent. We observed thin layers of carbonaceous mudstone, but no coal in these strata in Sierra County.

An important point is that the name Carthage Member is a preoccupied name and should not have been used for the name of a formal lithostratigraphic unit in New Mexico (use of duplicate names runs contrary to the North American Code of Stratigraphic Nomenclature). Thus, the first use of the place name Carthage for a lithostratigraphic unit in the United States was by Owen (1856), who used the name "Carthage limestone" for a Pennsylvanian-age unit in Kentucky. That name continues to be used in Kentucky, Illinois and Indiana (throughout the Illinois basin) as a formal, member-rank unit (e.g., Jacobson et al., 1985; Shaver et al., 1986). Therefore, the name Carthage Member of Hook et al. (1983) should be abandoned and replaced. Here, we replace it with the name Campana Member, named for the Cerro de la Campana—a set of hills near the abandoned coal-mining community of Carthage in Socorro County, where the type section of the Carthage Member is located.

At Flying Eagle Canyon, we measured two stratigraphic sections of the Tres Hermanos Formation, one is less detailed (Fig. A3.1) and the other more detailed (Fig. A3.4). At the less detailed section (Fig. A3.1), the Atarque Member is 13.5 m thick (Fig. A3.1, units 82–98) and composed of trough cross-bedded sandstone (individual beds 0.3–0.5 m thick), horizontally laminated sandstone (0.9–2.6 m), massive sandstone (0.5–0.7 m), shale (1.1 m), and a few covered (shale) intervals (0.5–1.5 m thick). The top of the Atarque Member is formed by a limy sandstone bed (0.6 m) that contains abundant bivalves (bivalve coquina). At the more detailed section (Fig. A3.4), the Atarque Member is 19 m thick and is also mostly trough cross-bedded sandstone and laminar sandstone with shale interbeds, and its topmost bed is also a bivalve coquina.

The Atarque Member is ~8 m thick at the head of Reynolds Canyon (Fig. A3.4), where it is composed of sandstone lithofacies similar to those at Flying Eagle Canyon. At Mescal Canyon (Fig. A3.3), the Atarque is essentially the same thickness and lithology as at Flying Eagle Canyon. Some sandstone beds of the Atarque Member at Mescal Canyon are very calcareous and weather to large, rounded, concretionary forms, often with coquinoid lenses of bivalve shells.

The overlying Campana Member is about 28–36 m thick at Flying Eagle Canyon, 28 m thick at the head of Reynolds Canyon and 50 m thick at Mescal Canyon. It is a slope-forming unit, comprised mainly of non-fissile mudstone and siltstone that is green, olive, or brownish with a few lenticular bodies of sandstone (0.3–2.7 m thick) that are either crossbedded, laminar bedded, or very calcareous, and weather to a nodular texture. Some mudstone layers are carbonaceous, but no coal layers were observed. At the ghost town of Carthage in Socorro County about 80 km to the north, coal beds in the Campana Member are also less than 1 m thick (Osburn, 1983).

The Campana Member at Flying Eagle Canyon begins with a 9.5 m thick interval (Fig. A3.1, units 99–107) that is composed of brown shale with two thin intercalations of massive sandstone (0.3 and 0.4 m thick) in the lower part and two intercalated beds of horizontally laminated sandstone (0.3 m thick) in the upper part. The overlying interval is approximately 12 m thick (units 108–117) and sandstone-dominated with intercalated shale. Sandstone includes horizontally laminated sandstone (0.4 and 1.8 m thick) and massive sandstone (0.6 and 1.5 m thick). The intercalated shale is brown, and the shale intervals are 1.5–3 m thick.

At the head of Reynolds Canyon (Fig. A3.4), the Campana Member is mostly mudrock with a few thin, intercalated beds of cross-bedded sandstone and more numerous, thin beds of massive sandstone. At Mescal Canyon (Fig. A3.3), the Campana Member is dominantly shale with thin limestone beds (<0.2 m) in the lower part, and sandstone beds (mostly trough cross-bedded sandstone, also planar cross-bedded, ripple-laminated and massive sandstone) in the upper part. Sandstone intervals are up to 2.7 m thick. Seager and Mack (2003, fig. 43) showed the upper 25 m of the Campana Member at Mescal Canyon as "offshore marine" shale with ammonites, but we cannot verify that observation or interpretation. Instead, the upper 25 m of the Campana Member in our Mescal Canyon A section (Fig. A3.3) is shale intercalated with bioturbated sandstone. There are some limestone concretions in the upper part of this interval, and the bioturbation indicates some marine influence on sedimentation. But, if the Fite Ranch Member is the transgressive shoreline of the offshore marine D-Cross Member of the Mancos Formation (see below), it is difficult to conceive how it would also be underlain by offshore marine deposits of the Campana Member.

Capping the Tres Hermanos succession is the Fite Ranch Member, which is 7 to 10 m thick and composed of light-colored, cross-bedded to massive sandstone having a few shale interbeds. At Flying Eagle Canyon (Fig. A3.1), the Fite Ranch Member is 2–7 m thick and consists of sandstone that is cross-bedded, laminar, or massive with some intercalated shale. At Mescal Canyon (Fig. A3.3), the Fite Ranch Member is a thin sandstone unit of dominantly trough cross-bedded sandstone and subordinate massive sandstone, and an intercalated thin mudstone bed. At the head of Reynolds Canyon (Fig. A3.4), the Fite Ranch Member consists mostly of horizontally laminated or massive sandstone beds, and its base is a trough cross-bedded sandstone overlain by a thin, ripple-laminated sandstone.

Paleontology and age

Fossils in the Tres Hermanos Formation are most abundant in the Atarque Member and are marine bivalves and rare gastropods. There are also some fossil oysters in coquinoid lenses in the Atarque and the Fite Ranch members (Fig. 8C). At Mescal Canyon, Hook et al. (2012) identified *Mytiloides mytiloides* in the Atarque Member and used that as the basis for an early Turonian age assignment. The overlying D-Cross Member of the Mancos Formation yields middle Turonian invertebrate fossils (see below) that provide a minimum age for the Tres Hermanos Formation.

Sedimentary petrography

Sandstone of the Atarque Member (Figs. A5.1E–H) commonly is fine to medium grained, well-sorted and consists of subangular to subrounded grains. The most abundant grain type is monocrystalline quartz (including rare porphyry quartz). Subordinate polycrystalline

quartz is present. Chert grains are a common constituent. Detrital feldspar grains are present in moderate amounts and consist of untwinned potassium feldspars, plagioclase, rare microcline and microperthite. Many detrital feldspars are slightly altered. The sandstone also contains fine-grained, brownish grains that represent altered detrital grains, probably volcanic rock fragments. Rare grain types are volcanic rock fragments, fine-grained metamorphic rock fragments, rock fragments composed of quartz and feldspar, micas (muscovite and biotite) and opaque grains. Broken fragments (xenomorphs) of zircon grains are common accessory minerals; less common are grains of greenish tourmaline. One thin section of sandstone from the Fite Ranch Member (Fig. A5.2A) shows that it is similar to the Atarque Member sandstone petrographically.

In some of the sandstone beds, authigenic quartz overgrowths on detrital quartz grains are a common cement type. Other sandstones contain coarse poikilotopic calcite cement that partly replaces detrital feldspar grains. Sandstone containing a few quartz overgrowths and small amounts of matrix are also present. All sandstone samples of the Tres Hermanos Formation are classified as subarkose (cf. Pettijohn et al., 1987). Following the classification of McBride (1963), most samples plot into the field of subarkose, and a few samples into the field of lithic subarkose. The average composition is $Q_{79}F_{15}L_6$ (see discussion of petrofacies below).

Depositional environments

Regionally, the Tres Hermanos Formation represents the upper part of the R1 regression and the lower part of the T2 transgression of the Western Interior Seaway (Molenaar, 1983). Thus, the Atarque Member represents the regressive shoreline facies at the end of R1, and the Fite Ranch Member represents the transgressive shoreline at the beginning of T2. The Campana Member represents fluvio-deltaic deposition landward of these shorelines, and the "turnaround point" between R1 and T2 is within the Campana Member.

According to Seager and Mack (2003), at Mescal Canyon, sandstone of the Atarque Member coarsens upward and grades from sandstone with symmetrical ripples to trough cross-bedded sandstone and sandstone with horizontal lamination. The degree of bioturbation decreases up section (Seager and Mack, 2003). According to these authors, the Atarque Member at Mescal Canyon represents a vertical stacking of lower shoreface deposits (bioturbated sandstone with wave oscillation ripples) to upper shoreface (cross-bedded sandstone with shell hash and vertical burrows) to foreshore deposits represented by horizontally laminated sandstone with vertical burrows.

However, our section of the Atarque Member at Mescal Canyon (Fig. A3.3) and that of Wallin (1983, fig. 7) show a different succession of lithofacies than does the section of Seager and Mack (2003). Our Mescal Canyon section of the Atarque Member shows a lower part with finer-grained, planar and ripple laminated sandstone overlain by an upper part composed of coarser-grained sandstone with trough cross-bedding, wave ripples and bioturbation. Coquina beds are intercalated in the lower and upper parts. Wallin (1983) interpreted the succession as a distributary-mouth bar of the Atarque Member above prodelta sandstone intercalated with shale of the upper part of the Carlile Member. At Flying Eagle Canyon and at the head of Reynolds Canyon, a coarsening-upward trend within the Atarque Member is not visible. The Atarque Member is composed of trough cross-bedded, horizontally laminated, and massive sandstone, alternating with covered (shale?) intervals. Sandstone at the top contains abundant bivalve shells. We interpret the succession as deposits of an upper shoreface to foreshore environment, in agreement with Seager and Mack (2003).

Seager and Mack (2003) interpreted the strongly bioturbated shale of the basal Campana Member above the Atarque Member as lagoonal deposits, the overlying sandstone with root structures and coal as coastal swamp deposits, the overlying thick sandstone as fluvial channels, and the mudstone with thin intercalated sandstone beds above as overbank and crevasse-splay deposits. Wallin (1983, fig. 16) interpreted the lower 6 m of the Campana Member as interdistributary bay and lacustrine deposits, overlain by fluvial channel, crevasse-splay and overbank floodplain deposits, and we concur with his interpretation.

Sandstones of the Fite Ranch Member were interpreted as lower shoreface deposits by Seager and Mack (2003). The uppermost sandstone of the Fite Ranch Member was posited to be a transgressive lag, which defines the flooding surface that separates the Tres Hermanos Formation from the overlying D-Cross Member of the Mancos Formation (Seager and Mack, 2003). Wallin (1983, fig. 18) considered the Fite Ranch Member to be transgressive coastal barrier deposits, a reasonable interpretation.

Mancos Formation–D-Cross Member

Lithostratigraphy

Dane et al. (1957) gave the name "D-Cross Tongue of Mancos Shale" to a shale-dominated unit overlying the Tres Hermanos Formation in the vicinity of D-Cross Mountain in northwestern Socorro County. Wallin (1983) extended recognition of the D-Cross into Sierra County.

Thus, the upper part of the Mancos Formation in Sierra County is the D-Cross Member, a 95–146 m thick interval of mostly gray and greenish-gray shale intercalated with some prominent sandstone beds, especially in its upper half. In Mescal Canyon, Hook et al. (2012) assigned these sandstone beds to the Gallup Formation. However, from the point of view of mappable lithostratigraphy, these sandstones are in a shale-dominated interval better assigned to the D-Cross Member (also see Molenaar (1983) and Seager and Mack (2003), who assigned these sandstones to the D-Cross.)

The D-Cross is an upward-coarsening succession of shale and siltstone, with much sandstone in the upper part. The shale is dark gray, weathering olive-gray, and changes from soft and flaky, calcareous clay-shale in the lower part to weakly laminated, silty shale in the upper part. Laminae and thin interbeds of siltstone and very fine sandstone increase in abundance upward. The most distinctive feature of the D-Cross is large septarian concretions that range up to a meter across and are composed of dark gray, dolomicritic limestone that weathers rusty orange. Ammonites and other marine fossils are present in some of these concretions.

In our two complete measured sections, the D-Cross is 95 m thick at Flying Eagle Canyon (Fig. A3.1) and 146 m thick at Mescal Canyon (Fig. A3.3), about 18 km to the south. Logs of eight oil-test holes suggest a thickness range from 62 to 165 m.

We measured three stratigraphic sections of the D-Cross Member: a complete section at Flying Eagle Canyon (Fig. A3.1) and another at Mescal Canyon (Fig. A3.3), and an incomplete section at the head of

Reynolds Canyon (Fig. A3.4). At Flying Eagle Canyon (Fig. A3.1), the lower part of the D-Cross Member (units 124–134) is 34.5 m thick and consists of shale with intercalations of trough cross-bedded sandstones that are lenticular, with a maximum bed thickness of 0.6 m; two thin beds (each 0.1 m thick) of massive sandstone; thin sandstone lenses intercalated in shale (unit 130); shale containing large sandy limestone concretions with oyster shells (0.4 and 1.5 m thick); and greenish-gray shale intervals (1.5–11 m thick). The upper part of the D-Cross Member is 60.5 m thick and composed of shale (individual shale intervals are up to 20 m thick), and intercalated sandstone units that are thicker than sandstone beds in the underlying, lower part of the D-Cross Member. The following sandstone lithotypes are present: trough cross-bedded sandstone; horizontally laminated sandstone; massive sandstone; rare, ripple-laminated sandstone; two oyster beds (coquina) in the upper part; and shale intervals (up to 20 m thick). The shale of unit 137 contains large limestone concretions.

At the head of Reynolds Canyon (Fig. A3.4), an incomplete section of the D-Cross Member is about 57 m thick. Here, the lower D-Cross is almost entirely greenish-gray shale with scattered limestone concretions, except for three thin (0.3–0.7 m thick), persistent beds of concretions, one with ammonites (unit 40).

At Mescal Canyon (Fig. A3.3), the lower 30 m of the D-Cross Member is mostly shale, whereas the upper 60 m include sandstone units (up to 8.1 m thick) alternating with shale and siltstone. The dominant sandstone lithofacies is trough cross-bedded sandstone (Fig. 8E), and, subordinately, horizontally laminated, planar cross-bedded, and massive sandstone. Several horizons are intercalated that contain large sandy limestone concretions (0.2–1.2 m in diameter). Some siltstone (units 76 and 78) and shale (units 88 and 94) intervals also contain concretions. Stratigraphically high in the member, an oyster coquina (0.3 m) is intercalated in shale (unit 93).

Paleontology and age

Cope (1871) named a mosasaur, *Liodon dyspelor,* based on bones supposedly collected "from the yellow beds of the Niobrara epoch of the Jornada del Muerto, near Fort McRae, New Mexico" (also see Cope, 1875; Russell, 1967). However, as Parris et al. (1997) demonstrated, the published provenance of this fossil was incorrect; it actually came from the Niobrara Formation of Kansas.

Kennedy et al. (2001, fig. 118) illustrated a specimen of the ammonite *Prionocyclus germari* collected from the D-Cross Member in Mescal Canyon. Also, at Mescal Canyon, Hook et al. (2012) listed an ammonite assemblage stratigraphically low in the D-Cross Member with *Coilopoceras inflatum, Hourcquia mirabilis* and *Prionocyclus macombi.* This is a "Juana Lopez age" assemblage of middle Turonian age. In strata they assigned to the lower part of the Gallup Formation, but that we include in the D-Cross Member, Hook et al. (2012) listed ammonites of the *Prionocyclus novimexicanus* and *P. germari* zones of Turonian age.

We collected bivalves and ammonites from the D-Cross Member at both Flying Eagle and Reynolds canyons (Figs. A6.2, A6.3) that are of Turonian age. These will be published more extensively elsewhere. The lower D-Cross includes the bivalves *Cameleolopha bellaplicata* (Shumard) and *Inoceramus dimidius* (White), and the ammonites *Coilopoceras inflatum* and *Prionocyclus macombi* (Meek), whereas the upper D-Cross contains the ammonite *Prionocyclus germari*, confirming the records reported by Hook et al. (2012).

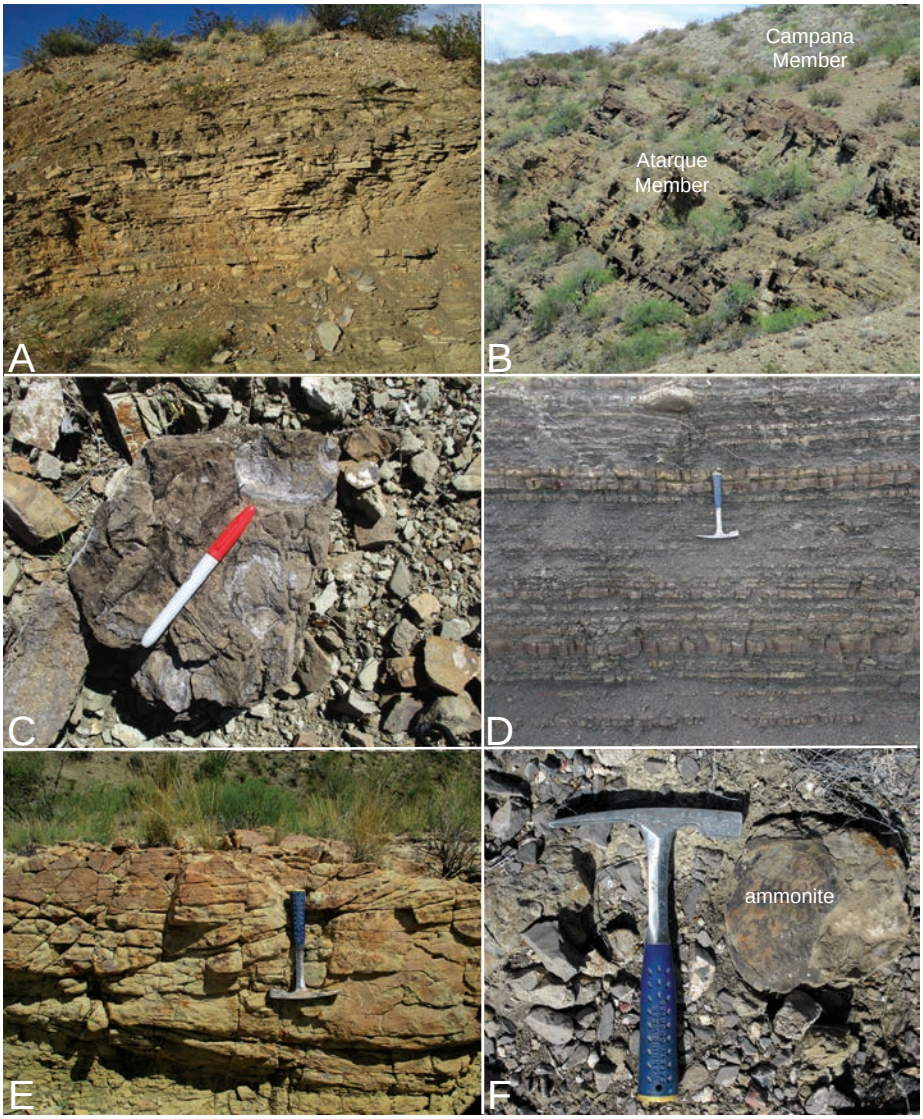

FIGURE 8. Photographs of selected outcrops of the Tres Hermanos Formation and D-Cross Member of the Mancos Formation in Sierra County. A, Lower part of Atarque Member at section at head of Reynolds Canyon. B, Atarque Member and lower part of overlying Campana Member at Mescal Canyon. C, Fossil oysters in Atarque Member at Mescal Canyon. D, Well exposed, cyclically bedded shale of D-Cross Member of Mancos Formation at Flying Eagle Canyon section. E, Sandstone bed stratigraphically high in D-Cross Member at Mescal Canyon. F, Ammonite fossil (*Coilopoceras inflatum*) in D-Cross Member at Flying Eagle Canyon. Rock hammer is 28 cm long.

FIGURE 9. Photographs of selected outcrops of the Gallup Formation at Mescal Canyon (A) and Flying Eagle Canyon (B).

Sedimentary petrography

In the D-Cross Member of the Mancos Formation, fine-grained sandstone is well-sorted and has a composition similar to the thin sandstone beds intercalated in the lower Mancos Formation and in the Tres Hermanos Formation: abundant monocrystalline quartz, subordinately polycrystalline quartz, chert grains, many detrital feldspar grains, altered brownish grains, and rare volcanic and metamorphic (phyllitic) rock fragments (Fig. A5.2B). The detrital grains are cemented by coarse blocky calcite; rarely, quartz grains display authigenic overgrowths of quartz. Sandstone samples from the D-Cross Member plot into the field of subarkose (cf. Pettijohn et al., 1987) or subarkose to lithic subarkose (cf. McBride, 1963). The average composition is $Q_{72}F_{16}L_{12}$.

Depositional environments

Regionally, the D-Cross Member represents the upper part of the T2 transgression and the lower part of the R2 regression of the Western Interior Seaway (Molenaar, 1983). Seager and Mack (2003) suggested that maximum water depth (the "turnaround point") is near the middle of the D-Cross, just below where thick sandstone beds are present (this would be unit 139 or 142 in our Flying Eagle Canyon section: Fig. A3.1; and unit 78 in our Mescal Canyon section: Fig. A3.3).

We infer that D-Cross shale beds without sandstone intercalations are offshore marine muds deposited below wave base. Dark gray, fissile shales that locally contain concretions and intercalated fine-grained sandstone beds with horizontal burrows and scattered bivalve shell fragments of the upper part of the D-Cross Member at Mescal Canyon are interpreted here as lower shoreface deposits. Thicker sandstone units displaying trough cross-bedding may represent upper shoreface deposits.

Gallup Formation

Lithostratigraphy

Sears (1925) named the "Gallup sandstone member of the Mesaverde formation" for the town of Gallup in northwestern New Mexico. Wallin (1983) was the first to assign strata to this unit in Sierra County. Because lithology and stratigraphic relationships here are a good match for those in the Gallup area, we accept and continue this usage, as have others (e.g., Seager and Mack, 2003; Hook et al., 2012; Mack et al., 2016).

In central Sierra County, the Gallup Formation is well exposed at Flying Eagle Canyon (Fig. A3.1) and at Mescal Canyon (Fig. A3.3). At both locations it is a prominent, light-colored interval of tabular bedded, bioturbated and cross-bedded sandstone with minor shale intercalations (Fig. 9). Unweathered colors are white and very pale orange, and weathered colors are moderate brown and light brown. The section of the Gallup Formation at Mescal Canyon we measured is ~32 m thick. At Flying Eagle Canyon the Gallup Formation is 19 m thick. These values compare to a range of 6 to 30 m in five oil-test holes.

At Flying Eagle Canyon (Fig. A3.1), the Gallup Formation is mostly sandstone. In the lower part, trough cross-bedded and horizontally laminated sandstone are present; the upper part is composed of finer-grained, horizontally laminated and massive sandstone. One coquina bed is intercalated in the middle of the formation. Shale is rare and intercalated

in the lower and middle parts of the Gallup Formation.

At Mescal Canyon (Fig. A3.3), the Gallup Formation is mostly composed of sandstone and minor shale and three coquina beds (each 0.3–0.6 m thick). Sandstone lithofacies are horizontally laminated, trough cross-bedded, ripple laminated, bioturbated, or massive. Trough cross-bedded sandstone contains abundant bivalve shells and shell fragments.

Paleontology and age

At Mescal Canyon, Hook et al. (2012) listed the bivalves *"Lopha" sannionis* (White), *Crassostrea glabbra* (Meek and Hayden), *Inoceramus cuvieri* (Sowerby), and *Mytiloides incertus* (Jimbo) from the Gallup Formation. They assigned the Gallup Formation to the *Prionocyclus germari* (Reuss) ammonite zone of late Turonian age, largely because *Mytiloides incertus* is not known from strata younger than the *P. germari* zone (Hook et al., 2012).

In Flying Eagle Canyon, we collected *"Lopha" sannionis* from the lower part of the Gallup Formation. Fragments of bivalves, fossil logs, and shark's teeth are also present locally.

Sedimentary petrography

Sandstone of the Gallup Formation (Fig. A5.2 C–F) is mostly fine to medium grained, moderately to well-sorted, and grains are dominantly subangular. The mineralogical composition is similar to sandstone of the Atarque Member of the Tres Hermanos Formation and consists mainly of monocrystalline quartz, subordinately polycrystalline quartz, many chert grains, many detrital feldspar grains, small amounts of volcanic rock fragments containing plagioclase laths, fine-grained brownish altered grains, rare fine-grained metamorphic rock fragments, and rare grains displaying spherulitic texture (derived from acidic volcanic rocks). Other rare grains include micas (muscovite and biotite), opaque grains, and zircon. Sandstone is cemented by coarse, blocky, partly poikilotopic calcite cement. Locally, authigenic quartz overgrowths on detrital quartz grains and small amounts of matrix are present.

Sandstone samples of the Gallup Formation are subarkose to sublitharenite according to the classification of Pettijohn et al. (1987) and subarkose, lithic subarkose and sublitharenite according to McBride (1963) The average composition is $Q_{78}F_{11}L_{11}$ (also see the section below on petrofacies).

Depositional environments

The Gallup Formation represents the shoreline of the R2 regression of the Western Interior Seaway (Molenaar, 1983). According to Molenaar (1973, 1974), in northern New Mexico the Gallup Formation is a succession of coastal barrier, strand plain or delta-front sandstones that grade seaward into offshore marine mudstone of the Mancos Formation and landward into nonmarine or brackish coastal-plain deposits of the coal-bearing Dilco Member of the Crevasse Canyon Formation.

At Mescal Canyon, Seager and Mack (2003) interpreted the upper part of the D-Cross Member and lower to middle parts of the Gallup Formation as prodelta, delta-front and distributary-mouth bar deposits, respectively. Coquina beds (oyster-bearing sandstones) above the distributary-mouth bar sandstones are interpreted by them as deposits of brackish bays on the lower delta plain. The upper part of the Gallup Formation is interpreted as delta-front deposits, over- and underlain by channel sandstones that probably represent distributary channels, tidal channels or estuaries (Seager and Mack, 2003). Wallin (1983, fig. 21) interpreted Gallup deposition as a progression upward from lower shoreface to upper shoreface deposits, capped by foreshore sandstones.

Flying Eagle Canyon Formation

Lithostratigraphy

In Sierra County, beginning with Harley (1934), much of the Cretaceous section above the lower Mancos or above the Tres Hermanos Formation has been assigned to the Mesaverde Formation (or Group) (Fig. 3). Seeking to introduce greater precision, Wallin (1983) introduced the term Crevasse Canyon Formation for these strata, and most subsequent authors followed suit. However, we find both Mesaverde and Crevasse Canyon to be inappropriate names for these strata in Sierra County, and propose to substitute locally derived names.

Mesaverde Formation (or Group) was originally the "Mesa Verde group" of Holmes (1877), named after the well-known mesa east of Cortez in southwestern Colorado. Holmes (1877) recognized three informal units in his "Mesa Verde group," and Collier (1919) named them the (ascending): Point Lookout Sandstone, Menefee Formation, and Cliff House Sandstone. These are strata of early-middle Campanian age, between the Montezuma Valley Member of the Mancos Formation below and the Lewis Formation above (e.g., Leckie et al., 1997). Thus, a strict application of the name Mesaverde should be as a group-rank unit to encompass these strata and their homotaxial (essentially correlative) strata to the south (e. g., Reeside, 1924).

In early, mostly reconnaissance-level work, Mesaverde Formation (or Group) was a useful lithostratigraphic term to apply to a substantial portion of the Cretaceous section in Sierra County when the architecture of that section was not understood in detail and its correlation remained imprecise. Now, we have progressed beyond such a general understanding, so a broad term like Mesaverde is no longer needed for Cretaceous strata in Sierra County.

Crevasse Canyon Formation has also been applied to much of the Cretaceous section in Sierra County, as a virtual synonym of earlier uses of Mesaverde (Fig. 3). However, the typical Crevasse Canyon Formation strata of west-central New Mexico have a very different stratigraphic architecture and lithologic content than do the strata termed Crevasse Canyon in Sierra County. Thus, the Crevasse Canyon in west-central New Mexico has two substantial intervals characterized by interbedded sandstone, siltstone, and mudstone containing thick, economically important coals: its basal Dilco Member and uppermost Gibson Member. This is quite different from the strata termed Crevasse Canyon Formation in Sierra County, which lack the thick coal zones, so use of the name Crevasse Canyon here is abandoned. The stratigraphic architecture observed in Sierra County, a lower mudstone-dominated unit and an upper sandstone-dominated unit with quartz and chert pebbles near the top, is a poor fit for the type Crevasse Canyon.

An excellent, locally derived name, Ash Canyon, already is available for the upper part of the "Crevasse Canyon" succession in Sierra County. For the lower part, only informal terms such as "coal-bearing member" and "barren member" have been applied previously. For the purpose of recent geologic mapping in the area, Cikoski et al. (2017) used the term "unit of Flying Eagle Canyon" for the lower unit.

We thus propose the term Flying Eagle Canyon Formation to refer to strata previously included in the lower part of the Mesaverde Formation (Group) in Sierra County (Fig. 3). The name is in reference to Flying Eagle Canyon in the southern Fra Cristobal Mountains, where the type section of the formation was measured (Fig. A3.1).

Recognition of (and in several cases, quadrangle-scale mapping of) the lithostratigraphic units we term Flying Eagle Canyon and Ash Canyon formations (see below) can be found in earlier work on the Cretaceous of Sierra County (e.g., Melvin, 1953; Mack and Seager, 1993; Seager, 1995b, c) that recognized that the "Mesaverde" or "Crevasse Canyon" strata can be divided into a lower, mudrock-dominated unit, and an upper, sandstone/conglomerate-dominated unit. Melvin (1963) termed these the Cuesta Pelado and Mescal Creek formations, but these names were never published. Seager (1995b, c) termed the lower unit the "main body" of the Crevasse Canyon Formation and the upper unit the Ash Canyon Member. The simplest nomenclatural approach here is to name the lower unit and, as did Seager (1995b, c), expand the concept of the Ash Canyon Member of Bushnell (1955a) to encompass the upper unit.

The Flying Eagle Canyon Formation is composed of non-fissile mudstone, siltstone, and lenticular to tabular bodies of weakly cemented sandstone. These strata erode to slopes and valleys, in contrast to the light-colored Gallup Formation below and the sandstone-dominated Ash Canyon Formation above. Thus, these formations are readily differentiated on the ground and in aerial imagery. Under various names, the Flying Eagle Canyon Formation appears as a mapping unit on several 1:24,000 scale geologic maps (Lozinsky, 1985; Mack and Seager, 1993; Seager, 1995b, 2007; Seager and Mack, 2005; Cikoski et al., 2017), and we are using it thus in a forthcoming geologic map of the Fra Cristobal Range.

With fair certainty, the Flying Eagle Canyon Formation can be identified on the logs of several oil-test holes drilled in northern Sierra County. However, only two of these completely penetrated the unit. Thus, the Flying Eagle Canyon Formation is about 120 m thick in the Summit #A-1 Mims test, drilled about 8 km north of Truth or Consequences, and 221 m thick in the Beard Oil #1 Jornada del Muerto test hole, drilled about 10 km southeast of Engle (Table A2.2). These thicknesses compare to 151 m measured at the type section and 480 m at Mescal Canyon. The relatively thin type section of the Flying Eagle Canyon Formation could reflect depositional thinning, an unconformable contact with the overlying Ash Canyon Formation, or tectonic thinning of the section not obvious in the field, or a combination of two or more of those causes.

The Flying Eagle Canyon Formation is mostly fine-grained strata with subordinate fine- to medium-grained sandstone intervals that are light gray, pale yellow, and light olive-gray. Fine-grained strata are composed of olive-gray to light olive-gray mudrock (mudstone, siltstone and shale) interbedded with very fine- to fine-grained sandstone. Sparse, impure coal is present close to the base. Mudstone and siltstone is largely dark green to olive, but some layers are dark red, purplish gray, and ochre yellow. Layering is absent to weakly developed in fine strata, but relatively thin (<1 m thick) interbeds of very fine- to fine-grained sandstone are commonly present; these interbeds variably exhibit horizontal laminations, ripplemarks, root traces, or burrows (Seager and Mack, 2003). Sandstone-dominated strata rarely exceed 15 m in thickness and are channel-fill complexes that are single- to multistorey (seldom more than two storeys), generally less than 6 m in overall thickness. The sandstone is in thin to very thick, tabular to lenticular beds that are internally cross-bedded (lithofacies St, Sp); medium to very thick beds commonly correspond to a single-storey channel-fill body, with tangential or planar foresets, and trough cross-bedding is commonly observed. Some sandstones are horizontal-planar laminated (Sh), ripple laminated (Sr), or massive (Sm). Paleoflow directions indicated on the Cikoski et al. (2017) map, based on trough orientations, are toward the north and east, which agrees with the findings of Wallin (1983). The sand is fine to medium grained, subangular (only a few subrounded grains) and well-sorted (unit description modified from Cikoski et al., 2017).

Impure coal is present at or within a few meters of the base of the Flying Eagle Canyon Formation (Fig. 10A–B). Carbonaceous layers up to about 30 cm thick are visible in the type section and also in the south bank of Reynolds Canyon, southeast of Bert Cook Well (Fig. A4.1). Coal is also present at about the same stratigraphic position in the Cutter sag, and formerly was mined on a small scale (Wallin, 1983).

The Flying Eagle Canyon and Tres Hermanos formations contain a similar suite of lithologies and can be difficult to distinguish when encountered in fault blocks. The most diagnostic features of the Flying Eagle Canyon, lacking in the Tres Hermanos, are giant (commonly 2 to 3 meters across) sandstone concretions that weather dark brown. The Flying Eagle Canyon Formation might also be mistaken for the younger José Creek Formation, but on close inspection, most sandstone in the latter unit contains a high proportion of volcanic rock fragments, and quartz is at most a minor constituent. Sandstone of the Flying Eagle Canyon Formation contains abundant quartz and much pink feldspar, but lacks volcanic clasts. Some poorly preserved plant stems and roots and a few pieces of silicified wood are present in the Flying Eagle Canyon Formation, but wood is far less common than in the overlying Ash Canyon Formation.

At the type section (Fig. A3.1), the Flying Eagle Canyon Formation is 151 m thick and can be divided into two intervals: (1) sandy lower part, approximately 82 m thick (Fig. A3.1, units 169–212); and (2) mudstone-dominated upper part, approximately 69 m thick (Fig. A3.1, units 213–230). In the lower part, sandstone forms thin (0.1–0.3 m) beds and lenses (Sh, Sm), and thicker sandstone units (up to 3.7 m thick) composed of trough cross-bedded sandstone (St), horizontally laminated sandstone (Sh), ripple-laminated sandstone (Sr), and shale intervals (Fm). The upper part is mostly shale (Fm) with a few intercalated sandstone units that are 0.1–1.2 m thick: massive (Sm), horizontally laminated (Sh), and ripple-laminated sandstone (Sr), and rare trough cross-bedded sandstone (St). Shale units are 1 m to more than 25 m thick.

The Fossil Forest section (Figs. 11A, A3.6) encompasses about 85 m of the upper part of the Flying Eagle Canyon Formation. The base of the formation is not exposed, but the overlying contact with the Ash Canyon Formation is well exposed. The exposed Flying Eagle Canyon strata are mostly shale (54% of the measured thickness) and somewhat less sandstone (46%). Most of the sandstone beds are trough cross-bedded, but some are laminar, and a few are massive or bioturbated.

In the Mescal Canyon B section (Figs. 10B, A3.5), the Flying Eagle Canyon succession is composed of alternating shale and sandstone, and rare conglomerate

FIGURE 10. Photographs of selected outcrops of the Flying Eagle Canyon Formation. A, Basal coaly beds overlain by channel sandstone, Flying Eagle Canyon. B, Basal coal bed at Mescal Canyon. C, Cross-bedded sandstone, Mescal Canyon. D, Calcareous sandstone, Mescal Canyon. E, Gray shale with ironstone beds, Mescal Canyon.

and coal beds. Two thin coal beds (units 3 and 5), each 0.3 m thick, are intercalated in brown shale near the base of the Flying Eagle Canyon Formation. Another thin coal bed (unit 68, 0.3 m thick) is developed on top of a sandstone interval about 224 m above the base (Fig. A3.5). Shale is dominantly brown, but in the upper part (Fig. A3.5, units 102–134) it is gray, olive gray and greenish gray. Brown shale of unit 60 contains large (0.5 m in diameter) calcareous sandstone concretions. Silicified, fossil logs are present in the lower 1 m of brown shale of unit 81. Dark yellowish orange shale (Fig. A3.5, unit 95) contains ironstone beds and concretions (Fig. 10E).

Sandstone of the Flying Eagle Canyon Formation at the Mescal Canyon B section (Fig. A3.5) is present as different lithotypes: (1) thin sandstone beds and lenses intercalated in shale are mostly massive (Sm), subordinately horizontally laminated (Sh), rarely ripple laminated (Sr), and trough cross-bedded (St). Bed thickness varies from 0.1 to 0.8 m. The calcareous sandstone of unit 97 contains oyster shells; (2) thicker sandstone units (1–13.2 m thick) are mostly trough cross-bedded (lithofacies St). Two types of trough cross-bedded sandstone can be distinguished: large-scale cross-bedding with thick cross-bedded sets (mostly 50–100 cm), and small-scale cross-bedding with thin cross-bedded sets (<50 cm). Some of the trough cross-bedded sandstones contain intraformational (mostly mudstone) rip-up clasts near their bases. Bioturbation is rare. Sandstone of unit 118 displays synsedimentary deformation structures (dewatering structures). Sandstone of unit 13 contains sandstone concretions in its uppermost part; subordinately, massive sandstone (Sm), ripple-laminated sandstone (Sr), and minor sandstone with planar cross-bedding (Sp) are present. One thin conglomerate bed (0.5 m) containing intraformational clasts (mudstone pebbles) and displaying trough cross-bedding (lithofacies Gt) is intercalated in the middle part of the formation at the base of a trough cross-bedded sandstone unit (Fig. A3.5, unit 82).

The contact of the Flying Eagle Canyon Formation with the overlying Ash Canyon Formation is marked by a change to lighter-colored, more resistant, more thickly bedded sandstone and a decrease in the amount of mudstone and siltstone. The contact is mapped at the base of the lowest thick, light-colored, quartz-rich, resistant bed of sandstone. This contact is typically sharp and erosive, but probably represents only a minor disconformity. It is likely that the lowest sandstone included with the Ash Canyon is not the same age throughout the study area. Seager and Mack (2003) reported that large-scale intertonguing takes place between lower Crevasse Canyon (Flying Eagle Canyon) and Ash Canyon strata in the Caballo Mountains.

Paleontology and age

Fossils of plants, marine bivalves, and a turtle are known from the Flying Eagle Canyon Formation. Lozinsky (1985) listed fossil plants from one locality near Mescal Canyon as "*Sequoia montana*" [sic], *Ficus planicostata* Lesquereux, cf. *Dryophyllum* sp., cf. *Laurophyllum wardiana* (Knowlton), cf. *Dillenites cleburni* (Lesquereux), *Cercidiphyllum* sp., and cf. *Quercus viburnifolia* Lesquereux (identifications by Coleman Robinson). Most of these taxa, at least at the generic level, are known from the late Campanian Fruitland or Kirtland formations in the San Juan Basin of northwestern New Mexico (e.g., Tidwell et al., 1981), but it is not clear that they are of precise biostratigraphic significance. Fossil wood is also present but unstudied.

The bivalve fossils include fragmentary oysters and are present in a few beds (see above). Lichtig and Lucas (2016) described a new species of turtle, *Neurankylus notos*, from the Flying Eagle Canyon Formation east of the Caballo Mountains (NMMNH locality 9158). This is likely the oldest record of *Neurankylus*, which is mostly a Campanian–Paleocene genus elsewhere (Lyson et al., 2016). Thus, the fossils currently known from the Flying Eagle Canyon do not provide a precise age assignment, although they are consistent with a possible minimum age of Campanian.

However, the base of the Flying Eagle Canyon Formation is no older than the underlying late Turonian Gallup Formation, and the lower part of the unit is homotaxial with the Dilco Coal Member of the Crevasse Canyon Formation in west-central New Mexico. This means the base and lowermost part of the Flying Eagle Canyon Formation are likely of Turonian age, and the unit probably includes Coniacian-age strata, though its upper age limit cannot be determined with available data.

Sedimentary petrography

In the Flying Eagle Canyon Formation (Figs. A5.2G–H, A5.3A–D), the grain size of sandstone is mostly very fine- to medium-grained but may locally range to coarse- to very coarse-grained; it is very seldom pebbly. Sorting ranges from poorly sorted in pebbly sandstone, but the more common fine- to medium-grained sands are mostly well-sorted. Detrital grains are subangular to subrounded. The most common grain types are monocrystalline quartz (including porphyry quartz), polycrystalline quartz (including stretched metamorphic), and abundant volcanic grains. Detrital feldspars are sparse (average 6%) and include potassium feldspars (untwinned, microcline, perthite) and plagioclase. Detrital feldspars are partly altered to clay minerals, and partly replaced by calcite cement. The sandstone also contains a few granitic rock fragments, rare volcanic chert grains displaying a spherulitic texture, and rare granophyric grains, metamorphic rock fragments and micas (muscovite and biotite). A few grains are composed of phyllosilicate minerals and represent altered grains such as feldspars. Sandstone contains small amounts of matrix. Authigenic quartz overgrowths on detrital quartz grains are common; rarely, authigenic feldspar overgrowths are also observed on detrital feldspar grains. Coarse, blocky calcite cement is present in some sections.

The average composition of sandstone of the Flying Eagle Canyon Formation is $Q_{84}F_6L_{10}$ (sublitharenite). Most samples plot into the field of sublitharenite, and rarely into the fields ofquartz arenite and subarkose (classification after Pettijohn et al., 1987). Following the classification of McBride (1963), most samples plot into the field of sublitharenite, and subordinately into the fields of lithic subarkose, and, rarely, subarkose and quartz arenite.

Depositional environments

To the north of Sierra County, the Crevasse Canyon Formation represents coastal deposits associated with the R2 regression, the overlying T3 transgression, and the R3 regression of the Western Interior Seaway, and was deposited primarily between the T3 and R3 paleoshorelines (Molenaar, 1983, fig. 9) along a belt that extended northwest to southeast from Gallup through Socorro to near Carrizozo. The R2 regression is recorded in Sierra County by the upper part of the D-Cross Member of the Mancos Formation, the Gallup Formation and the lowermost strata of the Flying Eagle Canyon Formation, the latter being homotaxial with the Dilco Coal Member of the Crevasse Canyon Formation to the northwest. Thus, the rocks in Sierra County are equivalent to the lower part of the Crevasse Canyon Formation and were deposited about 100–120 km south (southwest) of the T3 transgression shoreline. A thin sandstone bed containing oyster shells is present at our Mescal Canyon B section approximately 339 m above the base of the Flying Eagle Canyon Formation, indicating some marine influence on sedimentation (Fig. A3.5, unit 97). However, it is not certain that this is a record of the T3 transgression in Sierra County (see later discussion).

Seager and Mack (2003) interpreted the lower member of the Crevasse Canyon Formation (Flying Eagle Canyon Formation) as fluvial deposits. According to Seager and Mack (2003), sandstone beds of the Flying Eagle Canyon are mainly single-storey sand sheets and ribbons. Thicker sandstone units (thickness mostly 5–20 m) of the Flying Eagle Canyon Formation are mostly multistorey trough cross-bedded sandstone (St), rare planar cross-bedded sandstone (Sp), and locally contain trough cross-bedded fine-grained conglomerate (Gt) at the base. The thick sandstone units fine upward and grade into other lithofacies, such as Sh, Sr, Sl, and Sm—forming the architectural element channel (CH) in combination with sandy bedforms (SB), sensu Miall (1996, 2010). Mudstone units are assigned by us to the architectural element FF (overbank fines). Thinner sandstone intercalations (<2m thick) within the mudstones, represented by lithofacies St, Sh, Sr and Sm, are interpreted by us as crevasse-channel and crevasse-splay deposits (architectural elements CR and CS).

We thus interpret the Flying Eagle Canyon Formation as deposits of a sandy meandering to anastomosing fluvial system formed under semihumid to humid climatic conditions (indicated by gray colors of mudstone, "wet" paleosols (cf. Seager and Mack, 2003), and the presence of thin coal beds and fossil plant debris within the mudstone facies). Lateral variations in thickness and facies are present among the three measured sections illustrated here. At the type section, the upper Flying Eagle Canyon Formation consists of a high proportion of mudstone. At the Fossil Forest section, the exposed upper portion of the Flying Eagle Canyon Formation is more sandy. Thickness also varies considerably between sections of the Flying Eagle Canyon Formation.

"Engle coal field"

Lee (1905) coined the term "Engle coal field," but there is very little coal in this "field" and there has never been any commercial production. As Lee (1905, p. 240) well stated, "little development has been accomplished in the Engle area and its importance as a coal field is doubtful." Mason (1976) estimated that only about 0.2% of the Mesaverde strata in the northern Caballo Mountains are coal, and our measured stratigraphic sections suggest that may be a generous estimate. Thus, coal beds in our sections are almost entirely restricted to the basal Flying Eagle Canyon Formation and they are few in number (one to three beds) and mostly less than one meter thick (Figs. A3.1, A3.5). Wallin's (1983) use of the term "coal-bearing member" to refer to the lower part of the Mesaverde Formation thus is somewhat misleading, as that stratigraphic interval contains very little coal.

Ash Canyon Formation (revised)

Lithostratigraphy

In an unpublished thesis, Bushnell (1953, p. 17–22) named the Ash Canyon Mem-

ber of the Mesaverde Formation for Ash Canyon, a ravine at the south end of Elephant Butte Lake near Mescal Canyon. The first published mention of the unit is in Bushnell (1955a), who did not designate a type section, although the unit is well exposed along the lower reaches of Ash Canyon. As originally proposed, the Ash Canyon Member was restricted to a pebbly sandstone interval 30 to 60 m thick at the top of the Mesaverde or Crevasse Canyon Formation. Without explicitly revising the definition, Mack and Seager (1993) expanded the Ash Canyon to include about 365 m of "predominantly tan, medium-grained, cross-bedded lithofeldspathic sandstone interbedded with lesser amounts of olive-gray mudstone. Chert-pebble conglomerate lenses within sandstone beds are present locally, especially near the top of the unit." Seager and Mack (2003) carried this change forward, and it was mapped in the Cutter (Seager, 2007), Engle (Mack and Seager, 1993), and Upham (Seager, 1995b) geologic quadrangle maps.

In this report, we apply the expanded concept of the Ash Canyon Member as used by Mack and Seager (2003), and we elevate the unit in rank from a member to a formation. The Ash Canyon Formation is a thick interval of predominantly light-colored, quartzose, cross-bedded sandstone that forms bold ridges, in contrast to the darker, varicolored mudstone, siltstone, and lenticular-tabular sandstone of the valley-forming Flying Eagle Canyon Formation. Furthermore, in the Ash Canyon Formation: (1) sandstone intervals are typically several meters thick and are laterally continuous over 100–800 m; (2) mudstone-siltstone is subordinate or subequal compared to these sandstone intervals; and (3) the dominant sand size is medium-grained.

Using these criteria, the Ash Canyon Formation is readily identified on the ground and aerial images. The older definition of the unit (Bushnell, 1953) relied on the presence of quartz and chert pebbles that are erratically distributed, and mostly concentrated in its uppermost strata.

Close to Ash Canyon, at the Mescal Canyon C section (Fig. A3.7), the Ash Canyon Formation comprises units 74 through 124, and we consider this to be the principal reference section of the formation. At this section, the Ash Canyon Formation is ~216 m thick. Its base is a thick succession of sandstone and sparse conglomeratic sandstone that overlie relatively thick (10 m or more) mudstone-dominated slopes comprising the top of the Flying Eagle Canyon Formation. The top of the Ash Canyon Formation is beneath the stratigraphically lowest volcaniclastic sandstone at the base of the José Creek Formation. Thus, the Ash Canyon Formation at this reference section is a sandstone-dominated unit with minor conglomerate, lying between the mudrock-dominated Flying Eagle Canyon Formation (below) and the volcaniclastic strata of the José Creek Formation (above). In Sierra County, the Ash Canyon forms cliffs, ledges, and cuestas between the adjacent slope-forming units.

In general, the Ash Canyon Formation consists of sandstone interbedded with subordinate mudrock and siltstone. Sandstone is light-gray to pale-yellow on fresh surfaces, weathering light brownish, yellowish, and pinkish gray. Grain size varies from very fine to very coarse, but most of the sandstone is medium grained. Based on hand specimens, composition was estimated at 60 to 90% quartz, 10 to 30% feldspar, and 10% or less lithic fragments and possible heavy minerals. Fresh pink to orange feldspar is prevalent, but in some samples the feldspar is largely weathered to clay. However, samples examined petrographically (see below) contain more quartz, approaching quartz arenite in composition. The sandstone has a sparkly appearance due to quartz? overgrowths on the quartz grains; this feature aids identification of the unit in the field. The rock is typically porous but well indurated.

Sandstone complexes of the Ash Canyon Formation are commonly several meters thick (as much as 15 m to the south, cf. Seager and Mack, 2003) and are lenticular over 100–800 m on strike (Cikoski et al., 2017). Sandstone is extensively cross-bedded (within medium to very thick, tabular to lenticular beds), with common trough forms and tangential forests, although planar laminated or massive beds are locally present; paleoflow directions from the troughs are toward the east-northeast (Cikoski et al., 2017). The thick, ledge-forming sandstone intervals of the Ash Canyon Member are typically multistorey, whereas those in the Flying Eagle Canyon Member tend to be single-storey (Seager and Mack, 2003). Trough cross-bedding and cut-and-fill features are the most common sedimentary structures. Mudstone and siltstone of the Ash Canyon Formation are similar to mudstone and siltstone of the Flying Eagle Canyon Formation. Exposures of mudstone beds are generally confined to canyon walls.

Very thin to medium beds and lenses of pebbly sandstone and conglomerate are observed in the upper 50–60 m of the Ash Canyon Formation. Clasts are composed of rounded granules and pebbles of gray to black chert and clear to white quartz, quartzite, and siltstone rip-ups, with 1–5% silicious volcanic rock (aphanitic and gray), and traces of petrified wood (Cikoski et al., 2017). Pebbles are rounded, poorly sorted, and up to 5 cm in diameter.

The section at Mescal Canyon C (Fig. A3.7) is 525 m thick and includes the upper part of the Flying Eagle Canyon Formation, the entire Ash Canyon Formation, and the lower part of the José Creek Formation. Here, the Ash Canyon succession is relatively coarse, containing a high proportion of sandstone and conglomerate. This may reflect greater proximity to source area than the Ash Canyon strata to the north. Shale is brown, olive gray and olive green. Shale intervals are mostly less than 10 m thick (~21 m maximum thickness). Trough cross-bedded sandstone (St) is by far the most abundant lithotype and is present in intervals up to 50 m thick. Less common are massive sandstone beds (Sm, 0.1–1.2 m thick), ripple-laminated sandstone (Sr, 0.1–2 m thick), and horizontally laminated sandstone (Sh, 0.1–1m thick). Conglomerate is relatively abundant. Conglomerate in units 97–100 (Fig. A3.7) is mostly trough cross-bedded (Gt), and rarely massive (Gm), consisting largely of extraformational siliceous pebbles. Units 110 and 111 are two massive conglomerate units (Gm) composed of chert pebbles. Unit 113 is a sandstone containing lenses of massive, mudstone-pebble conglomerate (Sm and Gm).

The upper 66–67 m of the Ash Canyon Formation at the Mescal Canyon C stratigraphic section are composed of three thick shale units and three sandstone conglomerate units. The shale units are 11.2–14.5 m thick. The lower sandstone and conglomerate (units 115–118 in Fig. A3.7) is 19.1 m thick and composed of trough cross-bedded sandstone (St) and trough cross-bedded chert conglomerate (Gt). The sandstone unit in the middle (unit 120) is 5.5 m thick, with massive, tabular beds. The upper 5 m of the Ash Canyon Formation is composed of mudstone intercalated with trough cross-bedded pebbly sandstone to conglomerate (Gt) and coarse-grained, massive conglomerate (Gm). The latter conglomerate bed (unit 124, 1.2 m thick) is composed of chert pebbles and is the top bed of the Ash Canyon Formation at this locality.

At the Fossil Forest section (Fig. A3.6), the exposed thickness of the Ash Canyon Formation is 208 m. The succession is composed of sandstone, conglomerate, shale and siltstone. Shale units are up to 6.4 m thick; some of the shale units contain fossil logs. Covered intervals, which most likely also represent shale units, are up to 8.3 m thick. Sandstone and conglomerate mostly forms thicker units (up to 33 m thick) that are composed of the following lithotypes: (1) conglomerate as lenses within trough cross-bedded sandstone or as thin, trough cross-bedded (Gt) or massive (Gm) conglomerate beds; (2) trough cross-bedded sandstone, partly pebbly (St), is the most abundant lithotype; (3) sandstone with planar cross-bedding (Sp) is rare; (4) sandstone with low-angle cross-bedding (Sl) is rare; (5) horizontally laminated sandstone (Sh); (6) ripple-laminated sandstone (Sr); and (7) massive sandstone, partly bioturbated (Sm) is rare. Trough cross-bedded sandstone commonly is present as multistorey units, and rarely as single-storey units. A few fining-upward cycles are developed, grading from pebbly sandstone (St and Gt), into trough cross-bedded sandstone (St), and finally into horizontally laminated and ripple-laminated sandstone (Sh, Sr), overlain by siltstone and shale. A good example of a fining-upward cycle is the succession of units 64–70 (Fig. A3.6).

Beginning with Bushnell (1953) and continuing through Seager and Mack (2003), previous workers regarded the contact between the Ash Canyon and the overlying McRae (José Creek) strata as unconformable. In the field, an obvious topographic and lithologic break separates light-colored, pebbly, ridge-forming sandstone of the Ash Canyon from overlying darker, volcaniclastic, slope-forming sandstone, siltstone, and mudstone of the José Creek. Clean exposures of the contact, however, are few. One of the best exposures observed is in the large west-trending arroyo 2.3 km northeast of Kettle Top Butte (UTM 301029E, 3680720N). Sandstone at the base of this exposure is typical Ash Canyon, with quartz and chert granules. Overlying the sandstone is dark gray, carbonaceous mudstone about 3.5 m thick, above which is a sandstone bed, 3 m thick, that shares features of Ash Canyon and José Creek. This sandstone contains a high proportion of feldspar and volcanic lithic grains, but also has stringers of rounded chert and quartz granules, as in the Ash Canyon. The next higher sandstone is typical volcaniclastic José Creek. This outcrop indicates a transition, rather than an abrupt hiatus, between quartzose Ash Canyon sands to volcaniclastic sands of the José Creek.

Paleontology and age

Petrified wood is widespread and locally abundant in the Ash Canyon Formation. Segments of logs more than 50 cm across and several meters long are not unusual (Fig. 11B). An enormous log, 27 m long and 2 m across, was observed on the south side of Walnut Canyon in the Fra Cristobal Range (Hunter, 1986, first reported this log). This outlier of Ash Canyon Formation rests on Permian rocks and apparently was emplaced by large-scale gravity sliding. Nearly all fossil wood in the Ash Canyon Formation has weathered free of rock matrix, suggesting that it is derived from mudstone layers rather than sandstone. A few fossil stumps apparently in growth position have been observed, but these are far less common than in the overlying McRae Group. Unfortunately, the fossil wood illustrated and classified by Estrada-Ruiz et al. (2012a, b) is of no precise biostratigraphic significance.

Lucas et al. (2016) documented some poorly preserved dinosaur footprints from the Ash Canyon Formation near

FIGURE 11. Photographs of selected outcrops of the Ash Canyon and Double Canyon formations. A, Contact of Flying Eagle Canyon and Ash Canyon formations, Fossil Forest section. B, Fossil log in Ash Canyon Formation in Fossil Forest section. Note hammer for scale at center of image. C–D, Trough cross-bedded, silica-pebble conglomerate in the Ash Canyon Formation, Mescal Canyon section. E, Siliceous conglomerate of Double Canyon Formation in Fra Cristobal North section. F, Conglomerate of the Double Canyon Formation resting directly on Precambrian basement, northern tip of the Fra Cristobals.

Ash Canyon. These are likely ornithopod footprints, but of no precise biostratigraphic significance.

Sedimentary petrography

Fine-grained conglomerate of the Ash Canyon Formation is poorly sorted and composed of subrounded to rounded clasts in a sandy matrix. Clasts include two types of chert: (1) the dominant type is volcanic chert, which appears mostly brownish under plane light and partly displays a volcanic texture (spherulitic texture, small phenocrysts of quartz); and (2) sedimentary chert is mostly clear under plane light and shows outlines of fossils such as shell fragments, spicules and other skeletal grains (Fig. A5.4A–B). The sandy matrix of Ash Canyon conglomerate is composed of mono- and polycrystalline quartz, rare chert and detrital feldspars, a few grains of phyllosilicate minerals (altered feldspars?), and very rare phyllitic grains.

Sandstone of the Ash Canyon Formation (Figs. A5.3B–H, A5.4C) is mostly medium grained and moderately to well-sorted. Most of the detrital grains are subrounded. The most common grains are monocrystalline quartz (including a few porphyry quartz grains), polycrystalline quartz and abundant chert grains. Volcanic chert, which rarely displays ignimbrite texture and spherulitic texture, is more common than sedimentary chert. Detrital feldspars are rare and include microcline, perthite and untwinned grains. Granitic and volcanic rock fragments are rare. Sedimentary rock fragments (reworked siltstone) and metamorphic rock fragments composed of mica and quartz with well-developed schistosity are very rare. A few grains composed of clay minerals (altered feldspars?) are present. The sandstone is cemented by quartz, which occurs as authigenic overgrowths on detrital quartz grains. Calcite cement is present in small amounts. The sandstone also contains small amounts of matrix.

The average composition of sandstone of the Ash Canyon Formation is $Q_{92}F_3L_5$ (sublitharenite). Most of the sandstone samples plot into the field of quartz arenite, and subordinately into the field of sublitharenite. In the classification scheme of McBride (1963), most samples are sublitharenite and quartz arenite, rarely lithic subarkose. Thus, there is a mineralogical shift from the Flying Eagle Canyon Formation sandstones, which are mostly subarkoses, to the more mature quartz arenites of the Ash Canyon Formation.

Depositional environments

Like previous workers, we interpret the deposition of the Ash Canyon Formation as totally nonmarine by fluvial processes. At the principal reference section in Mescal Canyon (Fig. A3.7), the lower 19 m of the Ash Canyon Formation is a succession of sandy and pebbly channel-fill sediments (lithofacies St, subordinately Sh), with rare intercalations of conglomerate (Gt, Gm). These lithofacies types are combined into the architectural elements CH (channel), SB (sandy bedforms), and GB (gravel bars and bedforms) sensu Miall (1996, 2010). Floodplain deposits are absent. This succession probably represents deposits of a sand-dominated, braided fluvial system. The upper part of the Ash Canyon Formation, which is composed of alternating thick mudstone units (floodplain deposits, architectural element FF) and intercalated sandstone and conglomerate units (architectural elements CH and SB) is interpreted as deposits of a meandering to anastomosing fluvial system (cf. Miall, 1996, 2010).

At the Fossil Forest section (Fig. A3.6), ~208 m of the Ash Canyon Formation is exposed, and the deposits differ somewhat from the section at Mescal Canyon. The succession is composed of alternating sandstone units (mostly lithofacies St, rare Sh, Gm, Gt), forming local fining-upward sequences—we classify these as architectural elements CH (channel), SB (sandy bedforms), and mudstone units that we classify as floodplain deposits forming architectural element FF (overbank fines). Thinner sandstone units (<2 m) are interpreted as minor channels and thicker sandstone units (>2 m) as major channels of a sandy meandering to anastomosing fluvial system (see Miall, 1996, 2010).

According to Seager and Mack (2003), paleosols are common in the Ash Canyon Formation. The character of the paleosols—thin, gray A horizon, light colored E horizon, thick argillic B horizon—indicates well-drained soils that formed in a relatively humid climate.

McRae Group (change in rank)

Kelley and Silver (1952) gave the name "McRae formation" to a thick succession of sedimentary rocks that overlies the Ash Canyon Formation (our usage) in the Cutter sag. The name refers to old Fort McRae, a U.S. Army post that formerly (1869 to 1876) stood on the south side of McRae Canyon. Bushnell (1953, 1955b) divided the McRae Formation into two members: the José Creek (lower) and the Hall Lake (upper).

The McRae Formation is more than 1 km thick, and its two members have long been readily mapped at the scale of 1:24,000 (e.g., Lozinsky, 1985; Mack and Seager, 1993; Seager, 1995b, c; Cikoski et al., 2017). Distinctive lithology and substantial thickness of the José Creek and Hall Lake fully justify elevating these units to formations and the McRae to a group. In addition, we describe a new unit of formation rank, the Double Canyon Formation, which overlies the Hall Lake Formation at the top of the McRae Group.

José Creek Formation

Lithostratigraphy

As outlined by Bushnell (1953, 1955a, b), the José Creek Formation is the lower, drab-colored, sandstone and conglomerate-rich interval of the McRae Group (Figs. 12, A3.7–A3.10). The name refers to an intermittent stream that flows northwest to Elephant Butte Lake (Fig. 2). We measured a principal reference section of the José Creek Formation at José Creek, where it is approximately 203 m thick (Fig. A3.8). We also measured the lowermost part of the José Creek Formation at our Mescal Canyon C section (Fig. A3.7), and the uppermost part of the José Creek Formation at our Kettle Top, McRae Canyon, and Reynolds Canyon A sections (Figs. A3.9, A3.10).

Estimates based on outcrop width and average dip at three sites in the southwestern part of the Black Bluffs quadrangle yield José Creek Formation thicknesses of approximately 128, 171, and 174 m. Seager and Mack (2003) state a thickness of 170 m near Kettle Top Butte. Cikoski et al. (2017) report a thickness range of 80–130 m. Thickness increases to a maximum of about 200 m in the type area along José Creek. Farther southeast, the José Creek steadily thins, pinching out entirely at Yoast Draw east of the central Caballo Mountains, where the Hall Lake Formation overlies the Ash Canyon Formation with an angular unconformity (Seager and Mack, 2003).

The José Creek Formation is generally non-resistant to erosion and underlies valleys and gentle slopes. Sandstone and silicified volcanic ash form low ledges. Good exposures of the José Creek can be found along most of the arroyos south of Black Bluffs that drain into Elephant Butte Lake (Cikoski et al., 2017).

Lithologically, the José Creek Formation is composed of non-fissile siltstone and mudstone interbedded in roughly equal proportions with volcaniclastic fine- to coarse-grained sandstone, almost all beds exhibiting an olive color. Conglomerate and silicified volcanic ash are minor, but distinctive components, and the proportion of conglomerate increases to the south. Mudstone and siltstone are dominantly dark green, olive, and brownish gray. Red colors are rarely seen, and where present, may be the result of hydrothermal alteration. Mudrocks are massive and display pedogenic features, including root traces and blocky ped structure. Pedogenic carbonate nodules are generally absent. Levron (1995) and Buck and Mack (1995) classified most José Creek paleosols as Argillisols and attributed them to weathering under a humid to subhumid climate. Mudstone and siltstone layers range up to about 3 m thick and commonly contain thin, lenticular interbeds of sandstone.

Sandstone of the José Creek Formation displays various shades of gray, green, bluish gray, brown, and brownish gray, and tends to become darker on weathered surfaces than in fresh exposures. Most sandstone is weakly to moderately indurated and erodes to low, rounded outcrops. Grains are very fine to medium and poorly sorted. Sandstone bodies are typically 2 to 9 m thick and laterally continuous over tens to hundreds of meters, and bedding within these bodies is lenticular to tabular and thin to thick. Wavy lamination, cross-bedding, scour and fill features are developed in some layers. In contrast to all older Cretaceous units, the sand is composed dominantly of lithic grains derived from volcanic rocks, together with feldspar, and little or no quartz. Some sandstone beds of the José Creek Formation contain scattered, rounded and well-rounded granules, pebbles, and, rarely, small cobbles (up to 15 cm in diameter). These are predominantly intermediate to basic volcanic and intrusive rocks, but in some samples include clasts of intraformational siltstone, sandstone, and impure carbonate rock. As Bushnell (1953, 1955a, b) noted, overall proportion of conglomerate and the size of clasts in José Creek conglomerate increases toward the south, with boulders as large as 1 meter in diameter present near the south end of Elephant Butte Lake. Evidently, a volcanic center was located nearby.

The upper part of the José Creek Formation contains layers of rock that resemble bedded chert. These beds are white to light brown, yellow, or purple. The cherty beds exhibit a dull or vitreous luster and are generally densely jointed. The chert-like rock is present in individual layers less than 1 m thick and in thicker intervals interbedded with siltstone and mudstone. Lozinsky (1985) and Seager and Mack (2003) observed shards of volcanic glass in thin sections, indicating that these layers consist of silicified volcanic ash.

Along Cañon del Muerto southeast of old Fort McRae (UTM 303000E, 3672950N), large sandstone dikes and small faults are present in José Creek strata. The largest dikes are up to 15 cm wide and crosscut at least 3 m of strata. The filling is dominantly fine sandstone, containing scattered coarse grains and small granules.

At the principal reference section (Fig. A3.8), the José Creek Formation is 203 m thick and is mostly siltstone or shale (64% of the measured section), with less sandstone (29%), conglomerate and conglomeratic sandstone (5%), and volcanic ash and silcrete (2%). The most abundant lithotype is silty mudstone to siltstone, and subordinately mudstone (lithofacies Fsm). Individual siltstone-mudstone units are up to 15 m thick. Intercalated are thin beds (<1 m thick) of trough cross-bedded (St), horizontally laminated (Sh) or massive sandstone (Sm). Thicker sandstone units are also present and composed of trough cross-bedded sandstone (St) and subordinate horizontally laminated sandstone (Sh). Conglomerate is massive (Gm) or trough cross-bedded and contains clasts mostly of volcanic rocks (Gt). Minor lithotypes are a limestone interval (Fig. A3.8, unit 25) composed of wavy bedded and nodular limestone (lithofacies P), thin silcrete beds, and a thin volcanic ash layer containing fossil leaves.

At Mescal Canyon C, we measured the lowermost José Creek Formation (Fig. A3.7). Here, it is composed of olive-green mudstone (2.2–13.2 m thick beds), intercalated with trough cross-bedded sandstone (St; 1.2 and 5.8 m thick) and horizontally laminated (Sh) to massive (Sm) sandstone (3.1 m thick). These sandstones are volcanic litharenites.

We also measured the upper 5 to 10 m of the José Creek Formation at our Kettle Top, McRae Canyon, and Reynolds Canyon A sections (Figs. A3.9, A3.10). At these locations the uppermost José Creek strata are mostly olive-colored volcanic-litharenite sandstones. But at the Reynolds Canyon A section (Fig. A3.10), sandy siltstone beds are present just below the Hall Lake Formation that contain abundant fossils of plant foliage.

The José Creek and Hall Lake formations are differentiated chiefly by the drab green, brown, and olive-colored mudstone of the former in contrast with the maroon and purplish mudstone of the latter. It is likely that this reflects the climate change from relatively wet (José Creek) to relatively dry (Hall Lake) indicated by the paleosols (Buck, 1992; Levron, 1995; Seager and Mack, 2003), but more study of the color change is needed to confirm this inference. South of Kettle Top Butte, the José Creek-Hall Lake contact appears unconformable, as the Hall Lake has a basal conglomerate that contains rounded cobbles as large as 30 cm in diameter (Fig. A3.9, Kettle Top section, unit 5). North of Kettle Top Butte, the formation contact is either a minor disconformity or a transition through an interval of 3 m or less. In the south bank of Reynolds Canyon just above its confluence with Flying Eagle Canyon, the base of a lens of coarse sandstone at the base of the Hall Lake is slightly scoured into uppermost José Creek mudstone. Beyond the pinch-out of the sandstone lens, the contact continues to be sharp but parallel to bedding. Excellent exposures of the contact are also present near the northern edge of the Elephant Butte quadrangle in a west-trending arroyo 1.7 km east to northeast of Kettle Top Butte. In these exposures, greenish-gray and purplish-gray mudstone layers alternate through an interval about 3 m thick.

Paleontology and age

Fossil foliage and wood are locally common in the José Creek Formation. During our investigation, plant remains we observed include roots, stems, and foliage. Silicified wood was also found, but other than a stump in the José Creek principal reference section (Fig. 12D), none of it was in place. Upchurch and Mack (1998) documented fossil plants from the José Creek Formation. These authors used foliage to identify 40 to 50 species of ferns, conifers, cycads, and angiosperms; wood features were used to identify conifers, dicots, and monocots (likely palms). Estrada-Ruiz et al. (2012a, b) identified 10 types of dicots, three types of monocots, and seven types of conifers from wood in the José Creek Formation.

Lozinsky et al. (1984) and Wolberg et al. (1986) reported dinosaur fossils from the José Creek, but, as best as we can deter-

mine, all of these fossils actually came from the Hall Lake Formation. For example, we relocated and collected a sauropod femur that Lozinsky et al. (1984, fig. 6) illustrated. They identified the stratigraphic level as José Creek Formation, but we determined it to be Hall Lake Formation (Fig. A3.11, NMMNH locality 11834).

Amato et al. (2017, fig. 4) reported U-Pb ages from the José Creek Formation in the Cutter sag (southwestern part of the Engle quadrangle: see Seager and Mack, 2003, fig. 49). In ascending stratigraphic order, the reported weighted means are 74.9 ± 0.7 Ma, 74.6 ± 0.6 Ma and 75.2 ± 1.3 Ma. These ages are laser ablation-inductively coupled plasma mass spectrometry ages (LA–ICPMS), which are less precise than isotope dilution-thermal ionization mass spectrometry (ID-TIMS) ages (Bowring et al., 2006; Schoene, 2014). Nevertheless, they are Campanian ages, and thus likely a reasonable approximation of the age of part of the José Creek Formation, given correlation of the volcaniclastic strata of the José Creek to the Copper Flat volcanic complex, which is at least in part of Campanian age (see later discussion).

Sedimentary petrography

In a petrographic study of the José Creek Formation based on 8 samples, Hunter (1986) reported 58 to 76% lithic grains, 24 to 40% feldspar, and 0 to 3% quartz. This composition places the sandstone samples into the field of lithic arenites. Lithic grains were 97 to 100% of volcanic origin, and the feldspar grains were dominantly plagioclase. A single sample from the base of the José Creek Formation contained 21% quartz and only 4% feldspar. Some of that sand was likely recycled from the underlying Ash Canyon Formation or reflects gradation between the Ash Canyon and José Creek lithosomes.

Basal sandstones from the José Creek section (Fig. A5.4D–F) differ significantly in composition from the lithic arenites typically encountered in the José Creek Formation, however, and the dominant grain type is monocrystalline quartz. The sandstone also contains many chert grains of volcanic origin, and many detrital feldspar grains, including potassium feldspars (mostly untwinned, a few perthitic grains) and plagioclase displaying polysynthetic twinning. Many of the feldspar grains are altered. Minor grain assemblages include volcanic rock fragments of acidic to intermediate composition, chert grains displaying spherulitic texture, granitic rock fragments containing coarse-grained quartz and feldspar, and fine-grained schistose metamorphic rock fragments composed of quartz and micas. Detrital muscovite, biotite, and chlorite are very rare. A few grains composed of fine-grained phyllosilicate minerals are present

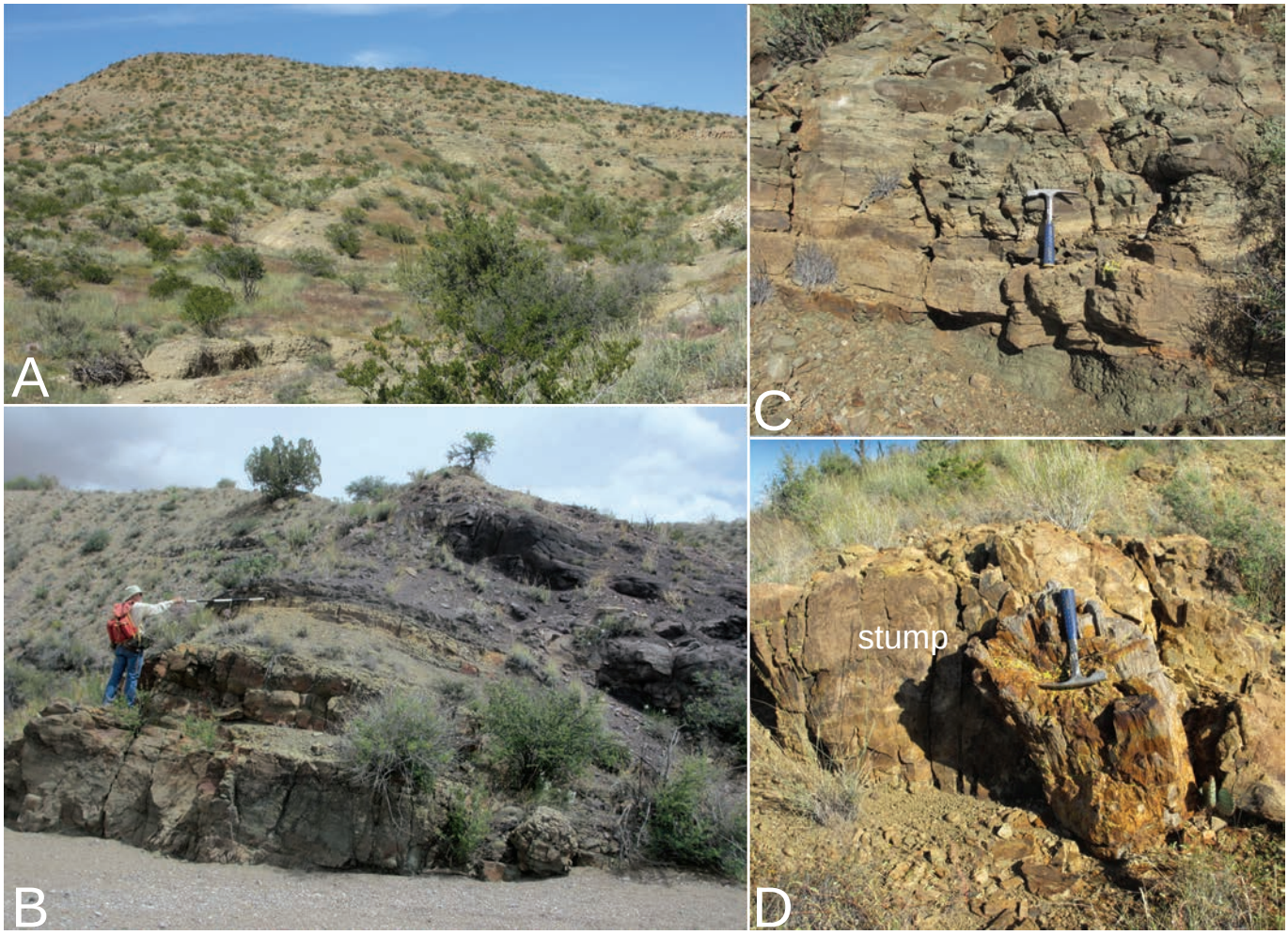

FIGURE 12. Photographs of selected outcrops of the José Creek Formation. A, Overview of lower-middle part of the José Creek principal reference section. B, Contact of José Creek and Hall Lake formations (staff held at contact) in Reynolds Canyon. C, Sandstone bed in principal reference section of José Creek Formation. D, Fossil stump in principal reference section of José Creek Formation.

that probably represent altered feldspar grains. Accessory minerals are zircon, titanite, tourmaline, and opaque grains. The sandstone contains small amounts of matrix and blocky calcite cement that randomly replaces detrital feldspar grains. Locally, authigenic quartz overgrowths are present on detrital quartz grains.

The average composition of sandstones of the basal José Creek Formation at the José Creek section is $Q_{81}F_6L_{13}$ and are sublitharenite to subarkose, using the classification scheme of Pettijohn et al. (1987). Most samples plot into the field of sublitharenite, and rarely into the fields of lithic subarkose and subarkose, following the classification scheme of McBride (1963).

Depositional environments

Deposition of the José Creek Formation was by fluvial processes (Bushnell, 1953; Wallin, 1983; Seager and Mack, 2003). The siltstone-mudstone facies represents floodplain deposits (overbank fines; architectural element FF). Thin sandstone beds represent small channel fills (lithofacies St) and sheetflood deposits (lithofacies Sm, Sh), and may be assigned to architectural element SB (sandy bedforms). Seager and Mack (2003) interpret the thin intercalated sandstone beds as crevasse-splay deposits.

Thicker sandstone units and, subordinately, massive, and cross-bedded conglomerate (Gm, Gt), represent major channels composed of multistorey crossbed sets (St). The intercalated thin limestone unit is interpreted based on field observations (it includes rhizoliths) as pedogenic carbonate (lithofacies Pc), and the silcrete beds represent altered volcanic ash beds (siliceous tuffs of Seager and Mack, 2003). Whether the ash was deposited directly by the wind or transported by water is not certain.

The José Creek Formation probably represents deposits of a sandy braided to anastomosing fluvial system with thick floodplain deposits that likely accumulated on the distal edge of a volcaniclastic apron surrounding one or a cluster of volcanoes to the southwest. According to Seager and Mack (2003), José Creek paleosols indicate deposition under subhumid climatic conditions (also see Buck, 1992; Levron, 1995).

Hall Lake Formation

Lithostratigraphy

Bushnell (1953, 1955a) named the Hall Lake Member as the upper of two divisions of the McRae Formation. The name refers to Hall Lake, which was formerly the official name for Elephant Butte Lake (Reservoir). Bushnell (1955a, p. 15) imprecisely located the type section "on the east shore of the lake, northeast of Elephant Butte and south of McRae Canyon." Bushnell (1953) described the section, which measures approximately 490 m thick, with the base under water and the top faulted against older units. With reference to the geologic map of Lozinsky (1985), Bushnell's type section probably extends northwest from near the mouth of Beaver Canyon through the area known as "The Jungles." Aerial imagery suggests that this is a well-exposed, gently dipping section with no significant internal faults.

Another continuous section, moderately dipping and without faults, is present east of Double Canyon and south of Flying Eagle Canyon. We did not measure the section, but a minimum thickness of approximately 730 m was obtained through geometric construction. A steeply dipping section, northwest of Flying Eagle Canyon near its mouth, also is at least 700 m thick. In this area, the Hall Lake Formation has conformable lower and upper contacts with the José Creek and Double Canyon formations, respectively. Southeast of the type area, the Hall Lake thins markedly because of truncation of the upper part beneath the Eocene Love Ranch Formation. Thus, at Yoast Draw east of the central Caballo Mountains, Seager and Mack (2003) reported that the Hall Lake is less than 15 m thick.

We did not measure a "complete" section of the Hall Lake Formation, but instead measured sections of the lower 200 m or less at Kettle Top (Fig. A3.9), McRae Canyon (Fig. A3.9), Reynolds Canyon (Fig. A3.10), and Cottonwood Canyon (Fig. A3.11). We also measured the upper 25 m of the Hall Lake Formation at the type Double Canyon section (Fig. A3.12). At these sections and elsewhere, the Hall Lake Formation consists largely of reddish brown to maroon (locally light green) mudstone (Fig. 13A), with subordinate lenticular sandstone tongues (Fig. 13D) that are locally conglomeratic (Fig. 13E), and very sparse silicified volcanic ash. In the Black Bluffs quadrangle, the sandstone bodies may be up to 30–70 m thick and extend over 20–150 m lateral distances (Cikoski et al., 2017). The mudstone intervals are up to approximately 23 m-thick beds that are soft and deeply weathered, forming low, hummocky terrain. Blocky structure together with slickensides and carbonate nodules (Fig. 13B), are interpreted as pedogenic features associated with paleosols. Inclined carbonate stringers (along slip fractures) and vertical cylinders (after roots) are also developed (Fig. 13C). Excellent exposures of such features are present along Flying Eagle Canyon about 600 m below the junction with Reynolds Canyon. Buck and Mack (1995) classified paleosols of the Hall Lake as calcisols and vertic calcisols, suggesting a climate more arid than that which prevailed during José Creek deposition, possibly accounting for the reddish color of the mudstones.

Sandstone in the Hall Lake Formation displays various shades of green, blue, purple, and reddish gray. In the upper part of the formation, the prevalent color is medium to dark gray with a purplish cast. Cikoski et al. (2017) describe channel fills in the Black Bluffs quadrangle as typically single storey (1 to 3 m thick) but locally multistorey and 4–6 m thick; these consist of medium to thick, tabular to lenticular beds that are internally massive (Sm), horizontal-planar laminated (Sh), or cross-bedded (tangential foresets, up to 20 cm high, with local trough forms; St). We've found that the thicker sandstone units (mostly 1–8 m thick) are mostly composed of trough cross-bedded multistorey sandstone (St), subordinately of planar cross-bedded (Sp) and horizontally laminated sandstone (Sh). Bedding varies from thin to very thick. Some sandstone beds are nearly massive, and these rocks exfoliate like a plutonic rock. Large-scale cross-bedding is faint to prominent, depending on weathering. Grain size varies from fine to very coarse, with pebbles to small cobbles locally present, and is mostly medium to very coarse grained on the Black Bluffs quadrangle (Cikoski et al., 2017). Clastic dikes were noted in several outcrops.

Based on field observations, sandstone of the Hall Lake is feldspathic litharenite, similar to sandstone of the José Creek Formation. Quartz varies from zero to a few percent of rock volume. However, based on thin-section study, Hunter (1986) reported Hall Lake sandstone to consist of 43 to 66% lithic grains, 13 to 30% feldspar grains, and 15 to 27% quartz. One of Hunter's samples contained 55% quartz and only 29% lithic fragments. According to Hunter, lithic grains are mostly of volcanic origin, but metamorphic and plutonic rock fragments are more abundant relative to José Creek sandstone.

Local conglomeratic strata are typically composed of thin lenticular beds

that are 0.6–2.2 m thick, and massive or trough cross-bedded (Gm, Gt). South of Kettle Top, the Hall Lake Formation has a basal conglomerate that contains rounded cobbles as large as 30 cm in diameter. The cobbles consist of white, gray, and pink quartzite; pink and red porphyritic rhyolite, gray to pink granite, and greenish-gray, intermediate volcanic rocks. Sparse conglomerate layers are also present higher in the Hall Lake throughout the study area. Intermediate and mafic volcanic rocks continue to dominate, but clasts of red to pink granite, chert, quartzite, and quartz become increasingly common toward the top of the formation. This may indicate a petrographic trend of gradation into the overlying Double Canyon Formation.

Some Hall Lake units display a fining-upward trend, starting with Gt, grading into St and finally into Sh (Fig. 13D). Another common lithofacies consists of thin (mostly 20–40 cm) carbonate beds (pedogenic calcretes), which are partly nodular and sometimes contain root traces (lithofacies P).

Without specifying localities, Lozinsky (1985) reported layers of white to light red, silicified volcanic ash in the Hall Lake Formation in the Elephant Butte quadrangle. We observed no such lithology in the Hall Lake, and suspect that the silicified layers reported by Lozinsky are in the younger Double Canyon Formation (see below).

The contact between the Hall Lake Formation and the overlying Double Canyon Formation was mapped at the base of the lowest significant greenish, bluish, or olive-gray mudstone or conglomerate bed, in contrast to the prevalent dark reddish and purplish- gray mudstone of the Hall Lake. The contact appears to be gradational and conformable near the type area of the Hall Lake Formation.

Paleontology and age

Fossils that represent several genera of dinosaurs from the lower part of the Hall Lake Formation indicate that these rocks are latest Cretaceous (Maastrichtian or Lancian) in age, which is ~66 to 68 Ma (Lucas et al., 2012). Lee (1907b) first reported fossils from what later was named the Hall Lake Formation, consisting of dinosaur bones and a skeleton of "*Triceratops*." A few bones of this skeleton, preserved in the Smithsonian collection (Fig. A6.4), are only diagnostic of a large ceratopsian dinosaur, not of *Triceratops* or any other genus. Subsequent publications on vertebrate-fossil assemblages of the Hall Lake Formation include: Lozinsky et al. (1984), Wolberg et al. (1986), Gillette et al. (1986), Lucas et al. (1998a, 2017a, 2017b), Sullivan et al. (2005), Suazo et al. (2014), Sullivan and Lucas (2015), Dalman and Lucas (2017), and Lichtig and Lucas (2017).

Fossil turtle and dinosaur bones are present 24, 29, and 32 m above the base of the Hall Lake Formation at the McRae Canyon section, in the upper part of the Kettle Top section, and in the Reynolds Canyon A section (Figs. 13F, A3.9, A3.10). These stratigraphic sections make it possible to put many of the vertebrate fossil localities in the Hall Lake Formation into stratigraphic context, and the bulk of the assemblage (including the most identifiable dinosaur fossils) comes from low in the formation, 24–141 m above its base (Figs. A3.9, A3.10). This interval yields a jaw of *Tyrannosaurus rex* (Fig. A6.5; 43 m above the base), partial skeletons of a new ceratopsian genus originally assigned to *Torosaurus* (24–43 m above the base), and a femur of the sauropod dinosaur *Alamosaurus* (141 m above the base). Sullivan and Lucas (2015) referred to this vertebrate assemblage as the Armendaris local fauna, and, like previous workers (Lozinsky et al., 1984; Wolberg et al., 1986; Gillette et al., 1986; Lucas et al., 1998a), considered it to be of late Maastrichtian (Lancian) age. This is because records of *Tyrannosaurus* and *Alamosaurus* are of Lancian age in Texas, Utah, and the San Juan Basin of northwestern New Mexico (Lucas et al., 2012).

The only other fossils we observed in the Hall Lake Formation are large vertical, meniscate burrows we assign to *Taenidium*. These were encountered in sandstone at two separate localities in Reynolds Canyon in the lower 100 m of the formation (Fig. A3.10).

Amato et al. (2017, fig. 4) reported a U-Pb age of 73.2 ± 0.7 Ma on a tuff bed about 10 m above the base of the Hall Lake Formation. However, this Campanian age is from a tuff stratigraphically just a short distance below late Maastrichtian dinosaur fossils, so we question its reliability. In particular, the MSWD (mean square of weighted deviates) value of 1.7 for the dated sample reported by Amato et al. (2017, p.1218) suggest that the analytical data the weighted mean was calculated from are too scattered given the reported uncertainty (e.g., Schoene, 2014). What is needed to resolve the apparent conflict between the U-Pb age and dinosaur biostratigraphy is an ID-TIMS date from the Hall Lake tuff (to possibly estimate a more precise numerical age), and possibly more biostratigraphic data.

The presence of latest Cretaceous dinosaur fossils in the lower part of the Hall Lake Formation suggests that the upper part of the formation may be Paleocene in age. Because it contains a succession of paleosols, suggesting extended episodes of soil development, this unit may have accumulated over a long interval of time.

Sedimentary petrography

Sandstone and conglomerate of the Hall Lake Formation (Figs. A5.5–A5.6) is distinctive petrographically. Most conglomerates contain a mixture of intermediate volcanic types with 0–25% siliceous clasts and 0–10% granite (based on Cikoski et al., 2017). Intraformational conglomerate is poorly sorted, clast supported, and consists of partly recrystallized carbonate clasts (most likely derived from the reworking of paleocaliche beds), some containing a few small quartz grains. Sand-sized detrital quartz grains (mostly monocrystalline quartz), and a few detrital feldspar grains are present. The conglomerate is cemented by calcite. Pebbly sandstone is moderately to poorly sorted, the sand grains are angular to rounded, and is cemented by calcite.

Coarse-grained sandstone of the Hall Lake Formation is moderately sorted and composed of monocrystalline quartz (including volcanic quartz), some polycrystalline quartz, many detrital feldspars, volcanic rock fragments, rare granitic and metamorphic rock fragments, and a few chert grains (Fig. A5.5A–C). The detrital feldspars include plagioclase and potassium feldspar, are mostly altered to different degrees, and are partly replaced by calcite. Some large volcanic rock fragments are composed of zoned plagioclase phenocrysts with hypidiomorphic texture, partly altered and embedded in fine-grained volcanic matrix (Fig. A5.5D–H). Some phenocrysts are altered to chlorite (originally probably hornblende or pyroxene).

Fine- to medium-grained sandstone (Fig. A5.6F–H) is moderately to well-sorted. The grains are angular to subangular in fine-grained sandstone and subangular to subrounded in medium-grained sandstone. The sandstone contains abundant monocrystalline quartz (including volcanic

quartz), a few polycrystalline quartz grains, abundant detrital feldspars, a few granitic rock fragments and a few volcanic rock fragments composed of feldspars. The detrital feldspar fraction includes many untwinned feldspar grains (probably orthoclase), plagioclase, rare microperthitic grains and rare microcline. Volcanic rock fragments and volcanic chert grains are common constituents. Schistose metamorphic and granophyric rock fragments are very rare. A few volcanic chert grains display the spherulitic texture typical of rhyolitic volcanic rocks. Detrital muscovite and chlorite are rare, and biotite is very rare. The sandstone contains many opaque grains. A few detrital grains are almost completely altered to clay minerals (originally feldspars?). Volcanic rock fragments contain abundant feldspar and a few quartz phenocrysts. The sandstone is cemented by coarse poikilotopic calcite; locally, some matrix and diagentic chlorite are present.

Most sandstones of the Hall Lake Formation plot into the field of lithic arenite, and a few sandstone samples plot into the field of arkose. The average composition is $Q_{45}F_{24}L_{31}$ (lithic arenite). Most samples are classified as feldspathic litharenite, and rarely as lithic arkose, according to the classification of McBride (1963).

Depositional environments

All workers have suggested that deposition of the Hall Lake Formation was wholly nonmarine and involved fluvial processes (Hunter, 1986; Buck, 1992; Buck and Mack, 1995; Levron, 1995; Seager et al., 1997; Seager and Mack, 2003). The mudstone facies of the Hall Lake Formation is interpreted as floodplain deposits. Thin sandstone and conglomerate intercalations represent small channel fills (St, Gt) and sheetflood deposits (Sh, Sm). Thicker sandstone units are interpreted as major channels (multistorey, cross-bedded sandstone and conglomerate) forming architectural element CH (channel) and SB (sandy bedforms).

The Hall Lake Formation represents deposits of an extensive muddy floodplain with minor and major channels of a braided to anastomosing fluvial system. Red mudstones and common pedogenic carbonates indicate deposition under relatively dry climatic conditions (Buck, 1992; Buck et al., 1992; Buck and Mack, 1995; Seager and Mack, 2003).

Double Canyon Formation (new)

Lithostratigraphy

In the vicinity of Black Bluffs and Kettle Top Butte, between the southern end of the Fra Cristobal Range and Elephant Butte Lake, a previously undescribed succession of sedimentary rocks overlies the Hall Lake Formation. At least 425 m thick, these strata include mudstone that is mostly greenish, bluish gray, or olive gray. Sandstone bodies are commonly arkosic and relatively coarse-grained, locally bearing silicified logs, but also include variable volcaniclastic fragments. Conglomerate beds are of mixed lithologies but generally contain more granitic clasts than seen in the Hall Lake Member. Locally, there are prominent beds of silicified volcanic ash. These beds show some resemblance to the José Creek Formation, and Lozinsky (1985) mapped them as such near the northern edge of his study area. Lozinsky mapped the contacts of what he identified as the José Creek Formation (Member) as faulted, but we found clean exposures demonstrating that the previously undescribed strata overlie the Hall Lake with a normal, depositional contact (Fig. A4.1). The level of Elephant Butte Lake has dropped substantially since the 1980s, revealing outcrops that were under water when Lozinsky conducted his field work.

The name Double Canyon Formation is proposed for these previously undescribed strata. The name refers to Double Canyon, a two-forked ravine near the eastern shore of Elephant Butte Reservoir (Fig. A4.1). The type section is a south-facing hogback ridge 1.6 km north-northeast of Kettle Top Butte at the northern edge of the Elephant Butte 7.5-minute quadrangle (Figs. 14, A4.1, A3.12). From about 3 km north-northeast of the type section, one can walk southward through a continuous, gently dipping succession from the Ash Canyon Formation through the José Creek and Hall Lake formations to the Double Canyon Formation (Fig. A4.1). Wherever we have observed the top of the Double Canyon, it is either in fault contact with older units (as it is at the type section) or concealed by Quaternary alluvium.

We recognize the Double Canyon as a new formation because it is distinct from the older Hall Lake and from any younger Cenozoic formation known in the region. In the Caballo Mountains to the south, the Eocene(?) Love Ranch Formation unconformably overlies the Hall Lake Formation (Seager and Mack, 2003). Characterized by conglomerates that are locally boulder-bearing and red to gray sandstone and mudstone, the Love Ranch is markedly dissimilar to the Double Canyon. Although it is confined to a small geographic area, the Double Canyon Formation is mappable (Fig. A4.1; also see Cikoski et al., 2017) and provides important insights into the tectonic evolution of the area (see later discussion).

We have identified the Double Canyon Formation in three separate fault blocks (Fig. A4.1). The first is the south-dipping hogback that contains the type section. The second fault block, immediately northwest of the first, has synclinal structure; here the base of the Double Canyon Member may intertongue with the underlying Hall Lake Member. The third outcrop area, called "McRae Forest" because of the abundance of fossil wood, is northeast of Black Bluffs and 3 to 4 km north of the other exposures. Here, the base of the Double Canyon is in fault contact with older rocks, and the upper contact is concealed by Quaternary alluvium (Fig. A4.1).

At the type section, the Double Canyon is 131 m thick, with the upper contact faulted (Fig. A3.12). At the McRae Forest section (Figs. A4.1, A3.13), the Double Canyon is about 310 m thick, with the lower contact faulted and the upper contact covered by Quaternary sediments. Two prominent, ridge-forming intervals of chert that are present in the southern area (type section) are absent in the northern area (McRae Forest). The higher of the silicified intervals (a single bed of chert) lies about 115 m above the base of the formation. Thus, assuming that the silicified layers are faulted out of the section at McRae Forest, the Double Canyon Formation has a minimum composite thickness of 425 m along the eastern side of Elephant Butte Lake.

The Double Canyon Formation is definitely absent northeast of the Caballo Mountains, where the Eocene Love Ranch Formation truncates the Hall Lake Formation. No information on the Double Canyon is available from the borehole logs that we examined (the Double Canyon Formation was not a recognized unit when the logs were interpreted). The Beard Oil #1 Jornada del Muerto test, drilled about 11 km southeast of Engle, possibly penetrated as much as 1070 m of McRae Group, but formations were not differentiated, and part of the thickness could include Love Ranch and younger units. No samples are available for this drill hole.

The Double Canyon Formation is composed of interbedded mudstone, siltstone, sandstone, conglomerate, and bedded chert. These rocks have some features in common with older parts of the McRae Group, but other features are unique to the Double Canyon Formation. Chief among the unique features are: (1) a greater proportion of quartz in the sandstone, (2) coarse conglomerate with common pebbles and cobbles of granite mixed with volcanic and silicic clasts, and (3) thick chert intervals and layers that form ridges.

In general, the Double Canyon Formation consists of pale brown to white to light gray sandstone and pebbly sandstone beds, interbedded with greenish, bluish, and olive-gray mudstone and siltstone. Purplish and reddish-gray hues are subordinate. These colors may explain why Lozinsky (1985) mapped strata in the Double Canyon type area as José Creek. Also, the Hall Lake–Double Canyon contact was submerged beneath Elephant Butte Reservoir at the time of Lozinsky's mapping.

Mudstone and siltstone of the Double Canyon Formation are non-fissile and non-resistant to erosion. Thin sandstone interbeds are common, but carbonate nodules are sparse. Sandstone in the lower part of the Double Canyon Formation is mostly light gray, light brownish gray, or greenish gray. These sands are relatively coarse-grained, poorly sorted, and composed of roughly equal proportions of quartz, feldspar, and lithic fragments. Quartz content is as high or higher (commonly about 20% to 40%) than many sandstones elsewhere in the McRae Group. Many of the sandstone beds are conglomeratic and contain 20–30% quartz granules and pebbles together with subrounded to well-rounded clasts of granitic rocks, volcanic rocks, chert of various colors, and mudstone rip-up clasts. Large silicified fossil logs and stumps are present (e. g., Fig. 14D–E).

Amalgamated channel-fill complexes are as much as 7 m thick. Individual sandstone channel fills are thick to very thick, display tangential foresets up to 20 cm tall, and, locally, trough forms or horizontal-planar laminated beds. There are also tabular beds that are internally cross-stratified or horizontal-planar bedded (laminated to 30 cm thick) (Cikoski et al., 2017).

Pebbly sandstone is commonly in very thin to medium, tabular to lenticular beds, some showing low-angle cross-stratification. Pebbles are subangular to rounded and moderately sorted. Small cobbles are rarely present. In general, sand is dominantly medium- to coarse-grained, subangular to subrounded, moderately to well-sorted, and composed of feldspar, quartz, and minor volcanic lithic grains; up section, sand becomes less arkosic, with more volcaniclastic lithic grains (description slightly modified from Cikoski et al., 2017).

Two intervals of chert are present in the Double Canyon Formation in the type section. The upper interval (Fig. A3.12, unit 44; Fig. 14C) is a single bed 1.3 m thick and caps the north to south hogback just west of the fork of Double Canyon, and also holds up a south-dipping hogback at the Double Canyon type section. The lower silicified unit is about 30 m lower in the section and averages about 6 m thick, and in our measured section is two distinct beds (Fig. A3.12, units 37 and 39). Colors are primarily light gray, pink, or yellowish orange, and some layers are greenish to olive. Some of the rock is dense and breaks with conchoidal fractures. Other layers are distinctly granular and may be, at least in part, silicified siltstone and sandstone. The upper unit displays a channel geometry, with the lower contact truncating beds beneath. The lower unit does not have a channel form and contains interbeds of olive to greenish-gray siltstone and mudstone.

Overlying the lower chert beds at Double Canyon is an interval of coarse, pebbly

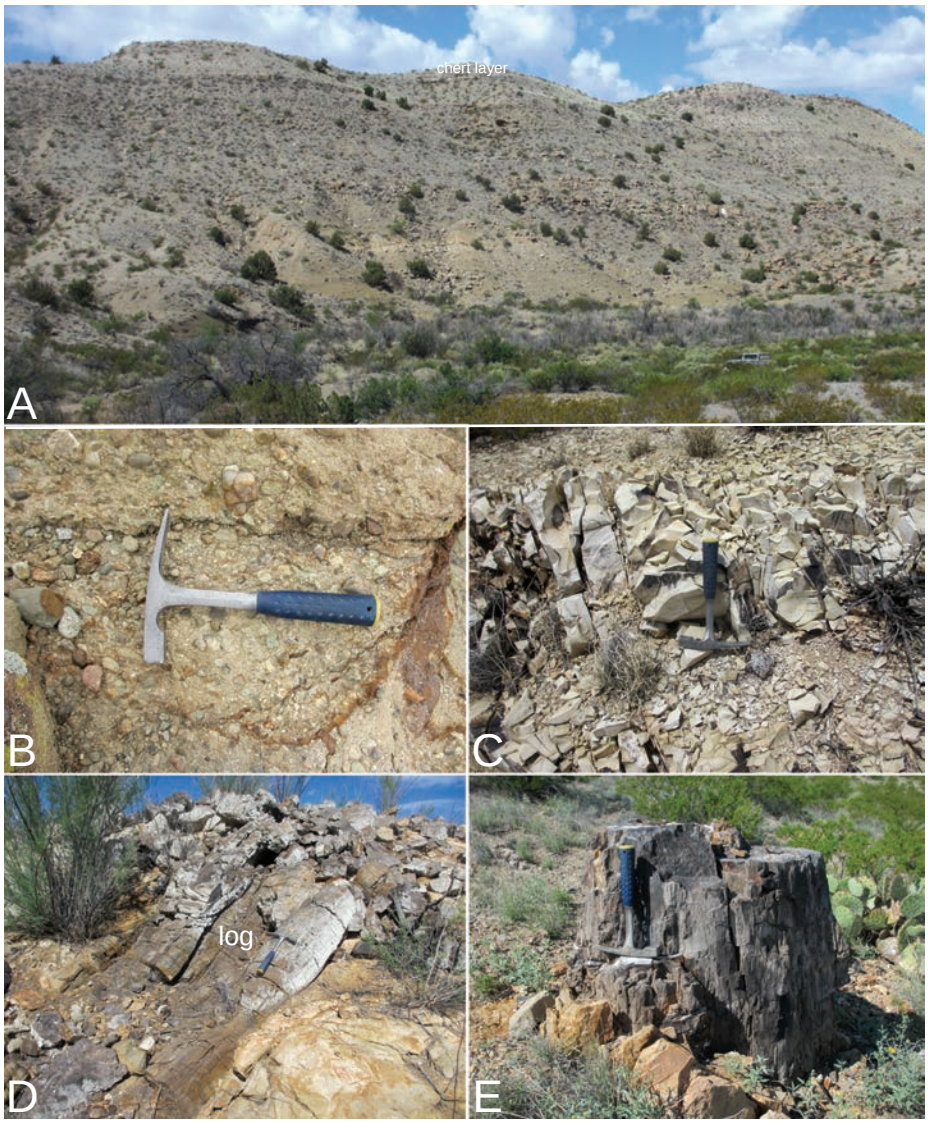

FIGURE 14. Photographs of selected outcrops of the Double Canyon Formation. A, Overview of most of type section. View is looking southwest at ridge approximately 70 m high. Light-colored beds at crest of ridge are chert layers, units 37, 39, and 44 in the measured section (Fig. A3.12). B, Silica-pebble conglomerate. C, Volcanic ash (silcrete) bed. D, Fossil log near base of section. E, Fossil stump in Double Canyon Formation at McRae Forest section.

sandstone that weathers to large, rounded outcrops. This sandstone is composed largely of feldspar, with a smaller proportion of lithic grains and less than 10% quartz. Pebbles include basalt, porphyritc volcanic rocks, chert, and quartz. Large-scale, high-angle crossbeds are prominent. Interbedded with the sandstone is greenish to bluish-gray mudstone.

At the type section of the Double Canyon Formation (Fig. A3.12), the following lithofacies types are distinguished: (1) thick, olive to gray mudstone successions, up to 17 m thick (lithofacies Fm); (2) a single, thin, massive sandstone bed (Sm) intercalated in mudstone (Fig. A3.12, unit 46); (3) thicker sandstone conglomerate units consisting of massive (lithofacies Gmm and Gm) and trough cross-bedded conglomerate (Gt), trough cross-bedded sandstone (St; most abundant lithofacies), rare, horizontally laminated sandstone (Sh), and massive sandstone (Sm); and (4) chert beds that are likely silicified volcanic ash layers. Sandstone beds at the type locality locally display soft-sediment deformation structures and contain fossil wood.

At the McRae Forest section (Fig. A3.13), the exposed thickness of the Double Canyon Formation is 272 m, and the contact with the underlying Flying Eagle Canyon Formation is a fault. The succession is composed of abundant mudstone and covered units, sandstone, subordinate conglomerate and one limestone bed (calcrete) near the middle of the exposed section. Mudstone and covered units are up to 18.1 m thick. Mudstone is mostly greenish, but also displays red and rarely yellowish hues.

In the McRae Forest section conglomerate and sandstone units are mostly less than 3 m thick. Conglomerates are trough cross-bedded (Gt), massive (Gm), rarely matrix supported (Gmm), and are up to 3 m thick. The unit 13 conglomerate at the (faulted) base of the Double Canyon Formation is composed of quartzite, granite and volcanic clasts with diameters up to 10 cm. The conglomerate of unit 15 contains clasts of granite and quartzite up to 20 cm in diameter. The most common sandstone lithotype is trough cross-bedded sandstone (St), which is present as single-storey beds up to 0.8 m thick and multistorey units up to 3.7 m thick. Horizontally laminated sandstone (Sh) intervals are up to 9.5 m thick. Massive sandstone (Sm) is also common, mostly as thin beds (<1 m) and rarely as thicker units up to 2.6 m thick.

Paleontology and age

Fossils from the Double Canyon Formation observed in this study are limited to terrestrial plant material (wood), including some of the fossil wood documented by Estrada-Ruiz et al. (2012a, b) and attributed by them to the José Creek Formation (Fig. 14E). Unfortunately, these fossil woods are of no precise biostratigraphic value. Thus, the age of the Double Canyon Formation cannot be determined with available data.

Sedimentary petrography

Sandstone of the Double Canyon Formation is fine- to coarse-grained and partly pebbly. The sandstone is moderately sorted, and the pebbly sandstone is poorly sorted. The grains are subangular to subrounded. Common grain types are monocrystalline and polycrystalline quartz, feldspars, volcanic rock fragments, and volcanic chert grains (Fig. A5.6A–E). Less common are granitic rock fragments (Fig. A5.6D). Schistose metamorphic rock fragments and mica (biotite) are rare. Feldspars include untwinned grains (mostly orthoclase), plagioclase, microcline, and microperthite. Some of the feldspars appear fresh but most are altered. Volcanic rock fragments exhibit feldspar (plagioclase) phenocrysts and other, smaller volcanic grains (Fig. A5.6E). Rarely, volcanic chert displaying spherulitic? texture is present. The sandstone contains small amounts of matrix.

Due to the high content of feldspars, most sandstones of the Double Canyon Formation plot into the field of arkose; subordinately, sandstones plot into the field of subarkose, sublitharenite, and lithic arenite (classification scheme of Pettijohn et al., 1987). The average composition is $Q_{55}F_{19}L_{26}$ (arkose). In the classification scheme of McBride (1963), most sandstones are feldspathic litharenite, subordinately lithic subarkose, and rarely lithic arkose.

Depositional environments

The lithofacies association of the Double Canyon Formation indicates that it represents fluvial deposits of floodplains and major channels of a braided to anastomosing fluvial system (Miall, 1996, 2010). The channel deposits are generally coarser-grained than in the underlying formations of the McRae Group.

Mudstone facies of the Double Canyon Formation are interpreted as floodplain deposits. An intercalated thin, massive sandstone bed (Fig. A3.13, unit 96) probably formed during a sheetflood event. The thicker conglomerate-sandstone units are interpreted as architectural element CH (channel; lithofacies Gt, St), in combination with element SG (sediment gravity-flow deposits including debris flow; lithofacies Gmm) and element SB (sandy bedforms; lithofacies St, Sh, Sm). The chert beds in the Double Canyon type section are most likely silicified volcanic ash beds, though some textures and structures suggest that some fluvial working or reworking of siliceous material may have been involved in their deposition.

Northern Fra Cristobal Mountain Outcrops

At the northern tip of the Fra Cristobal Range (just into Socorro County) is a small area (less than 2 km^2) of flat-lying to gently dipping sedimentary rocks consisting largely of sandstone (Fig. 2). These strata are juxtaposed with Precambrian granitic rocks to the south along a high-angle, east-striking fault (Fig. 15). Immediately south of the fault in this area, sandstone and boulder conglomerate lie on the granite with a horizontal, depositional contact (Fig. 11F).

Cserna (1956) mapped these rocks as Mesaverde Formation, but did not explain his choice. Using lithologic criteria, McCleary (1960), and Kelley and McCleary (1960) favored the younger McRae, either the José Creek Formation or José Creek–Hall Lake transition zone. Hunter (1986) called the rocks "North Fra Cristobal beds," and considered them to belong to an undetermined part of the McRae Formation.

The sedimentary rocks at the northern tip of the Fra Cristobal Mountains are mainly sandstone but include interbeds of conglomerate (Fig. 11E–F) and sandstone with chert clasts and grains that may represent silicified volcanic ash (Fig. A3.14). The predominant sandstones are light gray or yellowish to brownish gray, fine to very coarse grained, and composed of roughly 60 to 90% quartz, 10 to 30% lithic grains that are mostly chert, and a few percent to 20% feldspar. Sparkly overgrowths are present on quartz grains. The sandstone is laminated to thickly bedded, and exhibits planar cross-lamination together with larger-scale planar and trough cross-bedding. Many beds contain

rounded pebbles of quartz and white, gray, and black chert that range up to about 8 cm in diameter (Fig. 11E). The rock is well indurated and erodes to fairly continuous ledges. Talus-covered slopes between ledges may be underlain by less-resistant lithologies such as mudstone, but no exposures were found. Lack of mudstone exposures handicaps interpretation, because mudstone color and character would help to distinguish candidate formations.

The silica-rich sandstone beds at the northern tip of the Fra Cristobal Mountains are white to light greenish gray, vitreous to semi-vitreous, and break with conchoidal fracture. Beds are about 20 to 150 cm thick, and small pieces of chert are present as angular rip-up clasts within sandstone. Chert-like rocks in the José Creek and Double Canyon Formations in the southern part of the range have been interpreted as silicified volcanic ash. Specifically, the lower part of the Double Canyon Formation contains greenish, chert-like rock.

South of the fault, conglomerate composed of granitic cobbles up to 30 cm across in a sandstone matrix lies with a channel-form contact on Precambrian granitic rock (Fig. 11F). The conglomerate fines upward into sandstone compositionally and texturally similar to that found north of the fault. Angular clasts of chert like those observed north of the fault, are present in the sandstone and imply that sedimentary rocks on both sides of the fault are more or less the same formation and age. The narrow fault zone and lack of strong deformation suggest that displacement was modest, just enough to place Precambrian rocks below the valley floor on the north (Fig. 15). Large-displacement faults that strike east-west are uncommon elsewhere in the range.

The only fossils we observed were nondescript, twig-like impressions and casts of woody plant material in sandstone and in chert. McCleary (1960, p. 22) reported "Petrified wood is present, including palm wood." Hunter (1986, p. 60) mentioned "leaf and wood impressions." If the wood is palm (e.g., *Palmoxylon*), its age could be Cretaceous (and no older) or Paleogene.

The stratigraphic identity of the strata at the northern end of the Fra Cristobal Mountains cannot be positively determined. The Cambrian Bliss Formation and the Pennsylvanian Red House Formation, which rest directly on Precambrian basement elsewhere in the range, can be ruled out based on their very different lithologic composition (most of their sandstones are quartz arenites). Initially we considered the Ash Canyon Formation, based on quartz-rich sandstone containing rounded quartz and chert pebbles. We now disfavor the Ash Canyon because the pebbles are too large, the sandstone contains too much feldspar, and the Ash Canyon lacks so many chert clasts or grains. Moreover, as W.H. Seager (written communication to W. J. Nelson, 2017) pointed out, finding the Ash Canyon in direct contact with Precambrian basement is contrary to regional trends. The deposits in question are unlike the volcanic litharenite that characterizes the José Creek and Hall Lake formations, and likewise, bears little resemblance to the Love Ranch or any younger Cenozoic deposits.

Partially by elimination, our preferred assignment is to the Double Canyon Formation. Arkose and subarkose sandstone, conglomerate with granite pebbles and cobbles, and layers of siliceous rock, some of which are green, characterize this unit to the south. The age of the Double Canyon has not been precisely determined, it is younger than the Hall Lake Member, which contains late Maastrichtian (latest Cretaceous) dinosaurs, and older than the Eocene Love Ranch Formation. Most likely, the Double Canyon is largely, if not entirely, Paleocene age strata.

On this basis, we infer that the granitic core of the Fra Cristobal range was uplifted and eroded during latest Cretaceous to Paleocene time, consistent with earlier interpretations by Kelley and McCleary (1960). In contrast, Nelson (1986) interpreted this outcrop as McRae overlying Precambrian above a detachment fault, but, like Kelley and McCleary (1960), we see the contact as depositional. Granitic cobbles and pebbles in the upper Hall Lake and Double Canyon formations near the southern end of the range likely were derived from this uplift.

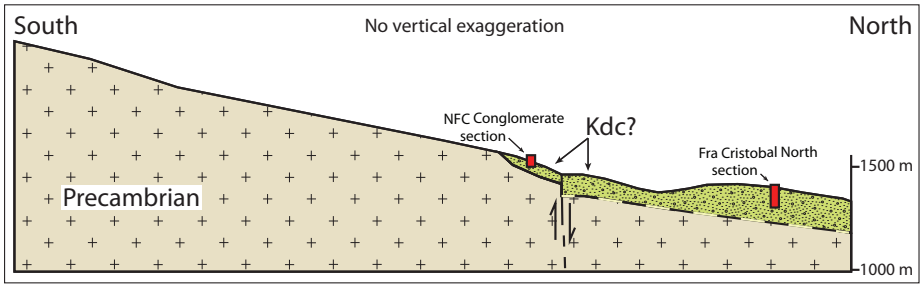

FIGURE 15. Cross section through Cretaceous outcrops at the northern end of the Fra Cristobal Mountains. Kdc = Double Canyon Formation.

Discussion

Petrofacies

Based on thin-section point counts, we can identify five petrofacies in the Cretaceous strata of central Sierra County, two in marine sandstones and three in fluvial sandstones (Fig. 16). In the lower, dominantly marine deposits of the Cretaceous section in Sierra County, sandstones of the Dakota Formation are characterized by high textural and compositional maturity. Dakota sandstones are composed almost entirely of quartz-monocrystalline, polycrystalline, and microcrystalline or cryptocrystalline quartz (the latter types are referred to as "chert" here), and are therefore classified as quartz arenite.

All other sandstones in the marine interval (lower interval of Mancos Formation, Atarque Member, D-Cross Member, Gallup Formation) are very similar in composition to one another, and are somewhat less mature than those of the Dakota Formation. The most common grain type is quartz, but moderate amounts of detrital feldspars and rock fragments are also present. Most of these sandstones are classified as subarkose, and some are sublitharenites (classification of Pettijohn et al., 1987).

Within the fluvial facies (Flying Eagle Canyon Formation through McRae Group), three petrofacies can be distinguished:

1. Petrofacies A of higher compositional maturity, characterized by a high percentage of quartz (monocrystalline, polycrystalline and chert) and comparatively low amounts of detrital feldspars and lithic fragments (Q>70, F<18, L<25). This petrofacies includes sandstone of the Flying Eagle Canyon, Ash Canyon and, locally, the basal José Creek formations. Within this petrofacies, Flying Eagle Canyon sandstones (dominantly sublitharenite) are least mature, and Ash Canyon sandstones (quartz arenite and sublitharenite) are more mature.

2. Petrofacies B of lower compositional maturity, including sandstones of the basal José Creek, Hall Lake and Double Canyon formations. The Hall Lake and Double Canyon formations contain relatively high amounts of lithic fragments and detrital feldspar grains, but the proportion of lithic fragments is notably less than that of Petrofacies C (José Creek Fm). Double Canyon sandstones have higher quartz content, and Hall Lake sandstones have slightly larger amounts of feldspar and lithic fragments. Overall, Double Canyon sandstones display a wider range in composition, from lithic arenite to sublitharenite, subarkose, and arkose. Hall Lake sandstones are less variable in composition, consisting mostly of lithic arenites and subordinate arkoses.

3. Petrofacies C. Sandstones of the José Creek Formation are almost exclusively composed of volcanic rock fragments and detrital plagioclase. These lithic arenites have a unique composition compared to other post-Gallup lithostratigraphic units.

Thus, José Creek, Hall Lake, and Double Canyon sandstones are characterized by significantly higher amounts of lithic fragments and detrital feldspars than Flying Eagle and Ash Canyon sandstones—even when microcrystalline quartz (chert) is included in the lithic fraction. Lithic fragments in the Hall Lake and Double Canyon formations are dominantly derived from intermediate and silicic volcanic rocks. Detrital feldspars (plagioclase) in these formations are also mostly derived from volcanic rocks, and a small part (particularly microcline and perthite) from granitic source rocks. Carbonate clasts derived from the reworking of pedogenic calcrete also form a substantial component of individual sandstone and conglomerate beds in McCrae Group deposits. Other sedimentary rock fragments (such as reworked siltstone fragments) are rare.

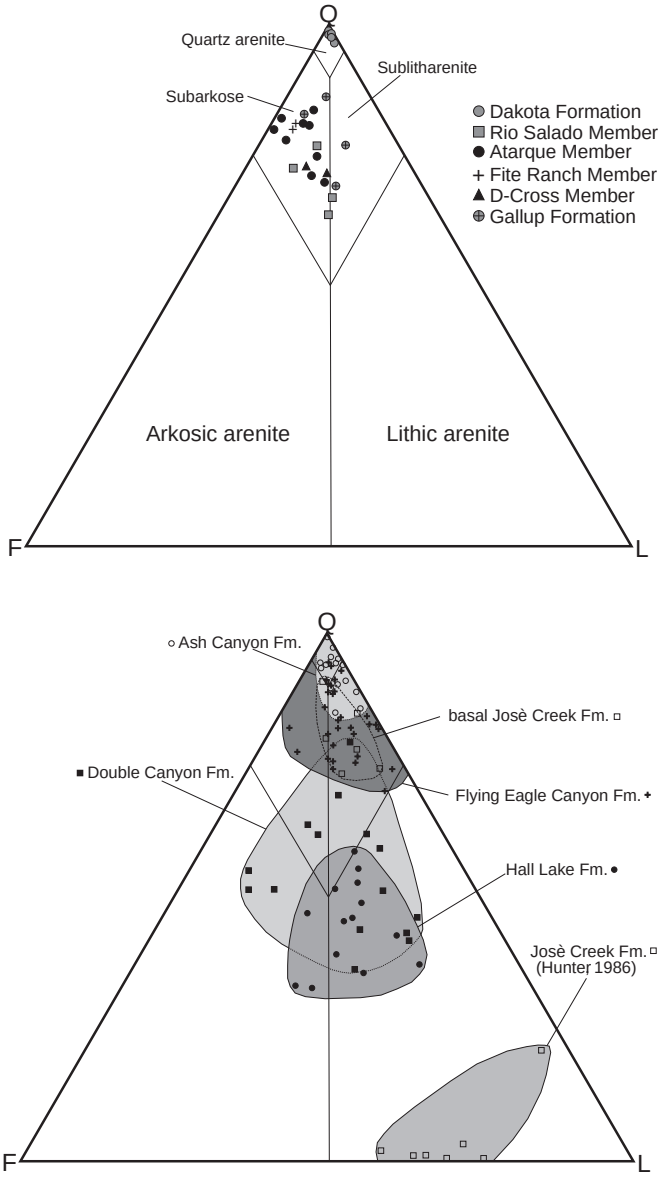

FIGURE 16. Ternary diagrams illustrating petrofacies of Cretaceous sandstones in central Sierra County, using the classification scheme of Pettijohn et al. (1987).

Similar results were noted by Wallin (1983) and Hunter (1986), who considered chert grains as lithic fragments rather than quartz. Hunter (1986) reported a very high quartz content for sandstones of the Ash Canyon Formation and indicated that sandstones of the José Creek and Hall Lake formations are almost exclusively composed of lithic fragments and plagioclase feldspars.

Basal José Creek sandstones, according to our results, are characterized by high quartz content and belong to petrofacies A, whereas the bulk of the José Creek sandstones belong to petrofacies C. Hall Lake and Double Canyon sandstones belong to petrofacies B. Hall Lake and Double Canyon sandstones and most of the José Creek sandstones are "feldspathic sandstones" (containing more than 5% detrital feldspar). They may also be termed "volcanic arkoses" or "plagioclase arkoses" (sensu Folk, 1974), due to the high amount of detrital plagioclase derived from volcanic rocks and the presence of abundant intermediate to silicic volcanic lithic fragments. Such sediments indicate nearby volcanic activity. Deposition must have been relatively rapid because of the susceptibility of feldspar to weathering. Abundance of fresh feldspar and granitic rock fragments in the upper McRae Group also suggests provenance from nearby Precambrian granitic rocks. We propose that the northern part of the Fra Cristobal Range was undergoing uplift related to Laramide tectonic activity during deposition of the sediments there.

Timing of Laramide deformation

Previous reconstructions of Laramide tectonism in southern New Mexico (Seager, 1983; Seager and Mack, 1986, 2003; Seager et al., 1997) primarily address the

region south of the Fra Cristobal Range. This investigation provides some insights into Laramide uplift within and close to the Fra Cristobals and points to areas in which further research is required.

As discussed by Seager and Mack (2003), the Cretaceous succession from the Dakota Formation through the Ash Canyon Formation represents deposition in the Laramide foreland basin. The upper part of the Ash Canyon Formation contains the first evidence for regional uplift, in the form of sedimentary chert clasts that are not found in older units. These cherty gravels and associated quartzose sands probably were derived from Paleozoic rocks undergoing erosion on those uplifts. In particular, limestone of the Pennsylvanian Gray Mesa Formation may have provided an abundant local source of chert. Closer analysis of chert pebbles in the Ash Canyon, particularly a search for included fossils, might strengthen supposition regarding possible source rocks.

The José Creek Formation records the onset of significant volcanism close to the study area. Seager and Mack (2003, p. 48) referred to "an apparently collapsed stratovolcano located east-northeast of Hillsboro" in western Sierra County as a likely source. Ranging from fine ash to boulder-sized clasts, volcanic material overwhelmed other types of sediment in the José Creek (also see Hunter, 1986).

The Hall Lake and Double Canyon formations reflect somewhat reduced deposition of volcaniclastic sediment combined with increasing erosion of nearby basement uplifts. Extensive areas of Precambrian basement were exposed, supplying arkosic sand and granitic pebbles and cobbles to the Cutter sag area. The Rio Grande uplift to the southwest was a major contributor (Seager and Mack, 1986) and likely was accompanied by uplift of what is now the northern Fra Cristobal Range. The apparent deposition of Double Canyon strata directly on Precambrian basement at the northern end of the range provides the strongest evidence for uplift inthat area.

To refine these conclusions, more accurate dating of the upper Hall Lake and Double Canyon units (and the Love Ranch Formation) is required. Dinosaur fossils establish the age of the lower Hall Lake, but younger strata have yielded only fossil wood and other plant remains of poorly constrained age. Radioisotopic dating of apparent volcanic ash layers in the Double Canyon Formation could potentially be fruitful.

Geologic history

A comprehensive understanding of the Cretaceous strata in Sierra County allows a more detailed interpretation of their relationship to Cretaceous strata to the north and to geologic events of Cretaceous time in New Mexico. We summarize these events in the context of broad transgressive-regressive cycles of deposition in the Western Interior Seaway (Weimer, 1960; Molenaar, 1983) and in terms of the Laramide orogenic history discussed above (Fig. 17).

Cretaceous deposition in Sierra County was initiated during the T1 transgression of the Western Interior Seaway during middle-late Cenomanian time. Deposition began with fluvial and then paralic-near shore deposits of the Dakota Formation, followed by open-marine deposition of the Graneros Member of the Mancos Formation. The T1 transgression culminated with relatively low clastic input during deposition of the Greenhorn Member of the Mancos. The succeeding Turonian R1 regression began with marine deposition of the Carlile Member of the Mancos Formation followed by shoreline and coastal plain deposits of the Atarque and Campana members (respectively) of the Tres Hermanos Formation.

The onset of the late Turonian T2 transgression is marked by shoreline deposits of the Fite Ranch Member of the Tres Hermanos Formation. Where the R1–T2 turnaround is in the underlying Campana Member is not clear. Open-marine deposition of the lower D-Cross Member of the Mancos Formation records the culmination of the T2 transgression.

The upper sandy part of the D-Cross Member represents the onset of the R2 regression of late Turonian-early

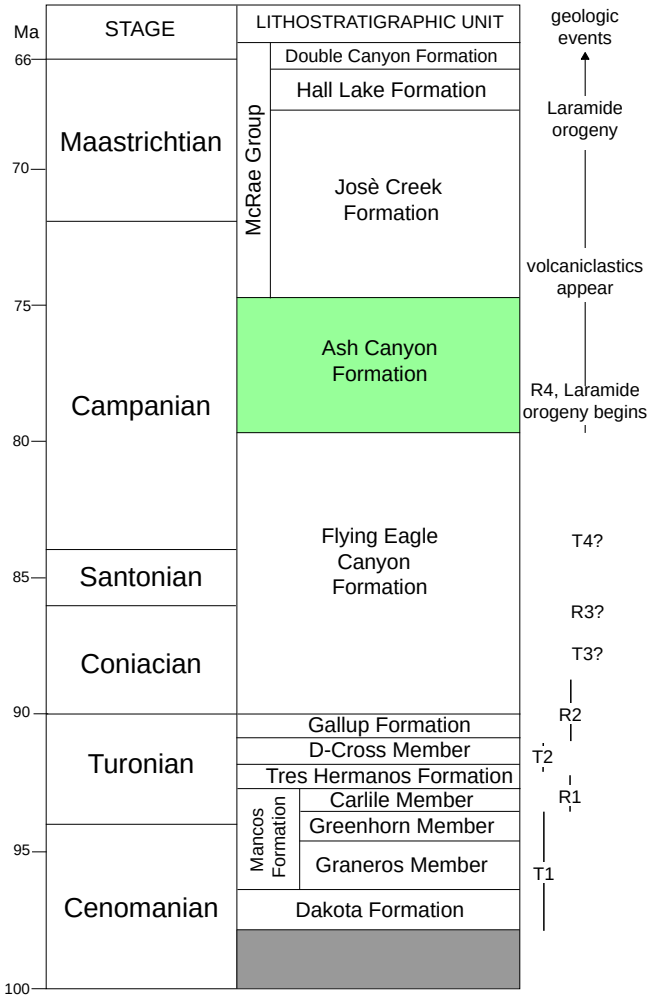

FIGURE 17. Summary of age assignments and geological events recorded by the Cretaceous strata in Sierra County.

Coniacian time. The Gallup Formation represents shoreline deposits of that regression, overlain by coastal plain deposits of the lower part of the Flying Eagle Canyon Formation.

Above this clear record of the T1–R1 and T2–R2 cycles, there is no obvious record in Sierra County of the late Coniacian T3 transgression, early Santonian R3 regression, and the middle-late Santonian T4 transgression. This reflects the fact that Sierra County was at least 100 km landward (south) of the T3 and T4 shorelines, which were located north of Socorro (Molenaar, 1983, figs. 9–10). Brackish water bivalves (oysters) in beds in the upper part of the Flying Eagle Canyon Formation may record one of these transgressions, but no age data are available by which to make a precise correlation. If we consider the Flying Eagle Canyon Formation to encompass the time from the last phase of R2 through T4, then it is essentially equivalent to the entire Coniacian and Santonian stages, or about 6 million years (Fig. 17).

The R4 regression is of early Campanian age and also marks the onset of the Laramide orogeny (e. g., Kauffman and Caldwell, 1993). We hypothesize that deposition of the upper part of the Ash Canyon Formation most likely reflects that tectonic event, so it represents an inland river system homotaxial to the early Campanian Menefee Formation of northern New Mexico, which is the coastal plain deposit of the R4 regression. Biostratigraphic or other age data are needed to test this hypothesis.

The base of the McRae Group records the first significant influx of volcanic detritus into the Cretaceous section of Sierra County. A likely source of this detritus was the Copper Flat complex, a Late Cretaceous magmatic center located near Hillsboro in southwestern Sierra County (Seager et al., 1997; McMillan, 2004), although other evidence of similar-aged volcanic centers could be buried by younger rift basin fill between Copper Flat and Truth or Consequences. Radioisotopic ages of the igneous rocks of the Copper Flats complex are late Campanian, ~74–75 Ma, to (for younger intrusions) early Maastrichtian (~70 Ma) (McLemore et al., 1999; McMillan, 2004). Radioisotopic ages indicate that the Josè Creek Formation may have been deposited quickly between 76–74 Ma (Amato et al., 2017). This suggests that the onset of McRae Group deposition was a late Campanian event and that the base of the José Creek Formation is ~75 Ma (Fig. 17).

The age of the lower part of the Hall Lake Formation is constrained by dinosaur biostratigraphy as late Maastrichtian (~66–68 Ma). Although treated here as units of Cretaceous age, the upper Hall Lake Formation and the Double Canyon Formation may be of Paleocene age. The overlying Love Ranch Formation of likely Eocene age represents the final pulse of the Laramide orogeny in Sierra County.

Acknowledgments

We are particularly grateful to Ted Turner for permission to work on the Armendaris Ranch, and to former ranch manager Tom Waddell, who assisted our access to the ranch and our fieldwork there in many ways. We are also grateful to the U. S. Bureau of Land Management for permitting our paleontological fieldwork on Federal lands in and around the Caballo Mountains. M. Brett-Surman and R. J. Emry made access to the Smithsonian fossil collection possible. P. Sealey provided help with invertebrate fossil identifications. In the field, we received diverse assistance from A. Cantrell, S. Dalman, A. Erickson, D. Koning, A. Lichtig, J. Sayler and T. Suazo, for which we are grateful. We also thank C. Cikoski, D. Koning and W. Seager for their insights on several aspects of the data and interpretations presented here. Careful reviews by B. Black, D. Koning and NM Geology editor B. Allen improved the content and clarity of the manuscript.

References

Amato, J.M., Mack, G.H., Jonell, T.N., Seager, W.R., and Upchurch, G.R., 2017, Onset of the Laramide orogeny and associated magmatism in southern New Mexico based on U-Pb geochronology: Geological Society of America Bulletin, v. 129, p. 1209–1226.

Barker, I.R., Moser, D.E., Kamo, S.L., and Plint, A.G., 2011, High-precision U-Pb zircon ID-TIMS dating of two regionally extensive bentonites: Cenomanian Stage, western Canada foreland basin: Canadian Journal of Earth Sciences, v. 48, p. 543–556.

Bauer, R.D., 1989, Nearshore depositional environments, sediment dispersal, and provenance of the Dakota Sandstone, Caballo Mountains, south-central New Mexico [M.S. thesis]: Las Cruces, New Mexico State University, 64 p.

Bowring, S.A., Schoene, B., Crowley, J.L., Ramezani, J., and Condon, D.J., 2006, High-precision U-Pb zircon geochronology and the stratigraphic record: progress and promise, *in* Olszewski, T., ed., Geochronology: Emerging Opportunities: Paleontological Society Papers, v. 11, p. 23–43.

Buck, B.J., 1992, Deterioration of paleoclimate in the Late Cretaceous, indicated by paleosols in the McRae Formation, south-central New Mexico [M.S. thesis]: Las Cruces, New Mexico State University, 69 p.

Buck, B.J., and Mack, G.H., 1995, Late Cretaceous (Maastrichtian) aridity indicated by paleosols in the McRae Formation, south-central New Mexico: Cretaceous Research, v. 16, p. 559–572.

Buck, B.J., Mack, H.H., and Upchurch, G.R., Jr., 1992, Paleosols and paleoflora of the Upper Cretaceous (Maastrichtian) McRae Formation, south-central New Mexico, and their implications to paleoclimate: New Mexico Geology, v. 14, p. 77.

Bushnell, H.P., 1953, Geology of the McRae Canyon area, Sierra County, New Mexico [M. S. thesis]: Albuquerque, University of New Mexico, 106 p.

Bushnell, H.P., 1955a, Mesozoic stratigraphy of south-central New Mexico, *in* Fitzsimmons, J.P., ed., South-Central New Mexico: New Mexico Geological Society, Guidebook 6, p. 81–87.

Bushnell, H.P., 1955b, Stratigraphy of the McRae Formation, Sierra County, New Mexico: The Compass of Sigma Gamma Epsilon, v. 33, p. 9–17.

Cikoski, C.T., Nelson, W.J., Koning, D.J., Elrick, S., and Lucas, S.G., 2017, Geologic map of the Black Bluffs 7.5-minute quadrangle, Sierra County, New Mexico: New Mexico Bureau of Geology and Mineral Resources, Open-File Geologic Map OF-GM 262, scale 1:24,000.

Coates, A.G., and Kauffman, E.G., 1973, Stratigraphy, paleontology and paleoenvironmenmt of a Cretaceous coral thicket, Lamy, New Mexico: Journal of Paleontology, v. 47, p. 953–968.

Cobban, W.A., and Reeside, J.B., Jr., 1952, Correlation of the Cretaceous formations of the United States: Geological Society of America Bulletin, v. 63, p. 1011–1044.

Cobban, W.A., Hook, S.C., and Kennedy, W.J., 1989, Upper Cretaceous rocks and ammonite faunas of southwestern New Mexico: New Mexico Bureau of Mines and Mineral Resources, Memoir 45, 137 p.

Cobban, W.A., Hook, S.C., and McKinney, K.C., 2008, Upper Cretaceous molluscan record along a transect from Virden, New Mexico to Del Rio, Texas: New Mexico Geology, v. 30, p. 75–92.

Collier, A.J., 1919, Coal south of Mancos, Montezuma County, Colorado: U. S. Geological Survey, Bulletin 691, 296 p.

Collins, D.S., 1999, Laramide and post-Laramide stratigraphy and tectonism on the southeast flank of the Fra Cristobal Mountains, New Mexico [M.S. thesis]: Golden, Colorado School of Mines, 116 p.

Cope, E.D., 1871, [Verbal communication on pythonomorphs]: Proceedings of the American Philosophical Society, v. 11, p. 571–572.

Cope, E.D., 1875, The Vertebrata of the Cretaceous formations of the West: U. S. Geological Survey of the Territories Report 2, 303 p.

Cross, W., and Purington, C.W., 1899, Telluride folio, Colorado: U.S. Geological Survey, Geologic Atlas of the United States Folio, GF-57, 18 p., map scale 1:62,500.

Cserna, E.G., 1956, Structural geology and stratigraphy of the Fra Cristobal quadangle, Sierra County, New Mexico [Ph.D. dissertation]: New York, Columbia University, 104 p.

Dalman, S.G., and Lucas, S.G., 2017, A new chasmosaurine ceratopsid from the Hall Lake Member of the McRae Formation (Maastrichtian), south-central New Mexico: New Mexico Geological Society, 2017 Annual Spring Meeting, Proceedings Volume, p. 23, http://nmgs.nmt.edu/meeting/2017/NMGS_Spring_Meeting_Program_2017.pdf

Dane, C.H., Landis, E.R., and Cobban, W.A., 1971, The Twowells Sandstone Tongue of the Dakota Sandstone and the Tres Hermanos Sandstone as used by Herrick (1900), western New Mexico: U.S. Geological Survey, Professional Paper 750-B, p. B17–B22.

Dane, C.H., Wanek, A.A., and Reeside, J.B., Jr., 1957, Reinterpretation of section of Cretaceous rocks in Alamosa Creek Valley area, Catron and Socorro Counties, New Mexico: American Association of Petroleum Geologists Bulletin, v. 41, p. 181–196.

Darton, N.H., 1922, Geologic structure of parts of New Mexico: U. S. Geological Survey, Bulletin 726, p. 173–275.

Darton, N.H., 1928, "Red beds" and associated formations in New Mexico: U.S. Geological Survey, Bulletin 794, 356 p.

Doyle, J.C., 1951, Geology of the northern Caballo Mountains, Sierra County, New Mexico [M.S. thesis]: Socorro, New Mexico Institute of Mining and Technology, 51 p.

Droser, M.L., and Bottjer, D.J., 1986, A semiquantitative field classification of ichnofabrics: Journal of Sedimentary Petrology, v. 56, p. 558–559.

Estrada-Ruiz, E., Upchurch, G.R., Jr., Wheeler, E.A., and Mack, G.H., 2012a, Late Cretaceous angiosperm woods from the Crevasse Canyon and McRae formations, south-central New Mexico, USA: part 1: International Journal of Plant Science, v. 173, p. 412–428.

Estrada-Ruiz, E., Parrott, J.M., Upchurch, G.R., Jr., Wheeler, E.A., Thompson, D.L., Mack, G.H., and Murray, M.M., 2012b, The wood flora from the Upper Cretaceous Crevasse Canyon and McRae formations, south-central New Mexico, USA: a progress report, *in* Lucas, S.G., McLemore, V.T., Lueth, V.W., Spielmann, J.A., and Krainer, K., eds., Geology of the Warm Springs Region: New Mexico Geological Society, Guidebook 63, p. 503–518.

Ewing, T.E., 2012, Geology and hydrocarbon resource potential of Cretaceous strata in the Jornada del Muerto, Sierra and Socorro counties, New Mexico, *in* Lucas, S.G. McLemore, V.T., Lueth, V.W., Spielmann, J.A., and Krainer, K., eds., Geology of the Warm Springs Region: New Mexico Geological Society, Guidebook 63, p. 569–580.

Ewing, T.E., and Colpitts, R.M., 2012, Thermal maturity in the Engle coal field and Mescal Canyon, Sierra County, New Mexico, *in* Lucas, S.G. McLemore, V.T., Lueth, V.W., Spielmann, J.A., and Krainer, K., eds., Geology of the Warm Springs Region: New Mexico Geological Society, Guidebook 63, p. 71.

Folk, R.L., 1974, Petrology of sedimentary rocks: Austin, Hemphill Publishing Company, 190 p.

Gilbert, G.K., 1896, The underground water of the Arkansas Valley in eastern Colorado: U.S. Geological Survey, Annual Report 2, p. 551–601.

Gillette, D.D., Wolberg, D.L., and Hunt, A.P., 1986, *Tyrannosaurus rex* from the McRae Formation (Lancian, Upper Cretaceous), *in* Clemons, R.E., King, W.E., Mack, G.H., and Zidek, J., eds., Truth or Consequences Region: New Mexico Geological Society, Guidebook 37, p. 235–238.

Harley, G.T., 1934, The geology and ore deposits of Sierra County, New Mexico: New Mexico Bureau of Mines and Mineral Resources, Bulletin 10, 22 p.

Hattin, D.E., 1975, Stratigraphy and depositional environments of Greenhorn Limestone (Upper Cretaceous) of Kansas: Kansas Geological Survey, Bulletin 209, 128 p.

Hattin, D.E., 1987, Pelagic/hempelagic rhythmites of the Greenhorn Limestone (Upper Cretaceous), *in* Clemons, R.E., King, W.E., Mack, G.H., and Zidek, J., eds., Northeastern New Mexico: New Mexico Geological Society, Guidebook 38, p. 237–247.

Head, C.F., and Owen, D.E., 2005, Insights into the petroleum geology and stratigraphy of the Dakota interval (Cretaceous) in the San Juan Basin, *in* Lucas, S.G., Zeigler, K.E., Lueth, V.W., and Owen, D.E., eds., Geology of the Chama Basin: New Mexico Geological Society, Guidebook 56, p. 434–444.

Herrick, C.L., 1900, Report of a geological reconnaissance in western Socorro and Valencia Counties, New Mexico: American Geologist, v. 25, p. 331–346.

Holmes, W.H., 1877, Report [on the San Juan District, Colorado]; Part I, Geology; in Hayden, H.V., Ninth annual report of the United States Geological and Geographical Survey of the Territories, embracing Colorado and parts of adjacent territories, being a progress of the exploration for the year 1875: U.S. Geological and Geographical Survey of the Territories (Hayden), Annual Report [9], p. 237–276.

Hook, S.C., 1983, Stratigraphy, paleontology, depositional framework, and nomenclature of marine Upper Cretaceous rocks, *in* Chapin, C.E., and Callender, J.F., eds., Socorro Region II: New Mexico Geological Society, Guidebook 34, p. 165–172.

Hook, S.C., and Cobban, W.A., 1981, Late Greenhorn (mid-Cretaceous) discontinuity surfaces, southwest New Mexico: New Mexico Bureau of Mines and Mineral Resources, Circular 180, p. 5–21.

Hook, S.C., and Cobban, W.A., 2013, The Upper Cretaceous (Turonian) Juana Lopez beds of the D-Cross Tongue of the Mancos Shale in central New Mexico and their relationship to the Juana Lopez Member of the Mancos Shale in the San Juan Basin: New Mexico Geology, v. 35, p. 59–81.

Hook, S.C., and Cobban, W.A., 2015, The type section of the Upper Cretaceous Tokay Tongue of the Mancos Shale (new name), Carthage coal field, Socorro County, New Mexico: New Mexico Geology, v. 37, p. 27–46.

Hook, S.C., Mack, G.H., and Cobban, W.A., 2012, Upper Cretaceous stratigraphy and biostratigraphy, *in* Lucas, S.G., McLemore, V.T., Lueth, V.W., Spielmann, J.A., and Krainer, K., eds., Geology of the Warm Springs Region: New Mexico Geological Society, Guidebook 63, p. 413–430.

Hook, S.C., Molenaar, C.M., and Cobban, W.A., 1983, Stratigraphy and revision of nomenclature of upper Cenomanian to Turonian (upper Cretaceous) rocks of west-central New Mexico: New Mexico Bureau of Mines and Mineral Resources, Circular 185, 54 p.

Hunter, J.C., 1986, Laramide synorogenic sedimentation in south-central New Mexico: petrologic evolution of the McRae basin [M.S. thesis]: Golden, Colorado School of Mines, 75 p.

Jacobson, R.H., Trask, C.B., Ault, C.H., Carr, D.D., Gray, H.H., Hasenmueller, W.A., Williams, D., and Williamson, A.D., 1985, Unifying nomenclature in the Pennsylvanian System of the Illinois basin: Illinois Academy of Science Transactions, v. 78, p. 1–11.

Kauffman, E.G., and Caldwell, W.G.E., 1993, The Western Interior basin in space and time, *in* Caldwell, W.G.E., and Kauffman, E.G., eds., Evolution of the Western Interior basin: Geological Association of Canada, Special Paper 39, p. 1–30.

Kauffman, E.G., Powell, J.D., and Hattin, D.E., 1969, Cenomanian–Turonian facies across the Raton basin: The Mountain Geologist, v. 6, p. 93–118.

Kelley, V.C., and McCleary, J.T., 1960, Laramide orogeny in south-central New Mexico: American Association of Petroleum Geologists Bulletin, v. 44, p. 1419–1420.

Kelley, V.C., and Silver, C., 1952, Geology of the Caballo Mountains: University of New Mexico, Publications in Geology 4, 286 p.

Kennedy, W.J., Cobban, W.A., and Landman, N.H., 2001, A revision of the Turonian members of the ammonite subfamily Collignoniceratinae from the United States Western Interior and Gulf Coast: Bulletin of the American Museum of Natural History, v. 267, 148 p.

Keyes, C.R., 1905a, Geology and underground water conditions of the Jornada del Muerto, New Mexico: U. S. Geological Survey, Water-supply and Irrigation Paper, no. 123, 42 p.

Keyes, C.R., 1905b, Geological structure of the Jornada del Muerto and adjoining bolson plains: Proceedings of the Iowa Academy of Science, v. 12, p. 167–169.

Landis, E.R., Dane, C.H., and Cobban, W.A., 1973, Stratigraphic terminology of the Dakota Sandstone and Mancos Shale, west-central New Mexico: U. S. Geological Survey, Bulletin 1372-J, p. J1–J44.

Leckie, R.M., Kirkland, J.I., and Elder, W.P., 1997, Stratigraphic framework and correlation of a principal reference section of the Mancos Shale (Upper Cretaceous), *in* Anderson, O.J., Kues, B.S., and Lucas, S.G., eds., Mesozoic geology and paleontology of the Four Corners area: New Mexico Geological Society, Guidebook 48, p. 163–189.

Lee, W.T., 1905, The Engle coal field, New Mexico: U. S. Geological Survey, Bulletin 285, p. 240.

Lee, W.T., 1907a, Water resources of the Rio Grande valley in New Mexico and their development: U. S. Geological Survey, Water-supply Paper 188, 50 p.

Lee, W.T., 1907b, Note on the red beds of the Rio Grande region in central New Mexico: Journal of Geology, v. 15, p. 52–58.

Levron, R.Z., 1995, Morphology and geochemistry of paleosols of the José Creek Member of the McRae Formation (Cretaceous: Maastrichtian), south-central New Mexico [M.S. thesis]: Las Cruces, New Mexico State University, 104 p.

Lichtig, A.J., and Lucas, S.G., 2016, A new species of *Neurankylus* (Testudines: Baenidae) from the Upper Cretaceous Crevasse Canyon Formation, *in* Sullivan, R.M., and Lucas, S.G., eds., Fossil Record 5: New Mexico Museum of Natural History and Science, Bulletin 74, p. 117–119.

Lichtig, A.J., and Lucas, S.G., 2017, Fossil turtles of the Upper Cretaceous McRae Formation, Sierra County, New Mexico: New Mexico Geological Society, 2017 Annual Spring Meeting, Proceedings Volume, p. 42, http://nmgs.nmt.edu/meeting/2017/NMGS_Spring_Meeting_Program_2017.pdf

Lozinsky, R.P., 1982, Geology and late Cenozoic history of the Elephant Butte area, Sierra County, New Mexico [M.S. thesis]: Albuquerque, University of New Mexico, 142 p.

Lozinsky, R.P., 1985, Geology and late Cenozoic history of the Elephant Butte area, Sierra County, New Mexico: New Mexico Bureau of Mines and Mineral Resources, Circular 187, 40 p.

Lozinsky, R.P., Hunt, A., Wolberg, D.L., and Lucas, S.G., 1984, Late Cretaceous dinosaur discoveries from the McRae Formation, Sierra County, New Mexico: New Mexico Geology, v. 6, p. 72–77.

Lucas, S.G., and Anderson, O.J., 1998, Corals from Upper Cretaceous of south-central New Mexico, *in* Mack, G.H., Austin, G.S., and Barker, J.M., eds., Las Cruces Country II: New Mexico Geological Society, Guidebook 49, p. 205–207.

Lucas, S.G., and Estep, J.W., 1998, Cretaceous stratigraphy and biostratigraphy in the southern San Andres Mountains, *in* Mack, G.H., Austin, G.S., and Barker, J.M., eds., Las Cruces Country II: New Mexico Geological Society, Guidebook 49, p. 187–196.

Lucas, S.G., and Krainer, K., 2012, The Lower Permian Yeso Group in the Fra Cristobal and Caballo Mountains, *in* Lucas, S.G. McLemore, V.T., Lueth, V.W., Spielmann, J.A., and Krainer, K., eds., Geology of the Warm Springs Region: New Mexico Geological Society, Guidebook 63, p. 377–394.

Lucas, S.G., Hunt, A.P., and Kues, B.S., 1987, Stratigraphic nomenclature and correlation chart for northeastern New Mexico, *in* Clemons, R.E., King, W.E., Mack, G.H., and Zidek, J., eds., Northeastern New Mexico: New Mexico Geological Society, Guidebook 38, p. 351–354.

Lucas, S.G., Mack, G.H., and Estep, J.W., 1998a, The ceratopsian dinosaur *Torosaurus* from the Upper Cretaceous McRae Formation, *in* Mack, G.H., Austin, G.S., and Barker, J.M., eds., Las Cruces Country II: New Mexico Geological Society, Guidebook 49, p. 223–227.

Lucas, S.G., Anderson, O.J., and Estep, J.W., 1998b, Stratigraphy and correlation of middle Cretaceous rocks (Albian-Cenomanian) from the Colorado Plateau to the southern High Plains, north-central New Mexico, *in* Lucas, S.G., Kirkland, J.I., and Estep, J.W., eds., Lower and middle Cretaceous terrestrial ecosystems: New Mexico Museum of Natural History and Science, Bulletin 14, p. 57–66.

Lucas, S.G., Dalman, S.G., and Sullivan, R.M., 2016, Cretaceous dinosaur footprints from Sierra County, New Mexico, *in* Sullivan, R.M., and Lucas, S.G., eds., Fossil Record 5: New Mexico Museum of Natural History and Science, Bulletin 74, p. 151–152.

Lucas, S.G., Sullivan, R.M., and Spielmann, J.A., 2012, Cretaceous vertebrate biochronology, North American Western Interior: Journal of Stratigraphy, v. 36, p. 436–461.

Lucas, S.G., Estep, J.W., Boucher, L.D., and Anderson, B.G., 2000, Cretaceous stratigraphy, biostratigraphy and depositional envi-ronments near Virden, Hidalgo County, New Mexico, *in* Lucas, S.G., ed., New Mexico's Fossil Record 2: New Mexico Museum of Natural History and Science, Bulletin 16, p. 107–119.

Lucas, S.G., Dalman, S.G., Lichtig, A.J., Elrick, S., Nelson, W.J., and Krainer, K., 2017a, Stratigraphy and age of the dinosaur-dominated fossil assemblage of the Upper Cretaceous Hall Lake Member of the McRae Formation, Sierra County, New Mexico: New Mexico Geological Society, 2017 Annual Spring Meeting, Proceedings Volume, p. 47, http://nmgs.nmt.edu/meeting/2017/NMGS_Spring_Meeting_Program_2017.pdf

Lucas, S.G., Dalman, S.G., Lichtig, A.J., Elrick, S., Nelson, W.J., and Krainer, K., 2017b, Stratigraphic distribution and age of the dinosaurs of the Upper Cretaceous Hall Lake Member of the McRae Formation, Sierra County, New Mexico: Society of Vertebrate Paleontology, Abstracts of Papers, 77th Annual Meeting, p. 154, http://vertpaleo.org/Annual-Meeting/Annual-Meeting-Home/SVP-2017-program-book.aspx

Lyson, T.R., Joyce, W.G., Lucas, S.G., and Sullivan, R.M., 2016, A new baenid turtle from the early Paleocene (Torrejonian) of New Mexico and a species-level phylogenetic analysis of Baenidae: Journal of Paleontology, v. 90, p. 305–316.

Mack, G.H., 1987, Mid-Cretaceous (late Albian) change from rift to retroarc foreland basin in southwestern New Mexico: Geological Society of America Bulletin, v. 98, p. 507–514.

Mack, G.H., and Seager, W.R., 1993, Geologic map of the Engle quadrangle, Sierra County, New Mexico: New Mexico Bureau of Geology and Mineral Resources, Open-file Digital Geologic Map OF-GM 207, scale 1:24,000.

Mack, G.H., Lawton, T.F., and Giles, K.A., 1998, First-day road log from Las Cruces to Derry Hills and Mescal Canyon in the Caballo Mountains, *in* Mack, G.H., Austin, G.S., and Barker, J.M., eds., Las Cruces Country II: New Mexico Geological Society, Guidebook 49, p. 1–21.

Mack, G.H., Hook, S.C., Giles, K.A., and Cobban, W.A., 2016, Sequence stratigraphy of the Mancos Shale, lower Tres Hermanos Formation and coeval middle Cenomanian to middle Turonian strata, southern New Mexico, USA: Sedimentology, v. 63, p. 781–808.

Mason, J.T., 1976, Geology of the Caballo Peak quadrangle [M.S. thesis]: Albuquerque, University of New Mexico, 131 p.

McBride, E.F., 1963, A classification of sandstones: Journal of Sedimentary Petrology, v.33, p. 664–669.

McCleary. J.T., 1960, Geology of the northern part of the Fra Cristobal range, Sierra and Socorro Counties, New Mexico [M. S. thesis]: Albuquerque, University of New Mexico, 59 p.

McLemore, V.T., Munroe, E.A., Heizler, M.T., and McKee, D., 1999, Geochemistry of the Copper Flat porphyry and associated deposits of the Hillsboro mining district, Sierra County, New Mexico, USA: Journal of Geochemical Exploration, v. 67, p. 167–189.

McMillan, N.J., 2004, Magmatic record of Laramide subduction and the transition to Tertiary extension: Upper Cretaceous through Eocene igneous rocks of New Mexico, *in* Mack, G.H., and Giles, K.A., eds., The geology of New Mexico: a geologic history: New Mexico Geological Society, Special Publication 11, p. 249–270.

Meek, F.B., and Hayden, F.V., 1861, Descriptions of new Lower Silurian (Primordial), Jurassic, Cretaceous, and Tertiary fossils collected in Nebraska…, with some remarks on the rocks from which they were obtained: Proceedings of the Academy of Natural Sciences of Philadelphia, v. 13, p. 417–432.

Melvin, J.W., 1963, Cretaceous stratigraphy in the Jornada del Muerto region, including the geology of the Mescal Creek area, Sierra County, New Mexico [M.S. thesis]: Albuquerque, University of New Mexico, 121 p.

Miall, A.D., 1996, The geology of fluvial deposits. Sedimentary facies, basin analysis, and petroleum geology: Berlin, Springer Verlag, 582 p.

Miall, A.D., 2010, Alluvial Deposits, *in* James, N.P., and Dalrymple, R.W., eds., Facies models 4: Geological Association of Canada (GEOtext 6), p. 105–137.

Miller, M.F., and Smail, S.E., 1997, A semiquantitative field method for evaluating bioturbation on bedding planes: Palaios, v. 12, p. 391–396.

Molenaar, C.M., 1973, Sedimentary facies and correlation of the Gallup Sandstone and associated formations, northwestern New Mexico, *in* Fassett, J.E., ed., Cretaceous and Tertiary rocks of the southern Colorado Plateau: Durango, CO, Four Corners Geological Society, p. 85–110.

Molenaar, C.M., 1974, Correlation of the Gallup Sandstone and associated formations, Upper Cretaceous, *in* Siemers, C.T., Woodward, L.A., and Callender, J.F., eds., Ghost Ranch: New Mexico Geological Society, Guidebook 25, p. 251–258.

Molenaar, C.M., 1983, Major depositional cycles and regional correlations of Upper Cretaceous rocks, southern Colorado Plateau and adjacent areas, *in* Reynolds, M.W., and Dolly, E.D., eds., Mesozoic paleogeography of the west-central United States, Rocky Mountain paleogeography symposium 2: Denver, Rocky Mountain Section of the Society of Economic Paleontologists and Mineralogists, p. 201–224.

Nelson, E.P., 1986, Geology of the Fra Cristobal Range, *in* Clemons, R.E., King, W.E., Mack, G.H., and Zidek, J., eds., Truth or Consequences Region: New Mexico Geological Society, Guidebook 37, p. 83–91.

Nelson, W.J., Lucas, S.G., Krainer, K., McLemore, V.T., and Elrick, S., 2012, Geology of the Fra Cristobal Mountains, New Mexico, *in* Lucas, S.G., McLemore, V.T., Lueth, V.W., Spielmann, J.A., and Krainer, K., eds., Geology of the Warm Springs Region: New Mexico Geological Society, Guidebook 63, p. 195–209.

NMBGMR, 2003, Geologic map of New Mexico: New Mexico Bureau of Geology and Mineral Resources, 2 sheets, scale 1:500,000.

Obradovich, J.D., 1993, A Cretaceous time scale; *in* Caldwell, W.G.E., and Kauffman, E.G., eds., Evolution of the Western Interior basin: Geological Association of Canada, Special Paper 39, p. 1–30.

Osburn, J.C., 1983, Coal resources of Socorro County, New Mexico, *in* Chapin, C.E., and Callender, J.F., eds., Socorro Region II: New Mexico Geological Society, Guidebook 34, p. 223–226.

Owen, D.D., 1856, Report of the geological survey in Kentucky, made during the years 1854 and 1855: Frankfort, KY, A.G. Hodges, State Printer, 416 p.

Owen, D.E., and Owen, D.E., Jr., 2005, The White Rock Mesa Member of the Dakota Sandstone (Cretaceous) of the San Juan Basin, New Mexico and Colorado. A formal new lithostratigraphic unit to replace the informal "Dakota main body", *in* Lucas, S.G., Zeigler, K.E., Lueth, V.W., and Owen, D.E., eds., Geology of the Chama Basin: New Mexico Geological Society, Guidebook 56, p. 227–230.

Owen, D.E., and Sparks, D.K., 1989, Surface to subsurface correlation of the intertongued Dakota Sandstone-Mancos Shale (Upper Cretaceous) in the Zuni embayment, New Mexico, *in* Anderson, O.J., Lucas, S.G., Love, D.W., and Cather, S.M., eds., Southeastern Colorado Plateau: New Mexico Geological Society, Guidebook 40, p. 265–267.

Owen, D.E., Siemers, C.T., and Owen, D.E., Jr., 2007, Dakota and adjacent Morrison and lower Mancos stratigraphy (Cretaceous and Jurassic) in the Holy Ghost Spring quadrangle, land of pinchouts, *in* Kues, B.S., Kelley, S.A., and Lueth, V.W., eds., Geology of the Jemez Region II: New Mexico Geological Society, Guidebook 58, p. 188–194.

Owen, D.E., Forgas, A.M., Miller, S.A., Stelly, R.J., and Owen, D.E., Jr., 2005, Surface and subsurface stratigraphy of the Burro Canyon Formation, Dakota Sandstone, and intertongued Mancos Shale of the Chama Basin, New Mexico, *in* Lucas, S.G., Zeigler, K.E., Lueth, V.W., and Owen, D.E., eds., Geology of the Chama Basin: New Mexico Geological Society, Guidebook 56, p. 218–226.

Parris, D.C., Grandstaff, B.S., Denton, R.K., Jr., and Lucas, S.G., 1997, Type locality of *Liodon dyspelor* Cope (Reptilia: Mosasauridae): Proceedings of the Academy of Natural Sciences of Philadelphia, v. 147, p. 193–203.

Peterson, F., and Kirk, A.R., 1977, Correlation of the Cretaceous rocks in the San Juan, Black Mesa, Kaiparowits and Henry basins, *in* Fassett, J.E., and James, H.L., eds., San Jaun Basin III: New Mexico Geological Society, Guidebook 28, p. 167–178.

Pettijohn, F.J., Potter, P.E., and Siever, R., 1987, Sand and sandstone (2nd ed): New York, Springer-Verlag, 553 p.

Pike, W.S., Jr., 1947, Intertonguing marine and nonmarine Cretaceous deposits of New Mexico, Arizona, and southwestern Colorado: Geological Society of America, Memoir 24, 103 p.

Rankin, C.H., 1944, Stratigraphy of the Colorado Group, Upper Cretaceous, in northern New Mexico: New Mexico Bureau of Mines and Mineral Resources, Bulletin 20, 30 p.

Reeside, J.B., Jr., 1924, Upper Cretaceous and Tertiary formations of the western part of the San Juan Basin, Colorado and New Mexico: U.S. Geological Survey, Professional Paper 134, p. 1–70.

Russell, D.A., 1967, Systematics and morphology of American mosasaurs: Yale University Peabody Museum Bulletin 23, 241 p.

Schmitz, M.D., 2012, Radiometric ages used in GTS 2012; *in* Gradstein, F.M., Ogg, J.G., Schmitz, M.D., and Ogg, G.M., eds., The geologic time scale 2012: Amsterdam, Elsevier, p. 1045–1082.

Schoene, B., 2014, U-Th-Pb geochronology: Treatise on Geochemistry, v. 4, p. 341–378.

Seager, W.R., 1981, Geology of the Organ Mountains and southern San Andres Mountains, New Mexico: New Mexico Bureau of Mines and Mineral Resources, Memoir 36, 97 p.

Seager, W.R., 1983, Laramide wrench faults, basement-cored uplifts, and complimentary basins in southern New Mexico: New Mexico Geology, v. 5, p. 69–76.

Seager, W.R., 1995a, Geologic map of the Alivio quadrangle, Sierra and Doña Ana Counties, New Mexico: New Mexico Bureau of Geology and Mineral Resources, Open-file Digital Geologic Map OF-GM 204, scale 1:24,000.

Seager, W.R., 1995b, Geologic map of the Upham quadrangle, Sierra County, New Mexico: New Mexico Bureau of Geology and Mineral Resources, Open-file Digital Geologic Map OF-GM 205, scale 1:24,000.

Seager, W.R., 1995c [updated 2002], Geologic map of the Upham Hills quadrangle, Sierra and Doña Ana Counties, New Mexico: New Mexico Bureau of Geology and Mineral Resources, Open-file Digital Geologic Map OF-GM 113, scale 1:24,000.

Seager, W.R., 2005, Geologic map of the Prisor Hill quadrangle, Sierra County, New Mexico: New Mexico Bureau of Geology and Mineral Resources, Open-file Digital Geologic Map OF-GM 114, scale 1:24,000.

Seager, W.R., 2007, Geologic map of the Cutter quadrangle, Sierra County, New Mexico: New Mexico Bureau of Geology and Mineral Resources, Open-file Digital Geologic Map OF-GM 206, scale 1:24,000.

Seager, W.R., and Mack, G.H., 1986, Laramide paleotectonics of southern New Mexico: American Association of Petroleum Geologists, Memoir 41, p. 669–685.

Seager, W.R., and Mack, G.H., 2003, Geology of the Caballo Mountains, New Mexico: New Mexico Bureau of Geology and Mineral Resources, Memoir 49, 135 p.

Seager, W.R., and Mack, G.H., 2005, Geologic map of Apache Gap and Caballo quadrangles, Sierra County, New Mexico: New Mexico Bureau of Geology and Mineral Resources, Geologic Map 74, 2 sheets, map scale 1:24,000.

Seager, W.R., Mack, G.H., and Lawton, T.F., 1997, Structural kinematics and depositional history of a Laramide uplift-basin pair in southern New Mexico: implications for development of intraforeland basins: Geological Society of America Bulletin, v. 109, p. 1389–1401.

Sears, J.D., 1925, Geology and coal resources of the Gallup-Zuni basin, New Mexico: U.S. Geological Survey, Bulletin 767, 53 p.

Shaver, R.H., Ault, C.H., Burger, A.M., Carr, D.D., Droste, J.B., Eggert, D.L., Gray, H.H., Harper, Denver, Hasenmueller, N.R., Hasenmueller, W.A., Horowitz, A.S., Hutchison, H.C., Keith, B.D., Keller, S.J., Patton, J.B., Rexroad, C.B., and Wier, C.E., 1986, Compendium of Paleozoic rock-unit stratigraphy in Indiana–a revision: Indiana Geological Survey, Bulletin 59, 203 p.

Shumard, G.G., 1860, The geological structure of the "Jornada del Muerto," New Mexico: St. Louis Academy of Science Transactions, v. 1, p. 341–355.

Suazo, T.L., Cantrell, A.K., and Lucas, S.G., 2014, Newly discovered dinosaur fossils from the Upper Cretaceous (late Maastrichtian) McRae Formation, Sierra County, New Mexico: New Mexico Geological Society, 2014 Annual Spring Meeting, Proceedings Volume, p. 60, http://nmgs.nmt.edu/meeting/2014/Spring_Meeting_Program_2014.pdf

Sullivan, R.M., and Lucas, S.G., 2015, Cretaceous vertebrates of New Mexico, in Lucas, S.G., and Sullivan, R.M., eds., Fossil vertebrates in New Mexico: New Mexico Museum of Natural History and Science, Bulletin 68, p. 105–129.

Sullivan, R.M., Boere, A.C., and Lucas, S.G., 2005, Redescription of the ceratopsid dinosaur *Torosaurus utahensis* (Gilmore, 1946) and a revision of the genus: Journal of Paleontology, v. 79, p. 564–582.

Thompson, S. III, 1955a, Geology of the southern part of the Fra Cristobal Range, Sierra County, New Mexico [M.S. thesis]: Albuquerque, University of New Mexico, 75 p.

Thompson, S. III, 1955b, Geology of the Fra Cristobal Range, *in* Fitzsimmons, J.P., ed., South-Central New Mexico: New Mexico Geological Society, Guidebook 6, p. 155–157.

Thompson, S. III, 1961, Geology of the southern part of the Fra Cristobal Range, Sierra County, New Mexico: New Mexico Bureau of Mines and Mineral Resources, Open-file Report 380, 89 p. and map, scale 1:24,000.

Tidwell, W.D., Ash, S.R., and Parker, L.R., 1981, Cretaceous and Tertiary floras of the San Juan Basin, *in* Lucas, S.G., Rigby, J.K., Jr., and Kues, B.S., eds., Advances in San Juan Basin paleontology: Albuquerque, University of New Mexico Press, p. 307–332.

Tucker, M.E., 1988, Techniques in Sedimentology: Oxford, Blackwell Scientific Publications, 394 p.

Upchurch, G.R., Jr., and Mack, G.H., 1998, Late Cretaceous leaf megafloras from the José Creek Member, McRae Formation of New Mexico, *in* Mack, G.H., Austin, G.S., and Barker, J.M., eds., Las Cruces Country II: New Mexico Geological Society, Guidebook 49, p. 209–222.

Wallin, E.T., 1983, Stratigraphy and paleoenvironments of the Engle coal field, Sierra County, New Mexico [M.S. thesis]: Socorro, New Mexico Institute of Mining and Technology, 127 p.

Warren, R.G., 1978, Characterization of the lower crust-upper mantle of the Engle basin, Rio Grande rift, from a petrochemical and field geologic study of basalts and their inclusions [M. S. thesis]: Albuquerque, University of New Mexico, 156 p.

Weimer, R.J., 1960, Upper Cretaceous stratigraphy, Rocky Mountain area: American Association of Petroleum Geologists Bulletin, v. 44, p. 1–20.

White, C.A., 1878, Report on the geology of a portion of northwestern Colorado: U. S. Geological and Geographical Survey of the Territories, 10th Annual Report, p. 3–59.

Wilmarth, M.G., 1928, Lexicon of geologic names of the United States: U. S. Geological Survey, Bulletin 896, 2396 p.

Wolberg, D.L, Lozinsky, R.P., and Hunt, A.P., 1986, Late Cretaceous (Maastrichtian–Lancian) vertebrate paleontology of the McRae Formation, Elephant Butte area, Sierra County, New Mexico, *in* Clemons, R.E., King, W.E., Mack, G.H., and Zidek, J., eds., Truth or Consequences Region: New Mexico Geological Society, Guidebook 37, p. 227–234.

Appendices for this paper are available at: https://geoinfo.nmt.edu/repository/index.cfml?rid=20190002

Gallery of Geology

The trace fossil *Ophiomorpha* from the Upper Cretaceous Trinidad Sandstone, northeastern New Mexico

Spencer G. Lucas
New Mexico Museum of Natural History, Albuquerque, NM 87104

Trace fossils are structures in sedimentary rocks that record the interaction of organisms with sediment. Often thought of as "fossilized behavior," trace fossils are important archives of the activities of extinct plants and animals. Many trace fossils are also strong indicators of paleoenvironments, an observation that underlies the concept of ichnofacies. This is in part because specific organismal behaviors are often correlated with particular substrates. Many trace makers are also specific to a particular type of habitat, and this specificity provides an important tool in identifying and interpreting ancient environments.

One environmentally diagnostic trace fossil is the burrow *Ophiomorpha*, which indicates littoral to shallow-marine paleoenvironments (Buatois and Mángano, 2011). Thus, *Ophiomorpha* are found in virtually all of the shallow-marine or shoreline Upper Cretaceous

This outcrop just southwest of Raton, New Mexico, is characteristic of the Upper Cretaceous Trinidad Sandstone in the Raton Basin. The Trinidad forms a bold cliff of light-colored sandstone that accumulated in a nearshore environment above slope-forming shale of the offshore-marine, Upper Cretaceous Pierre Shale. Coal beds above the Trinidad Sandstone mark the base of the overlying, fluvio-deltaic deposits of the Upper Cretaceous Vermejo Formation.

A characteristic *Ophiomorpha* burrow in the Trinidad Sandstone at Vermejo Park, northeastern New Mexico. Note the nodose, "corn-cob" wall of the burrow, which branches in the lower left part of the photograph. For scale, the pen is approximately 14 cm long.

sandstone-dominated stratigraphic units in the San Juan Basin of northwestern New Mexico. In the Raton Basin of northeastern New Mexico, *Ophiomorpha* is particularly abundant in the Upper Cretaceous Trinidad Sandstone, which records the final retreat of the Western Interior Seaway from the state.

Ophiomorpha consists of cylindrical tunnels with diameters of 0.5 to 3 cm and burrow lengths of up to one meter. These burrows often form three-dimensional burrow systems comprising both vertical and horizontal tunnels. The tunnels usually branch at acute angles, and the branch points are often "swollen"—larger than the adjacent tunnel segments. Perhaps most characteristic of *Ophiomorpha* is the structure of the burrow wall, which is packed with discoidal, ovate brick-like pellets several millimeters in diameter, giving the burrow wall its diagnostic nodose exterior—a "corn-cob" texture.

An extensive literature on *Ophiomorpha* has been published (see, for example, the bibliographies in Müller, 1969; Kennedy and Sellwood, 1970; Häntzschel, 1975). Particularly important to understanding the trace fossil is the recognition that modern decapod crustaceans, in particular callianassid shrimp, make *Ophiomorpha*-like burrows (Weimer and Hoyt, 1964). This correlation of trace and trace maker has also found fairly direct support in Cretaceous strata of Delaware, where Pickett et al. (1971) reported fossilized callianassid claws associated with *Ophiomorpha* burrows. Today, the callianassid shrimp build such burrows by digging and then packing the burrow walls with pellets that the shrimp cement together. Swollen parts of the burrows are places where the shrimp turned around.

The oldest fossils of *Ophiomorpha* are from Pennsylvanian–Permian rocks (Chamberlain and Baer, 1973; Driese and Dott, 1984; Buatois et al., 2002; Carmona et al., 2004; though note that L. Buatois, written commun., 2019, now doubts that any of these Paleozoic records should be assigned to *Ophiomorpha*). Reports of *Ophiomorpha* in

These *Ophiomorpha* burrows in the Trinidad Sandstone at Vermejo Park, New Mexico, show preservation of not only the exterior burrow walls, but of the fill of the burrow, which is finer grained than the host rock. For scale, the pen is about 14 cm long.

New Mexico are restricted to Cretaceous rocks. In addition to being indicators of shallow-marine, shoreline environments, the burrows also create what has been called an ichnofabric in the strata that were burrowed. Thereby, the *Ophiomorpha* burrows can enhance the permeability and the vertical transmissivity of impermeable sediment. This takes place when the burrows are filled with a contrasting sediment derived from overlying deposits. Thus, if the encasing bed is impermeable and the fill is permeable, the preserved burrow creates anisotropic porosity and permeability (Pemberton and Gingras, 2005). Furthermore, the burrow may also pass through an impermeable layer that separates two permeable layers.

Thalassinoides is another crustacean burrow preserved in the Trinidad Sandstone at Vermejo Park, New Mexico. *Thalassinoides* and *Ophiomorpha* are fairly similar in size and branching style, but *Thalassinoides* lacks the nodose exterior burrow wall that is diagnostic of *Ophiomorpha*. For scale, the pen is approximately 14 cm long.

In the Raton Basin of northeastern New Mexico and southeastern Colorado, the Trinidad Sandstone is a sandstone-dominated lithostratigraphic unit that is up to 100 m thick (Lee, 1917; Johnson and Wood, 1956). It consists of light-gray to yellowish-gray, fine- to medium-grained feldspathic sandstone that is tabular bedded or cross bedded, forming a bold, light-colored cliff at most of its outcrops. The contact with the underlying Upper Cretaceous Pierre Shale is a transition zone of interbedded shale and sandstone representing a lower shoreface environment of deposition. A coal bed marks the base of the Upper Cretaceous Vermejo Formation above the Trinidad Sandstone.

The Trinidad Sandstone was deposited in delta-front and other shoreline settings as the Western Interior Seaway retreated to the east and northeast (Pillmore and Maberry, 1976). *Ophiomorpha* is common and particularly abundant at almost all outcrops of the Trinidad Sandstone. The *Ophiomorpha* in the Trinidad Sandstone are primarily vertical and are indicative of relatively high-energy, delta-front and distal-delta paleoenvironments. They are commonly associated with other trace fossils indicative of shallow-marine or shoreline paleoenvironments, such as *Thalassinoides*, *Aulichnus,* or *Teichichnus*. Wherever it is found, *Ophiomorpha* is a good indicator of shallow-marine settings, usually of relatively high energy of deposition.

References

Buatois, L.A., and Mángano, M.G., 2011, Ichnology: organism-substrate interactions in space and time: Cambridge, Cambridge University Press, 358 p.

Buatois, L.A., Mángano, M.G., Alissa, A. and Carr, T.R., 2002, Sequence stratigraphy and sedimentologic significance of biogenic structures from a late Paleozoic marginal- to open-marine reservoir, Morrow Sandstone, subsurface of Kansas, USA: Sedimentary Geology, v. 152, p. 99–132.

Carmona, N.B., Buatois, L.A., and Mángano, G., 2004, The trace fossil record of burrowing decapod crustaceans: evaluating evolutionary radiations and behavioural convergence: Fossils and Strata, v. 51, p. 141–153.

Chamberlain, C.K., and Baer, J.L., 1973, *Ophiomorpha* and a new thalassinoid burrow from the Permian of Utah: Brigham Young University Geology Studies, v. 20, p. 79–94.

Driese, S.G., and Dott, R.H., 1984, Model for sandstone-carbonate "cyclothems" based on upper member of Morgan Formation (Middle Pennsylvanian) of northern Utah and Colorado: American Association of Petroleum Geologists Bulletin, v. 68, p. 574–597.

Häntzschel, W., 1975, Trace fossils and problematica, in Teichert, C., ed., Treatise on Invertebrate Paleontology, Part W, Miscellanea, Supplement 1: Geological Society of America, and Lawrence, University of Kansas Press, 2nd ed., p. W1–W269.

Johnson, R.B., and Wood, G.H., Jr., 1956, Stratigraphy of Upper Cretaceous and Tertiary rocks of Raton Basin, Colorado and New Mexico: American Association of Petroleum Geologists Bulletin, v. 40, p. 707–721.

Kennedy, W.J., and Sellwood, B.W., 1970, *Ophiomorpha nodosa* Lundgren, a marine indicator from the Sparnacian of southeast England: Proceedings of the Geologists' Association, v. 81, p. 99–110.

Lee, W.T., 1917, Geology of the Raton Mesa and other regions in Colorado and New Mexico: U.S. Geological Survey Professional Paper 101, 221 p.

Müller, A.H., 1969, Zur Kentniss von *Ophiomorpha* (Miscellanea): Geologie, v. 18, p. 1102–1109.

Pemberton, S.G., and Gingras, M.K., 2005, Classification and characterizations of biogenically enhanced permeability: American Association of Petroleum Geologists Bulletin, v. 89, p. 1493–1517.

Pickett, T.E., Kraft, J.C., and Smith, K., 1971, Cretaceous burrows: Chesapeake and Delaware Canal, Delaware: Journal of Paleontology, v. 45, p. 209–211.

Pillmore, C.L., and Maberry, J.O., 1976, Depositional environments and trace fossils of the Trinidad Sandstone, southern Raton Basin, New Mexico: New Mexico Geological Society, Guidebook 27, p. 191–195.

Weimer, R.J., and Hoyt, J.H., 1964, Burrows of *Calianassa major*, Say, geologic indicators of littoral and shallow neritic environments: Journal of Paleontology, v. 38, p. 761–767.

New Mexico graduate student abstracts

New Mexico Geology recognizes the important research of graduate students working in M.S. and Ph.D. programs. The following abstracts are from M.S. theses and Ph.D. dissertations completed in the last 12 months that pertain to the geology of New Mexico and neighboring states.

New Mexico Institute of Mining and Technology

SOIL CHRONOSEQUENCE STUDY OF LONG VALLEY, NEW MEXICO: INSIGHTS INTO THE DEVELOPMENT OF SOILS ON PLEISTOCENE AND HOLOCENE MORAINE CATENAS
Feldman, Anthony D., M.S.

The history of glacial advance and retreat cycles in mountain watersheds is recorded in glacial landforms. The Sangre De Cristo mountain range in northern New Mexico contains some of the southernmost expansion of glacial activity in the Southwest during the Quaternary but there have been few studies correlating its glacial chronology to the Rocky Mountain glacial record. Glacial deposits within Long Valley, a glaciated valley in the Sangre de Cristo Mountains, were correlated with the glacial history of the southern Rocky Mountains and Wind River Range utilizing soil and landform properties. A soil profile development index (PDI) was calculated utilizing soil texture, structure, consistency, and color data. Organic carbon, hydroxalamine extractable (FeO) and dithionite extractable (FeD) iron oxides, and clay accumulation were also utilized to differentiate moraine age correlations. Soil development is observed to increase with age between soil catenas and at individual catenary positions. Utilizing the calculated PDI values, chemical and physical proxies, as well as field and DEM observations of moraine morphology, four Pleistocene glacial periods are observed within the Long Valley moraine sequence as well as two smaller rock glacier and peri-glacial periods during the Holocene. These cycles were correlated to the Bull Lake, Pinedale, Oldest Dryas, Youngest Dryas, and two periods during the latter half of the Holocene. Among moraine morphology parameters, summit width and flank slope best distinguished moraines of different ages. Profile mass content of FeD iron and clays increased with age while FeO iron and organic carbon profile mass content decreased with age. The soil PDI chronofunction had the highest correlation with the glacial age determinations, with chronofunctions for clay and the FeO/FeD ratio also representing good age discriminators. organic carbon, FeO, and FeD iron were not as useful in differentiation of moraine ages. Chronofunctions for catenas and moraine summits possessed the best age correlations, while toeslope chronofunctions did not correlate well with age.

USING HEAT AS A TRACER TO QUANTIFY DAILY SURFACE WATER-GROUNDWATER EXCHANGE IN THE EAST FORK JEMEZ RIVER, VALLES CALDERA, NM
Paulino Céspedes, Eva R., M.S.

Studying the temporal and spatial variations of flow is critical to understand the fate and transport of solutes within hyporheic environments. Exchange fluxes can vary with time due to hydrologic drivers such as seasonal variability in regional groundwater flow and discharge changes due to snowmelt and precipitation events. From an observational perspective, exchange fluxes and their dynamics can be estimated with the analysis of temperature time series collected within the stream sediments. In this work, we explore the strengths and limitations of two analytical methods to estimate vertical exchange fluxes from temperature time series. Both methodologies were sensitive to sensor spacing, instrument resolution, and magnitude and direction of the flux which resulted in overestimation, underestimation, or incorrect estimation of the velocity. The methods were used to estimate fluxes in the Jemez River located in The Valles Caldera Natural Preserve, NM, which served as an example of a typical low-gradient, meandering mountain stream where temporal and spatial variability of vertical exchange fluxes were analyzed along a riffle-pool-riffle sequence reach. Vertical fluid velocities varied from –1 to 1 m/d and groundwater-surface water exchange was attributed to pressure gradients due to the topography of the streambed, local groundwater flow systems, and localized small lateral flow paths originated at the meander bends.

HYDROGEOLOGY OF THE QUESTA AREA: END MEMBER MIXING ANALYSIS OF SHALLOW GROUNDWATER
Robinson, Kylian, M.S.

In order to understand a pattern of seasonal well failures at Questa, New Mexico, we developed an endmember mixing analysis (EMMA) model that embraces the small scale geological complexities of the northern Rio Grande Rift. Geochemical measurements from multiple datasets were compared to quantify the connection of surface water with the mountain block aquifer with the alluvial aquifer, and the alluvial aquifer with the volcanic aquifer.

Wells and springs were sampled once for major ions, trace metals, water and sulfur isotopologues, and age tracers ^{14}C and ^{3}H, while hydraulic head was measured seasonally throughout the course of three years. These data were analyzed under the rubric of EMMA to quantify mixing relationships and identify statistically significant differences between water types and data sets.

Multiple lines of evidence supported a close connection between groundwater supplying domestic wells and anthropogenic recharge derived from acequias. Groundwater mounding around the ditches produces a seasonal movement of the groundwater table, corresponding with the yearly groundwater recharge cycle. Water level variations observed in the alluvial aquifer varied significantly with the logarithm of distance from acequia, the well depth, and seasonal applications of flow allotments. Surface waters low in TDS and high in bicarbonate are broadly distributed at these times, driven by infiltration of seasonal snowmelt and peak streamflow. Geochemical mixing analysis suggested that about 27% of the domestic supply control-volume was mixed with water recharged recently from the surface, and this should be regarded as a minimum estimate.

Likewise, the heterogeneity of higher tritium values in the alluvial aquifer reflects that the groundwater recharge to the domestic well supply derives significantly from vertical infiltration out of the acequia system. Some wells access mixtures more strongly supplied by long-residence time recharge from the mountain block that has flowed across the Sangre de Cristo Fault (SDCF). Groundwater signatures of the endmembers show that solutes derived from primary chemical weathering of the Latir Peak Volcanic Field have the largest mixing fraction just west of the SDCF. Calcium is associated with high sulfate in the ambient geological system, reflecting the presence of gypsum in the caldera source watershed. The areas dominated by the two major background groundwater types, bicarbonate and sulfate, are found downgradient of the regions of recharge through alkaline rock types and metaluminous bodies respectively. This pattern requires significant subsurface connectivity across Quaternary normal faults of the eastern rift.

In the volcanic aquifer, longer-residence groundwater flow predominates. Small but consistent declines in the head of the volcanic aquifer amounting to 0.14 feet/ year were measured over the course of our study. Head levels in this region do not respond significantly to seasonal forcing, except where the aquifer is overlain and partially confined by saturated alluvium. Identification of the key distinguishing tracer boron at the Dacite Fault Zone crosscutting Guadalupe Mountain establishes that the volcanic aquifer receives measurable inflow from a deep-circulating hydrothermal system. Groundwater flow converges on the volcanic complex from northeast to east, as far north as Latir Creek West and as far east as the alluvial

valley where the Red River emerges at the SDCF. These cool and chemically variable waters mix thoroughly with upwelling fluids, creating a geochemically homogeneous solute composition in the volcanic aquifer. We conjecture that the observed aquifer head decline results from decreasing streamflow and watershed discharges observable at gaging stations that bracket the Red River Spring Zone (RRSZ).

Contaminant loading from the tailings impoundment into the RRSZ and elsewhere within the groundwater system increased in recent years (-2017) despite cutbacks in mine-dewatering discharges to the tailings impoundment. We identify two tailings leachate endmembers, one oxidizing and rich in uranium, the other more reducing and high in molybdenum, that correspond with samples from highly productive and poorly productive extraction wells, respectively. The EMMA model tends to under-predict mixing ratios compared with values derived from only the most mobile tracers and molybdenum. Ongoing changes in contaminant levels at the monitoring sites result from at least two independent causes. 1) Mixing relationships can be temporally variable because surfacewater infiltration varies each year with watershed yield. 2) Contaminant retardation due to ion exchange reactions in the subsurface becomes exhausted at some point in the aquifer, allowing progression of contaminants downstream.

Changes in the contaminant plume can be more precisely mapped by including some additional selected constituents in the analytes of the monitoring program, such as water isotopologues, boron, silica, and lithium. Sampling should be regularized to correspond with high and low infiltration seasons, in order to properly assess the different contributions of mixing and retardation to our observations. With a larger sample size and better-constructed covariance groups to support the mathematics, background values and anthropogenic changes alike can be modeled with greater confidence.

GEOMORPHIC HISTORY AND CHRONOLOGY OF QUATERNARY ALLUVIAL DEPOSITS IN THE SOCORRO AREA, CENTRAL RIO GRANDE RIFT, NEW MEXICO

Sion, Bradley D., Ph.D.

Fluvial terraces in the central Rio Grande rift record important Quaternary climatic and tectonic signals. Age control among Rio Grande terrace sequences in central and southern New Mexico is limited, so regional correlations are unreliable and important process-related questions about the mechanisms and rates controlling terrace formation and deformation cannot be addressed. I present a terrace chronology from the central New Mexico Socorro Basin from ^{36}Cl surface-exposure and ^{14}C ages to establish a firm foundation for Socorro Basin terrace stratigraphy, provide terrace correlations to adjacent rift basins, and test climate response models of terrace formation. Terrace stratigraphy and ^{36}Cl ages imply climatic controls on river incision from terraces that have surface-exposure ages of 26–29, 64–70, and 135 ka. Carbon-14 ages from detrital charcoal show that the most recent aggradation event persisted until at least 3 ka during the transition from glacial to modern climate conditions. Our terrace chronology supports existing climate-response models of terrace formation in arid environments and links tributary responses to the axial Rio Grande system throughout the central Rio Grande rift. Soil characteristics from dated terrace surface provide rates of dust and carbonate accumulation for durations of 0.5-800 kyrs. Soil development in arid and semiarid regions of the southwestern United States is predominantly controlled by influx of eolian dust. I use the ^{36}Cl and ^{14}C soil ages presented in Chapter 2, coupled with soil textures and the profile development index (PDI), to estimate rates of soil development in the Socorro area. The silt-and-clay and profilemass carbonate contents of the soils increase with soil age and yield power-law slopes of 0.33–0.34. The PDIs also increase at rates of 0.33 with increasing soil age and can be used to roughly estimate the ages of undated soils. The rate of soil development in the Socorro area is less than that estimated for soils in higher latitude regions of New Mexico, but is roughly similar to that estimated for soils farther south. This may be due in part to a regional climate gradient presently manifested by greater mean annual precipitation and cooler mean annual temperatures at higher latitudes and/or slower rates of eolian dust accumulation into the soil profile. Rio Salado terraces preserved at the surface and above the Socorro magma body (SMB) provide paleo-geodetic markers to interrogate the longevity of magmatism in the Socorro area. High-resolution elevations from Rio Salado terraces that cross surface-uplift contours document a prehistoric surface-uplift event above the SMB. Longitudinal terrace patterns are consistent with an arching event that began after 26 ka and ceased before 3 ka and cannot be explained by tectonic or fluvial mechanisms. This late Pleistocene-early Holocene surface uplift is related to a magma-emplacement event that predates modern magmatism and is collocated with geodetic uplift. The two temporally distinct surface-uplift events likely record episodic intrusion below the Socorro area since late-Pleistocene time. Magmatic activity may be rejuvinated via a stationary plumbing system inferred from seismic data. This study shows that the magmatic source-feeder system is stable and active over timescales of 10^4 yrs and demonstrates the utility of terraces as strain markers of low-amplitude, large-wavelength deformation caused by mid-crustal magmatic activity.

A TWO-YEAR STUDY OF FLASH FLOOD CHARACTERISTICS IN NEW MEXICAN AND ISRAELI EPHEMERAL CHANNELS

Stark, Kyle, M.S.

The Arroyo de los Piños has been chosen as a prime location to study sediment flux in New Mexico. It is a direct tributary of the Rio Grande and routes through typical formations found in the middle Rio Grande Valley. Two years of observations reveal a channel that floods 3–5 times a year from summer monsoon rains. Rainfall and water depth were recorded continuously at two locations in the watershed. According to these instruments, a minimum rainfall intensity of 3.5 mm/15min is required to generate runoff, regardless of location in the basin. Water depth, velocity, and vertically integrated suspended sediment samples were collected at the basin outlet. In total, 35 suspended sediment and 180 depth and velocity measurements were collected from nine events. A rating curve was developed using the discrete depth and velocity measurements and the resulting calculated discharges are used to compare the suspended sediment concentration (SSC) between samples. SSC ranged from 4,040 mg/L to 74,000 mg/L. Samples collected during the falling limb of the hydrograph were well correlated to discharge ($r^2 = 0.72$) while samples collected during the rising limb were moderately correlated ($r^2 = 0.39$).

Prior to the third year of study, a new sediment monitoring station was completed near the Piños watershed outlet. The new station includes seven different methods of measuring bedload and three methods to measure suspended load. Direct measurements of bedload are collected using Reid-type slots samplers while direct measurements of suspended are collected using automated water samplers. These direct measures are used to calibrate a host of surrogate technologies including microphones, geophones, seismometers, and hydrophones. Few ephemeral channels are studied worldwide and no ephemeral channel has been studied more than the Nahal Eshtemoa in the Negev desert in Israel. Sediment transport dynamics in the channel have been studied for over 25 years. Plate microphones, a surrogate technology to measure bedload flux, are calibrated in the Eshtemoa. Two methods of calibration were tested: a time-averaged method which has been traditionally used, and a mass-averaged method which is new to calibration in the Eshtemoa. The mass-averaged method is shown to be better in almost every way. It is more robust, particularly at lower transport rates, it is effective at all flood stages (rise, max, and fall of the hydrograph), and it is more consistent across events.

INFLUENCE OF LITHOLOGY AND DIAGENESIS ON MECHANICAL AND SEALING PROPERTIES OF THE THIRTEEN FINGER LIMESTONE AND UPPER MORROW SHALE, FARNSWORTH UNIT, OCHILTREE COUNTY, TEXAS

Trujillo, Natasha Andrea, M.S.

This thesis focuses on an evaluation of the caprock for a commercial-scale carbon storage project at the Farnsworth Unit (FWU) in Texas. The FWU is currently in the injection phase of this Southwest Regional Partnership for Carbon Storage (SWP) project, and the goal is to inject 1 million metric tons of anthropogenic CO_2 into

the Morrow B sandstone reservoir. The main lithologies within the caprock are mudstone, cementstone, and some coal. The mechanical properties of these lithologies, along with an understanding of the diagenetic history of each lithology, help determine how the caprock will react to stress perturbation resulting from elevated pore pressure due to injection of supercritical CO_2 into the underlying reservoir.

The principal objective of this work is to understand the lithologic and diagenetic controls on mechanical attributes of the caprock. Important diagenetic processes that have affected the rock include: carbonate precipitation, as concretions and possibly laterally extensive cementstone layers, as well as fracture fills. The fracture fills are commonly fibrous calcite "beef" filling subhorizontal fractures. These may have formed during an overpressurization event and are found throughout the Thirteen Finger Limestone. The carbonate cementstone lithology within the Thirteen Finger Limestone is largely authigenic and was sampled from the core in grid patterns to infer lateral continuity. Because most of the grids have an asymmetric shape, the layers may be laterally extensive. However, it cannot be ruled out that some of the "layers" are part of larger concretions. The elastic properties of all the different lithologies within the caprock can be used to determine the brittle/ductile nature of these rocks. The cementstone is the most brittle lithology within the caprock, whereas the mudstones are the most ductile. Fracture analysis of the core from the characterization wells constrain paleo-stress conditions and induced fractures from the core helped determine current stress conditions within the subsurface. Determining the three principal stress orientations and magnitudes help predict critically oriented fractures and faults that could reactivate from injection of CO_2.

Determining seal potential for the FWU involved evaluation of seal geometry, capacity, and integrity for the upper Morrow Shale and the Thirteen Finger Limestone. The mudstone lithologies overlying the fluvial reservoir facies are marine in origin and the cementstones are of diagenetic origin. As the caprock covers the sandstone reservoir, which is laterally restricted by deposition in a paleo-valley, the caprock lithologies are laterally extensive enough to form an effective trap. Therefore, the principal issues related to the ability of the caprock to inhibit the upward migration of petroleum and CO_2 are the sealing capacity of the caprock lithologies, and the likelihood of any seal bypass features, such as interconnected fracture networks. With the above constraints, I conclude that the seal capacity is excellent for the principal caprock lithologies.

Understanding geomechanical properties of the caprock and attendant fracture gradients help constrain the maximum injection pressure possible without fracturing, as well as the likelihood of seal bypass. The maximum pore pressure that can be attained at the reservoir/caprock interface without fracturing the caprock is 6518 psi (44.9 MPa). The caprock lithofacies at the boundary between caprock and reservoir is predicted to behave in a ductile fashion, and is therefore not conductive to creation of fracture bypass systems. Seal bypass from existing fault/fracture reactivation is the largest threat to this caprock system. If the operator of FWU continues to stay below the fracture gradient for the caprock, then there should be no issue with loss of seal integrity.

ESTIMATION OF FOCUSED RECHARGE FOR NEW MEXICO USING A SOIL-WATER-BALANCE MODEL: PYRANA

Xu, Fei, M.S.

Determining the rate and distribution of groundwater recharge helps in water planning, sustainable development in the future, and preventing contaminants from entering the aquifer. Regional statewide in-place groundwater diffuse recharge estimation has been attempted by using a distributed-parameter soil-water-balance model that simulates recharge on the daily time-step at a resolution of 250 x 250 m. The model, which is called the Evapotranspiration and Recharge Model (ETRM), used gridded precipitation, reference evapotranspiration, and soil property data as the main inputs. Because focused recharge (i.e., transmission loss in ephemeral channels) is an important contributor to groundwater recharge in semiarid-to-arid environments, a stochastic rainfall-runoff generation algorithm was developed to substitute for the original Hortonian overland flow scheme in the ETRM runoff generation procedure. The change in the core algorithm of the ETRM made the model able to incorporate both diffuse recharge and transmission losses in the first-order basin scale into the statewide recharge estimation. Thus, Python Recharge Assessment for New mexico Aquifers (PyRANA) is proposed to be a more appropriate name for the new version of the ETRM model. PyRANA results show high recharge in the mountainous areas and the karst landscape of the state up to about 20% of annual precipitation. The rest of the semiarid part of the state recharged around 4% of annual precipitation. Arid parts of the state received little in-place recharge. PyRANA recharge results are close to previous point studies conducted in southern New Mexico. The amount of focused recharge at larger scales (2nd to 3rd order streams and higher) can be calibrated on the watershed basis by comparing PyRANA runoff and flume records. The rainfall-runoff generation regime was developed using data from the Walnut Gulch Experimental Watershed, which is under a semiarid to arid climate setting. Therefore, future work should focus on validating PyRANA by adding statistical analysis of rainfall-runoff generation procedure in the mountainous areas.

CRUSTAL DEFORMATION RELATED TO EMPLACEMENT OF THE SOCORRO MAGMA BODY

Yao, Shuoyu, M.S.

The Socorro magma body is the second-largest known crustal magma body on Earth. It covers 3400 square kilometers, has a thickness of ~130 m, and is situated at 19 km depth below the surface. The magma body is located within the Rio Grande rift zone, in the crust below the southern Albuquerque basin, the Socorro basin, and the accommodation zone connecting these two basins. Previous surface-leveling and InSAR studies suggest that the Socorro magma body is still active; causing surface uplift with a maximum rate of 2.5–3.0 mm/year centered around San Acacia, New Mexico. The Socorro seismic anomaly is a seismically very active region of mainly upper crustal earthquakes above the magma body.

In this study, Socorro magma body emplacement processes are studied, constrained by the sill-related surface uplift and seismicity patterns. I use the general finite-element software package Abaqus® to build models of crustal deformation. The fundamental analysis method used for all experiments is a fully-coupled thermal-stress analysis, in which results from thermal analysis depend upon displacement results and vice versa. The 2-D elastic models are composed of two parts: the crustal block, and the sill which is embedded into the crustal block at 19 km depth. Surface uplift above the Socorro magma body is caused by thermal expansion of the crustal material and/or a direct effect from inflation of the sill (magma addition). The two effects, thermal and mechanical, are both also modeled separately to understand their individual contributions, and combined in one model. The models predict thermal evolution, crustal deformation, and associated stresses.

The modeling results show the following crustal evolution upon sill emplacement: (1) A thermal aureole develops around the sill, resulting in thermal expansion. The uplift pattern caused by thermal expansion during the sill emplacement phase is wider, and the uplift rate is larger, than the observed uplift pattern; (2) After cooling of the emplaced sill starts, surface uplift rates are at least an order of magnitude smaller than observed uplift rates, and are below InSAR detection limits; (3) Net uplift caused by sill inflation is an approximately linear function of magma overpressure; (4) The temperature evolution suggests that the sill solidifies on a time scale of a few hundred years after an injection event; (5) Sill inflation causes crustal stresses, with a zone of horizontal compression directly above the sill, and horizontal tension between ~13 km depth and Earth's surface; (6) The average surface uplift rate during one heating-cooling cycle of the sill emplacement due to the combined effect of thermal expansion and inflation is similar to the observed uplift pattern.

Based on these results, I develop a new model for Socorro magma body emplacement. Because a newly emplaced sill cools down rapidly to temperatures below those associated with

the formation of a crystal mesh, the currently imaged fluid sill must be younger than several hundred years, or, if it is older, a significant magma injection event must have occurred in the last few hundred years to maintain the molten status of the sill. The ongoing seismicity above the sill is interpreted to result from injection events, which stress the crust so that slip along favorably oriented faults occurs. If this is true, magma injection occurs every 5–10 years or so, concurrent with seismic swarms. The current surface uplift above the sill results from sill inflation, and longer-term thermal expansion.

New Mexico State University

PROVENANCE AND SEDIMENT DISPERSAL TRENDS FROM EARLY PERMIAN (WOLFCAMPIAN) NONMARINE STRATA OF THE ABO FORMATION (AND AGE-EQUIVALENT STRATA) IN NEW MEXICO
Bonar, Alicia L, M.S.

The Early Permian (Wolfcampian) nonmarine, clastic strata of the Abo Formation (and age-equivalent strata) record the final stage of synorogenic sedimentation associated with the Ancestral Rocky Mountain orogeny (ARM) in New Mexico. During this time, ARM deformation was characterized by at least eight basement-block uplifts that exposed a number of Proterozoic basement provinces throughout southwestern Laurentia. Sandstone modal composition trends and U-Pb detrital zircon geochronology from these strata provide a basis for constraining uplift history and detrital contributions from basement blocks to create a new sediment dispersal model for the Early Permian stage of ARM orogenesis in New Mexico.

Sandstone modal composition for the Abo Formation (and age-equivalent strata) is dominated by quartz and feldspar grains, with rare lithic fragments (Q=56%, F=42%, L=2%). Northern samples contain a majority of the potassium feldspar grains (K=19%), and there is an absence of potassium feldspar in southern samples (K<l%). Southern samples deposited in the Orogrande basin underwent diagenetic alterations, including albitization. Bulk U-Pb age trends (n=662) from Early Permian strata reveal a primary peak age of 1689 Ma (Mazatzal-Yavapai province), with secondary peaks at 1247 Ma (Grenville province/De Baca Group) and 1378 Ma (Granite-Rhyolite province/Mesoproterozoic granitoids). However, despite the lithologic homogeneity of these strata, U-Pb age spectra from individual samples (N=7) vary considerably throughout New Mexico. Strata in northeastern New Mexico exhibit a primary peak age of 1376 Ma (Sierra Grande uplift), whereas strata in south-central New Mexico have a primary peak age of 1251 Ma (Pedernal uplift). Strata in north-central New Mexico have primary peak ages of 1692–1694 Ma (southern Uncompahgre uplift), while strata in west-central New Mexico have a primary peak age of 1706 Ma with a secondary peak at 1451 Ma (northern Uncompahgre uplift). Two samples in southern New Mexico exhibit no primary peaks, but have a wide range of ages from 270–3106 Ma, and are both locally and distally sourced (Pedernal, Uncompahgre uplifts).

Data support a model in which the Uncompahgre, Sierra Grande, and Pedernal uplifts in New Mexico were actively contributing sediment during the Early Permian, while the Defiance-Zuni and Peñasco uplifts were inactive and onlapped before the end of Abo deposition. Fluvial systems flowed from north to south, and drainage networks were complex and interconnecting, transporting sediment from central Colorado to southern New Mexico by the Early Permian.

EVALUATING ALONG-ARC TRENDS IN SUBDUCTION CONTRIBUTIONS TO THE SOUTHERN CASCADES: INSIGHTS FROM BASALTIC MAGMA GEOCHEMISTRY
Cole, Meredith, M.S.

The Cascade arc is a continental volcanic arc, extending from northern California to British Columbia, formed by subduction of the Juan de Fuca plate and the Gorda and Explorer micro-plates under the North American plate. The traditional model for generating arc magmas requires mantle melting resulting from fluid-fluxing of the mantle with a "subduction component" consisting of H_2O-rich fluids and/or melts (e.g., Plank and Langmuir, 1993; Plank et al., 2005). In a "hot slab" subduction zone, such as Cascadia, the subducting slab is young and relatively hot, such that complete dehydration of the slab should occur in the forearc, leading to a reduced capacity for fluid-flux melting of the sub-arc mantle wedge (Syracuse et al., 2010). However, basalts with elevated H_2O contents and trace element compositions consistent with subduction component contributions are associated with volcanoes in the southernmost arc as well as monogenetic vents in central Oregon (Grove et al., 2002; Leeman et al., 2005; Ruscitto et al., 2010; Ruscitto et al., 2011; Walowski et al., 2016). Segmentation of the arc and possible variation in mantle source enrichment also complicate magma generation in the Cascades. A variety of mafic lava types are erupted in the Cascades, including low potassium tholeiites (LKT), intraplate basalts (IPB) and calc-alkaline basalts (CAB), which have implications for styles of melt generation. This thesis uses whole-rock and melt inclusion major and trace elements, melt inclusion volatile contents, whole-rock isotopic compositions, and $^{40}Ar/^{39}Ar$ eruption ages in order to investigate trends in subduction component contributions and mantle sources within the southern Cascades between Mt. Shasta and central Oregon. Water contents are lower (<2.8 wt.%) than the Cascade arc average (3.2 wt.% H_20; Plank et al., 2005); however, CAB and LKT magmas have evidence (elevated Sr, Ba, Pb) for varying levels (2–6%) of subduction component contributions. Intraplate basalt magmas have minimal evidence for subduction contributions, and instead represent decompression melts of an enriched sub-arc mantle. Along the arc, subduction component contributions appear to decrease from south to north. There is also a change in mantle source enrichment along the arc, with magmas from central Oregon deriving from a more enriched mantle than those from northern California and southern Oregon. It also appears that subduction component contributions may have decreased over time, while mantle source enrichment, at least in central Oregon, may have increased. Although the Cascades are a "hot" subduction zone, this thesis finds that both magmas with evidence for subduction contributions (CAB, LKT) and those without (IPB) are erupted within the arc and that subduction contributions to CAB and LKT magmas decrease northward along the arc.

INFLUENCE OF INHERITED CRUST ON THE MAZATZAL PROVINCE INTRUSIVE ROCKS: EVIDENCE FROM ZIRCON XENOCRYSTIC CORE AGES AND ISOTOPE GEOCHEMISTRY
Howland, Colby R., M.S.

U-Pb geochronology, zircon Hf isotope compositions, whole-rock geochemistry, and geologic mapping were used to understand the formation of the Mazatzal province in southern New Mexico and provide insight into lithospheric crustal growth during the Paleoproterozoic. The data indicate three pulses of Paleoproterozoic magmatism occurred in southern New Mexico at 1675 Ma, 1655 Ma, and 1630 Ma. These pulses of magmatism formed during different tectonic regimes. 1675 Ma igneous rocks are pervasively deformed felsic gneisses with more evolved Hf isotopes (εHf=+4.3) and contain xenocrystic (1737 ± 16 Ma and 1778 ± 13 Ma) zircon cores suggesting a component of recycling of Yavapai-age crust or sediment during their formation. Through time, Mazatzal-age plutons show an increase in their apparent $^{176}Lu/^{177}Hf$ ratios, indicating the progressive mixing of juvenile lithosphere with older evolved crust. Field relationships and U-Pb ages suggest that the deformation of the orthogneiss, schist, and amphibolite units in the northern San Andres Mountains occurred as a result of the Mazatzal orogeny (1670–1650 Ma). The 1655 Ma pulse of magmatism consists of 'S-type' or 'two mica' undeformed granites with high $Si0_2$ and Al_20_3, low MgO, and Nd model ages generally between 1.9–2.1 Ga. These data suggest the reworking of earlier 1675 Ma crust during crustal melting in a syn- or post-orogenic setting. The final pulse of magmatism (1630 Ma) is bimodal (mafic and felsic igneous rocks), has juvenile Hf compositions, and trace element geochemistry similar to a rift setting indicating that orogenic collapse of the overthickened Mazatzal lithosphere may have occurred at 1630 Ma.

University of New Mexico

NEW GEOCHEMICAL AND ISOTOPIC APPROACHES TO SHALLOW CRUST LANDFORM EVOLUTION
Decker, David, Ph.D.

Many researchers have studied the Guadalupe Mountains in detail and starting with King (1948), many of them have speculated about the timing of the uplift of the Guadalupe block. There are several competing hypotheses including Laramide, Basin and Range, and Rio Grande Rifting uplift scenarios. Using uranium-lead dating of scalenohedral spar found in small vug caves throughout the study area, I have dated the episodes of spar formation to two major phases, 36 to 33 Ma and 30 to 27 Ma. These two episodes of spar formation are in good agreement with the time frame of the ignimbrite flare up during the formation of the Basin and Range. I have also dated several older phases, all the way back to ~180 Ma, which all correspond to nearby (<100 km) known volcanic activity and provide a good argument for the hydrothermal genesis of the spar. By determining the depth of formation of the spar through a new speleogenetic model (supercritical CO_2), age dating the cave spar through U-Pb dating techniques, and finding the temperature of formation of the spar through a newly calibrated $\delta^{88}Sr$ thermometer and fluid inclusion assemblage analysis, I have been able to develop a thermochronometer in a region that has not had the typical apatite fission track and apatite thorium-helium methods available. Using this new method, along with U-Pb dating of calcite vein spar from the Border Fault Zone, I have constrained the timing of the uplift of the Guadalupe block to between 27 and 16 million years.

DENSE-ARRAY TELESEISMIC IMAGING OF THE SOUTHERN ALBUQUERQUE BASIN
Finlay, Tori S., M.S.

The southern Albuquerque basin is a complex area of high extension, multiple orogenies, and ongoing uplift from a midcrustal magma body in which geophysical coverage is sparse. In this thesis, I capitalize on recent innovations in dense-array processing techniques to create virtual source reflection profiles from five teleseismic events during the deployment of the Sevilleta array. The Sevilleta array consisted of ~800 vertical component nodes with ~300 m spacing deployed for 10 days in February of 2015. Virtual source reflection profiles are created by using the free surface of the earth as a virtual seismic source, yielding profiles that mimic active source seismic surveys. From the seventeen virtual source reflection profiles created, I am able to resolve mapped and buried geologic structures throughout much of the southern Albuquerque and northern Socorro basins. Furthermore, I present a unique case of teleseismic P-wave to Rayleigh wave conversion, which is a dominating feature along the western margin of the two basins. The dense instrument spacing makes it possible to detect these arrivals, which likely occur due to the strong impedance contrast between the rift basin sediments and bounding basement-cored fault blocks.

A SPELEOTHEM RECORD OF CLIMATE VARIABILITY IN SOUTHWESTERN NORTH AMERICA DURING MARINE ISOTOPE STAGE 3
Peinado, Justin G., M.S.

During Marine Isotope Stage 3 (MIS-3) of the last glacial period, there were rapid transitions between warm and cold climates referred to as Dansgaard-Oeschgerr (DO) events. In Southwestern North America (SWNA), two speleothem paleoclimate records document changes in moisture source delivery in response to DO-events during MIS-3, but do not address potential changes in effective moisture for the region. In this study, we introduce a new high-resolution speleothem paleoclimate record from Carlsbad Cavern in the Guadalupe Mountains. The speleothem, sample BC-5, grew continuously from 46–31 kya during the latter half of MIS-3, based on U-Th dating. We also tied stable isotope ($\delta^{18}O$ and $\delta^{13}C$) and trace element (Sr/Ca, Mg/Ca, and Ba/Ca) analysis to the U-series chronology to produce multiple high-resolution time-series. Our data further strengthens the shifting westerly storm-track hypothesis and suggest that DO-events led to changes in effective moisture. The stable isotope time-series displays DO-events and are clearly tied to other speleothem records from SWNA and the NGRIP ice core record. When compared to a Holocene speleothem record (BC-11) and a speleothem Asian Monsoon record, it becomes apparent that $\delta^{13}C$ is a record of local changes in effective moisture and vegetation. $\delta^{13}C$ also suggests an atmospheric ρCO_2 control on vegetation and speleothem calcite during the last glacial as has been suggested in other studies. Trace element analysis of BC-5 further supports the stable isotope interpretations. Sr/Ca, Mg/Ca, and Ba/Ca all strongly covary, indicating that they are controlled by similar processes, and are likely connected to changes in effective moisture and local karst processes.

BIRTH AND EVOLUTION OF THE VIRGIN RIVER: ~1 KM OF POST-5 MA UPLIFT OF THE WESTERN COLORADO PLATEAU
Walk, Cory J., M.S.

The uplift history of the Colorado Plateau has been debated for over a century with still no unified hypotheses for the cause, timing, and rate of uplift. $^{40}Ar/^{39}Ar$ dating of semi-continuous basaltic volcanism over the past ~6 Ma within the Virgin River drainage system, southwest Utah and southern Nevada, provides a way to calibrate differential river incision and compare patterns of basaltic migration, mantle velocity structure, channel steepness, lithology, incision history and the birth and evolution of the Virgin River. New detrital sanidine ages constrain the arrival of the Virgin River across the Virgin Mountains to a maximum depositional age of 5.9 Ma. Incision magnitudes and rates of the Virgin River show a stair-step increase in bedrock incision as the river crosses multiple N-S trending normal faults. Average calculated rates are 23 m/Ma in the Lake Mead block, 85 m/Ma in the combined St. George and Hurricane blocks, and 338 m/Ma in the Zion block. Block-to-block differential incision adds cumulatively such that the Zion block has been deeply incised ~1 km (~315 m/Ma) over 3.6 Ma relative to the Colorado River confluence. We test two hypotheses: 1) observed differential incision magnitudes and rates along the Virgin River system are a measure of mantle-driven differential uplift of the Colorado Plateau relative to sea level over the past ~5 Ma. 2) Observed differential river incision relates to river integration across previously uplifted topography and differential rock types with no post 5 Ma uplift. Strong correlations exist between high channel steepness (ksn) and low mantle velocities throughout the Virgin River drainage while weaker correlations exist between high ksn and resistant lithologies. Basaltic volcanism, which has migrated at a rate of ~18 km/Ma parallel to the Virgin River between ~13 and 0.5 Ma suggests a possible mantle-driven mechanism for the combined observations of differential uplift across faults and additional young Colorado Plateau epeirogenic uplift tracked by headward river propagation. Thus, we interpret the Virgin River to be a <4.5 Ma disequilibrium river system responding to ongoing upper mantle modification and related basalt extraction, which is driving ~1 km of young uplift of the western Colorado Plateau.

GLOBAL SEAWATER REDOX TRENDS DURING THE LATE DEVONIAN MASS EXTINCTION DETECTED USING U ISOTOPES OF MARINE CARBONATES
White, David A., M.S.

The Late Devonian extinction ranks as one of the 'big five' Phanerozoic extinctions affecting up to 80% of marine species and occurred during five distinct pulses spanning /or widespread marine anoxia. We test the marine anoxia hypothesis by analyzing uranium isotopes ($\delta^{238}U$) across a ~7 My interval of well-dated Upper Devonian marine carbonates from the Devil's Gate Limestone in Nevada, USA.

The measured $\delta^{238}U$ curve shows no co-variation with local anoxic facies, water-depth dependent facies changes, redox-sensitive metals, TOC, or diagnostic elemental ratios indicating the $\delta^{238}U$ curve was not controlled by local depositional or diagenetic processes and represents global seawater redox conditions. Two negative $\delta^{238}U$ shifts (indicating more reducing seawater) are observed with durations of ~3.8 My (late Frasnian) and ~1.1 My (early Famennian), respectively. Steady-state modeling of the observed -0.2 to -0.3‰ shifts in $\delta^{238}U$ points to a ~5–15% increase in the total area of anoxic seafloor during these excursions. The

late Frasnian negative shift is broadly coincident with the first extinction pulse (late rhenana Zone or lower Kellwasser event), whereas the early Famennian negative shift (lower-middle triangularis zones) does not coincide with the most intense Frasnian-Famennian boundary (F-F) extinction pulses (upper Kellwasser event). Compilations of local sediment redox conditions from Upper Devonian marine deposits with conodont zone-level age control indicates that the extinction pulses were coincident with widespread anoxic deposits accumulating in subtropical epeiric sea and some open-ocean settings supporting previous interpretations that widespread marine anoxia had an important influence on the Late Devonian extinction. The temporal relationships between global ocean redox trends represented by the $\delta^{238}U$ curve and the newly compiled subtropical marine redox sediment trends indicates Late Devonian global oceans and epeiric seas were in relatively good redox communication for the majority of the study interval except for a brief interval (<500 ky) spanning the F-F boundary.